

Electronic Thesis and Dissertation Repository

---

5-18-2022 1:00 PM

## Evaluating the utility of S100A7 in identifying oral dysplastic lesions that will progress to oral squamous cell carcinoma

Jeff Soparlo, *The University of Western Ontario*

Supervisor: Darling, Mark, *The University of Western Ontario*

A thesis submitted in partial fulfillment of the requirements for the Master of Science degree in Pathology

© Jeff Soparlo 2022

Follow this and additional works at: <https://ir.lib.uwo.ca/etd>



Part of the [Pathology Commons](#)

---

### Recommended Citation

Soparlo, Jeff, "Evaluating the utility of S100A7 in identifying oral dysplastic lesions that will progress to oral squamous cell carcinoma" (2022). *Electronic Thesis and Dissertation Repository*. 8547.  
<https://ir.lib.uwo.ca/etd/8547>

This Dissertation/Thesis is brought to you for free and open access by Scholarship@Western. It has been accepted for inclusion in Electronic Thesis and Dissertation Repository by an authorized administrator of Scholarship@Western. For more information, please contact [wlsadmin@uwo.ca](mailto:wlsadmin@uwo.ca).

## **ABSTRACT AND KEYWORDS**

**Title: Evaluating the utility of S100A7 in identifying oral dysplastic lesions that will progress to oral squamous cell carcinoma**

**Introduction:** Recently, S100A7 has been shown to be a potentially useful marker for identifying oral lesions at risk of transformation from dysplasia to squamous cell carcinoma. Our hypothesis is that high S100A7 protein expression predicts the transformation of oral epithelial dysplasia to malignancy. The objective of our study is to semi-quantitatively evaluate the level of S100A7 expression in dysplastic lesions which have transformed into oral squamous cell carcinoma using immunohistochemistry, and correlate these results with other methods of analysis including the standard 3-tier histopathological diagnosis, the 2-tier histopathological diagnosis, and S100A7 evaluation utilizing Straticyte™, a digital proprietary technique designed to communicate S100A7 expression in dysplastic tissue as a 5-year risk of malignant transformation. In addition, a pilot study evaluating the utility of QuPath, an open source software for bioimage analysis, will be assessed to determine if it more reliably correlates with the known outcomes of the sample populations. MAPK pathway proteins ERK1/2, p38, and JNK, will also be assessed for dysregulated phosphorylation in each of the sample populations.

**Methods:** Formalin fixed paraffin embedded specimens from 48 patients with oral squamous cell carcinoma, where from the same site, a non-cancerous biopsy had been previously obtained, were included in the study. Thirty five (35) patients with multiple biopsies of dysplasia which had not advanced to squamous cell carcinoma, and 25

patients with a diagnosis of hyperkeratosis were included as control groups. In addition to the 3-tier dysplasia diagnoses of mild, moderate and severe, 2-tier diagnoses of low grade or high grade were assigned to each of the tissue samples. Specimens were stained for S100A7 protein using a standard immunohistochemistry protocol. Expression of S100A7 was assessed semi-quantitatively, using an intensity and proportion scale, as well as by image analysis using Straticyte™ and QuPath. As S100A7 is associated with activation of the MAPK signaling pathway activity, phosphorylated proteins ERK1/2, p38, and JNK were also evaluated via immunohistochemistry.

**Results:** Manual scoring of S100A7 staining of epithelium in the three study populations was carried out and compared to the 3-tier and 2-tier grading schemes, Straticyte™, and QuPath. Manual scoring had strong correlational relationships with QuPath and Straticyte based on Pearson correlation coefficients, and allowed differentiation of dysplastic from the Control groups. Straticyte™, a test which utilizes a proprietary algorithm for the epithelial S100A7 stain assessment, allowed differentiation, of dysplastic tissue samples that progressed to OSCC, from those that did not ( $p < 0.05$ ).

**Conclusion:** S100A7 holds potential for assisting in the identification of patients with dysplastic oral premalignant lesions that have an increased risk of malignant transformation as compared to those who do not.

Key Words: S100A7, Oral Squamous Cell Carcinoma, Oral Dysplasia, Mitogen-Activated Protein Kinase, Pathology, immunohistochemistry, QuPath, Straticyte™

## **SUMMARY FOR LAY AUDIENCE**

Despite increased awareness for the risk factors of oral cancer, there continues to be an increase in the number of cases globally and in Canada. Unfortunately, the prognosis is still grim and mortality also continues to rise. It is typical for cancerous lesions within the oral cavity to arise from pre-existing lesions, which as a group are called potentially malignant oral lesions. Therefore, in an attempt to identify and treat these lesions early, biopsies are conducted by health care practitioners and the tissue is viewed with microscopy to identify lesions that are potentially cancerous before they become invasive and spread to other parts of the body. However, it can be difficult to identify which of these lesions will progress to cancer, especially early. In this study we looked at a protein that is found within cells of the mucosa, called S100A7, to see if we could identify a change in its expression in lesions that progress to cancer as compared to those that do not. We looked at tissue from patient biopsies from three categories: Those that eventually developed cancer, those that did not, and those that had lesions that demonstrated relatively normal tissue. We looked to see if there were differences in S100A7 between these groups. Our evaluation consisted of a manual score, in which we evaluated the tissue samples under the microscope and scored the S100A7 expression, a commercially available digital scoring method called Straticyte™ in which a proprietary algorithm is used to evaluate and score S100A7 expression to determine a 5-year risk of progression to cancer, and a pilot study to see if an open-source bioimage analysis software, QuPath™ had utility in evaluating the tissue consistently as well. We looked to see if any method more reliably identified lesions likely to progress to cancer as compared to the conventional 3-tier and 2-tier methods of diagnosing tissue dysplasia.

**DEDICATION**

I would like to thank my wife Lacy and my three boys, Parker, Kellan and Jake for being supportive.

**ACKNOWLEDGEMENT**

Dr. Darling, Thank you for your guidance and support throughout my project.

Dr. McCord, Thank you for discussion and support.

Drs. Khan and Howlett, thank you for taking the time to answer my questions and provide insight into not only my project but the process of masters research.

Thank you to Linda for your assistance throughout this process.

## TABLE OF CONTENTS

<b>ABSTRACT AND KEYWORDS</b>	<b>I</b>
<b>SUMMARY FOR LAY AUDIENCE</b>	<b>III</b>
<b>DEDICATION</b>	<b>IV</b>
<b>ACKNOWLEDGEMENT</b>	<b>V</b>
<b>LIST OF TABLES</b>	<b>X</b>
<b>LIST OF FIGURES</b>	<b>XIII</b>
<b>LIST OF ABBREVIATIONS</b>	<b>XVI</b>
<b>CHAPTER 1: LITERATURE REVIEW</b>	<b>1</b>
<b>1.1 Oral squamous cell carcinoma</b>	<b>1</b>
1.1.1 Epidemiology	1
1.1.2 Risk factors	2
1.1.3 Prognosis	3
1.1.4 Clinical identification	4
1.1.5 Management	6
1.1.6 Follow up	10
<b>1.2 Normal oral mucosa</b>	<b>10</b>
<b>1.3 Oral potentially malignant lesions</b>	<b>15</b>
1.3.1 Overview	15
1.3.2 Epidemiology	16
1.3.3 Risk factors	17
1.3.4 Leukoplakia	19
1.3.5 Erythroplakia	20
1.3.6 Malignant transformation	21
1.3.7 Management	25
<b>1.4 Dysplasia</b>	<b>27</b>
1.4.1 Introduction	27
1.4.2 Grading systems	29
1.4.3 Predictive value of grading systems	30
1.4.4 Management of oral epithelial dysplasia	33
<b>1.5 Theories of carcinogenesis: Field cancerization</b>	<b>34</b>

<b>1.6 Biomarkers for oral epithelial dysplasia</b>	<b>36</b>
1.6.1 Introduction	36
1.6.2 S100A7 in oral epithelial dysplasia and oral squamous cell carcinoma	37
1.6.3 Straticyte™	41
1.6.4 S100A7 in other cancer	42
<b>1.7 Mitogen activated protein kinase (MAPK)</b>	<b>44</b>
<b>1.8 Digital slide assessment and QuPath</b>	<b>46</b>
<b>CHAPTER 2: HYPOTHESIS AND AIMS</b>	<b>49</b>
<b>2.1 Hypothesis</b>	<b>49</b>
<b>2.2 Rationale</b>	<b>49</b>
<b>2.3 Aims</b>	<b>50</b>
<b>CHAPTER 3: MATERIALS AND METHODS</b>	<b>51</b>
<b>3.1 Case selection, review and diagnosis</b>	<b>51</b>
3.1.1 Case selection	51
3.1.2 Tissue grading and diagnosis	52
3.1.3 Binary scoring	52
3.1.4 Case organization	53
<b>3.2 S100A7</b>	<b>54</b>
3.2.1 Tissue preparation and staining	54
3.2.2 Establishment of optimal staining conditions	55
3.2.3 S100A7 immunohistochemistry	55
3.2.4 Staining controls	57
3.2.5 Microscopic evaluation of S100A7 manual scoring	58
<b>3.3 Straticyte™ assessment and risk determination</b>	<b>60</b>
3.3.1 Image and risk analysis	60
<b>3.4 QuPath image analysis</b>	<b>61</b>
<b>3.5 Mitogen-Activated Protein Kinase staining</b>	<b>62</b>
3.5.1 p38: immunohistochemistry protocol	62
3.5.2 ERK 1/2: immunohistochemistry protocol	64
3.5.3 JNK: immunohistochemistry protocol	65
3.5.4 Microscopic evaluation of MAPK stained tissue	67
<b>3.6 Statistical methods</b>	<b>68</b>
<b>CHAPTER 4: RESULTS</b>	<b>69</b>

<b>4.1 Results</b>	<b>69</b>
4.1.1 Patient Demographics	69
4.1.2 Lesion Location	71
4.1.3 Diagnosis	72
<b>4.2 Immunohistochemistry</b>	<b>75</b>
4.2.1 S100A7 qualitative evaluation of staining	75
4.2.2 Control group	76
4.2.3 Non-progressing dysplasia	78
4.2.4 Progressing to OSCC	79
<b>4.3 S100A7 staining</b>	<b>80</b>
4.3.1 S100A7 manual score assessment	80
4.3.2 Straticyte: S100A7 risk score	82
4.3.3 QuPath Assessment of S100A7 staining	85
<b>4.4 MAPK Activated Phosphorylation Staining</b>	<b>91</b>
<b>4.5 Statistical analysis</b>	<b>95</b>
4.5.1 Descriptive statistics	95
4.5.2 Tukey multiple comparison 3-tier and 2-tier diagnoses	97
4.5.3 Tukey multiple comparison S100A7 manual score	100
4.5.4 Tukey multiple comparison, Straticyte™ risk score	101
4.5.5 Tukey multiple comparison, QuPath score	102
4.5.6 Pearson correlation coefficients	105
4.5.7 QuPath correlation	110
<b>CHAPTER 5: DISCUSSION</b>	<b>114</b>
<b>5.1 Demographics</b>	<b>114</b>
5.1.1 Gender	114
5.1.2 Age	114
5.1.3 Lesion Location	115
5.1.4 Malignant Transformation	117
<b>5.2 Utility of predictive parameters of dysplasia</b>	<b>118</b>
5.2.1 3-Tier and 2-Tier dysplasia grading systems	118
5.2.2 S100A7 manual score	121
5.2.3 Straticyte™ assay for S100A7 staining	123
5.2.4 S100A7 manual score analysis: 3-tier, 2-tier and Straticyte™	124
5.2.5 QuPath assessment of S100A7 staining	126
<b>5.6 MAPK</b>	<b>127</b>
<b>5.7 Future considerations</b>	<b>127</b>
<b>5.8 Limitations</b>	<b>129</b>

<b>CHAPTER 6: CONCLUSION</b>	<b>132</b>
<b>6.1 Conclusion</b>	<b>132</b>
<b>BIBLIOGRAPHY</b>	<b>134</b>

## **LIST OF TABLES**

Table 1.1: List of oral potentially malignant lesions

Table 1.2: Criteria for identifying and grading oral epithelial dysplasia

Table 1.3: Grading scheme for oral epithelial dysplasia

Table 3.1: Criteria for identifying and grading oral epithelial dysplasia

Table 3.2: Cases retrieved and included in the study

Table 3.3: Intensity scores of S100A7 via light microscopic evaluation (manual scoring).

Table 3.4: Proportion score for S100A7 staining via light microscopic evaluation

Table 3.5: Straticyte™ 5-year probability of malignant transformation and risk category

Table 4.1: Control population gender and average age at first biopsy

Table 4.2: Non-progressing dysplasia population gender and average age at first biopsy

Table 4.3: Progressing population gender and average age in years at first biopsy

Table 4.4: Location of lesion within the oral cavity for each of the three study populations

Table 4.5: Control group diagnoses

Table 4.6: Non-progressing group diagnoses including the 3-tier dysplasia diagnosis

Table 4.7: 2-tier diagnoses for the Non-progressing group

Table 4.8: Progressing group diagnoses including the 3-tier dysplasia diagnosis

Table 4.9: Progressing group diagnoses including the 2-tier dysplasia diagnosis

Table 4.10: Straticyte™ 5-year risk for malignant transformation: Control group case numbers

Table 4.11: Straticyte™ 5-year risk for malignant transformation: Non-progressing group case numbers

Table 4.12: Straticyte™ 5-year risk for malignant transformation: Progressing group case numbers

Table 4.13: Raw score for QuPath assessed epithelial area, S100A7 staining, and percent of epithelium stained in a sub-population of Control tissue samples

Table 4.14: Raw score for QuPath assessed epithelial area, S100A7 staining, and percent of epithelium stained in a sub-population of the Non-progressing tissue samples

Table 4.15: Raw score for QuPath assessed epithelial area, S100A7 staining, and percent of epithelium stained in a sub-population of the Progressing tissue samples

Table 4.13: Descriptive statistics for the 3-tier and 2-tier diagnoses, S100A7 manual scoring, and Straticyte™ risk score.

Table 4.14: Tissue samples excluded from statistical analysis and reason for exclusion

Table 4.15: ANOVA output for 3 tier diagnosis, 2 tier diagnosis, Manual S100A7 scores and Straticyte™ risk scores.

Table 4.16: Tukey multiple comparison between each of the populations (Control, Non-progressing, Progressing) against one another with the 3-tier and 2-tier diagnoses.

Table 4.17: Tukey multiple comparison between each of the populations (Control, Non-progressing, Progressing) against one another with the S100A7 manual score.

Table 4.18: Tukey multiple comparison between each of the populations (Control, Non-progressing, Progressing) against one another with the Straticyte™ risk score.

Table 4.19: Descriptive statistics for the 3-tier and 2-tier diagnoses, S100A7 manual score, Straticyte™ risk score and QuPath score for the QuPath tested tissue samples.

Table 4.20: Tukey multiple comparison between each of the populations (Control, Non-progressing, Progressing) against one another with the 3-tier, 2-tier, S100A7 manual score, Straticyte™ risk score and QuPath score.

Table 4.21: All Populations. Pearson correlation coefficient table for the 3-tier, 2-tier, S100A7 manual score, and Straticyte™ risk score.

Table 4.22: Progressing population. Pearson correlation coefficient table for the 3-tier, 2-tier, S100A7 manual score, and Straticyte™ risk score.

Table 4.23: Non-progressing population. Pearson correlation coefficient table for the 3-tier, 2-tier, S100A7 manual score, and Straticyte™ risk score.

Table 4.24: Control population. Pearson correlation coefficient table for the 3-tier, 2-tier, S100A7 manual score, and Straticyte™ risk score.

Table 4.25: All Populations. Pearson correlation coefficient table for the 3-tier, 2-tier, S100A7 manual score, and Straticyte™ risk score and QuPath.

Table 4.26: Progressing population. Pearson correlation coefficient table for the 3-tier, 2-tier, S100A7 manual score, and Straticyte™ risk score and QuPath.

Table 4.27: Non-progressing dysplasia. Pearson correlation coefficient table for the 3-tier, 2-tier, S100A7 manual score, and Straticyte™ risk score and QuPath.

Table 4.28: Control. Pearson correlation coefficient table for the 3-tier, 2-tier, S100A7 manual score, and Straticyte™ risk score and QuPath.

## LIST OF FIGURES

Figure 1.1: Demonstration of types and anatomical location of mucosa within the oral cavity

Figure 1.2: Layers of keratinized mucosa.

Figure 3.1 Staining controls: Representative high and low risk S100A7. A) High risk S100A7 staining with antibody and B) no antibody. C) Low risk S100A7 staining with antibody and D) no antibody

Figure 3.2: Straticyte™ image analysis. Control from the gingiva with detail containing ROI in red

Figure 4.1: Average age of patients at initial biopsy from each of the three study populations: Control, Non-progressing, and Progressing

Figure 4.2: Case 6: Hyperkeratosis, from gingiva. A) H&E stain, B) S100A7 Stain, C) QuPath™ total epithelial area, D) QuPath™ S100A7 total area, E) Straticyte™ ROI analysis, F) Straticyte™ analysis.

Figure 4.3: Case 9: Moderate/High grade dysplasia, from soft palate. A) H&E stain, B) S100A7 stain, C) QuPath™ total epithelial area D) QuPath™ total S100A7 area E) Straticyte™ analysis, F) Straticyte™ ROI analysis.

Figure 4.4: Case 4: Mild/Low grade dysplasia, from lateral tongue. A) H&E stain, B) S100A7 stain, C) QuPath™ total epithelial and S100A7 area, D) Straticyte™ analysis, E) Straticyte™ ROI analysis

Figure 4.5: Dot Plot for S100A7 manual scores for each of the three populations

Figure 4.6: Average S100A7 manual score for all three populations calculated from the intensity and proportion score

Figure 4.7: Median S100A7 manual scores for the Control, Non-progressing and

Progressing populations calculated from the intensity and proportion score

Figure 4.8.: Dot plot for calculated Straticyte™ 5 year risk score for each of the three populations

Figure 4.9: Average Straticyte™ 5 year risk score for malignant transformation.

Figure 4.10: Median Straticyte™ 5 year risk score for malignant transformation.

Figure 4.11: Average percent of epithelial area stained with S100A7 when assessed with QuPath

Figure 4.12: Median percent of epithelial area stained with S100A7 when assessed with QuPath

Figure 4.13: Dot plot for subpopulation QuPath S100A7 intensity and proportion scores for each of the three populations

Figure 4.14: Average intensity and proportion score for the subpopulation of QuPath assessed tissue samples when S100A7 area staining is assessed with QuPath

Figure 4.15: Median intensity and proportion score for the subpopulation of QuPath assessed tissue samples when S100A7 area staining is assessed with QuPath

Figure 4.16: Dot Plot for S100A7 manual scores the subpopulation of tissue samples that underwent QuPath assessment

Figure 4.17: Average S100A7 manual score for the subpopulation of QuPath assessed tissue samples

Figure 4.18: Median S100A7 manual score for the subpopulation of QuPath assessed tissue samples

Figure 4.19: Erk1/2 staining, Case 2 Control group

Figure 4.20: Erk1/2 staining, Case 26 Non-progressing group

Figure 4.21: Erk1/2 staining Case 4 Progressing group

Figure 4.22: p38 staining, Case 2 Control group

Figure 4.23: p38 staining, Case 26 Non-progressing group

Figure 4.24: p38 staining, Case 4 Progressing group

Figure 4-25: JNK staining, Case 2 Control group

Figure 4.26: JNK staining, Case 26 Non-progressing group

Figure 4.27: JNK staining, Case 4 Progressing group

**LIST OF ABBREVIATIONS**

OSCC	Oral squamous cell carcinoma
WHO	World Health Organization
HPV	Human Papilloma Virus
SCC	Squamous cell carcinoma
QoL	Quality of life
CT	Computed tomography
MRI	Magnetic resonance imaging
US	Ultrasound
PET	Positron emission tomography
TNM	Tumour, node, metastasis
ORN	Osteoradionecrosis
PORT	Post-operative radiation therapy
5-FU	5 fluorouracil
OPML	Oral potentially malignant lesion
H&E	Hematoxylin and eosin
DNA	Deoxyribonucleic acid
EDC	Epidermal differentiation complex
SPRR	Small proline rich proteins
LCE	Late cornified envelope
NK cell	Natural killer cell
iTRAQ	Isobaric tag for relative and absolute quantitation
RT-PCR	Reverse transcription polymerase chain reaction

YWHAZ	14-3-3 protein zeta/delta
PTHA/PTMA	Prothymosin
hnRNPK	heterogeneous nuclear ribonucleoprotein K
IHC	Immunohistochemistry
mRNA	messenger ribonucleic acid
IL-8	Interleukin 8
ELISA	Enzyme-linked immunosorbent assay
RNA	Ribonucleic acid
ERK	Extracellular signal related kinase
JNK	Jun kinase
MAPK	Mitogen activated protein kinase
MAPKKK	Mitogen activated protein kinase kinase kinase
MAPKK	Mitogen activated protein kinase kinase
G1/S	Growth 1 phase/synthesis phase
Rb	Retinoblastoma protein
CIN	Cervical intraepithelial neoplasia
FFPE	Formalin fixed paraffin embedded
EDTA	Ethylenediaminetetraacetic acid
TBS-T	Tris Buffered Saline-0.01% Triton X
TBS	Tris Buffered Saline
H <sub>2</sub> O <sub>2</sub>	Hydrogen peroxide
HRP	Horseradish peroxidase
DAB	3,3'-Diaminobenzidine

ROI	Region of interest
PBS	Phosphate buffered solution
ANOVA	Analysis of variance
FOM	Floor of mouth
TUGSE	traumatic ulcerative granuloma with stromal eosinophilia

## **CHAPTER 1: LITERATURE REVIEW**

### **1.1 Oral squamous cell carcinoma**

#### **1.1.1 Epidemiology**

Oral squamous cell carcinoma (OSCC) is a clinically significant malignant lesion affecting many people worldwide as it remains a significant cause of morbidity and mortality. Management of the malignancy is dependent upon both local and distant spread, therefore, early identification of tissue that is at risk of transforming into squamous cell carcinoma is thought to be essential in reducing harm to patients.

According to 2020 data from the World Health Organization, Oral and lip cancer accounts for 377 713 new cases this year, and 177 757 deaths, which is a slight increase from 2012 data, when approximately 300 400 new cases of oral squamous cell carcinoma occurred, with 145 400 deaths that year (1)(2). The total incidence is highest in South-central Asia with 174 448 cases, and the greatest cumulative risk is in Melanesia (Fiji, France, New Caledonia, Papua New Guinea, Solomon Islands, Vanuatu). The greatest total incidence is among men with 264 211 cases as compared to women with 113 502.

With respect to mortality, the greatest total number is again in South-central Asia with 98 015 with the highest cumulative risk in Melanesia at 0.82. Men had the highest death rate with a total of 125 022 deaths, while woman accounted for 52 735 deaths. North America sees 27 469 new cases annually, with total mortality of 4985(1). As the burden continues to be high, the diagnosis and management of oral potentially malignant lesions remains an important issue within healthcare, and methods leading to improved outcomes still stands to have significant benefit for a large population. As many oral squamous cell carcinomas arise from pre-existing lesions, biopsy and management of these lesions has

played a large role in our attempts to reduce the risk of OSCC (3). Of all head and neck cancers, 90% are squamous cell carcinoma (4).

Head and neck cancers originate in one of the oral cavity, oropharynx, nasopharynx, hypopharynx, and larynx. While anatomically close, the oral cavity and oropharynx are separate entities. The oral cavity can be divided anatomically into specific zones, some of which are at increased risk of malignant transformation relative to others, such as the ventrolateral tongue, and floor of mouth, which are at greater risk than the dorsal tongue and hard palate (5). This may be attributed not only to the settling of carcinogenic agents within these areas, but also due to the rapid rate of turn over that was found in the floor of mouth and ventral tongue relative to the dorsal tongue and hard palate. In addition, the tonsillar pillars and soft palate are also high risk sites (5).

### **1.1.2 Risk factors**

Tobacco use and alcohol consumption are the greatest risk factors for OSCC. In a large pooled analysis consortium regarding the effects of tobacco use and alcohol consumption from 2009, it was noted that 72% of all head and neck cancers were related to the use of either or both of these. The combined use resulted in a synergistic effect, and the risk of carcinogenesis was greater than either entity when used alone (6). Smoking imparts the greatest risk to the upper aerodigestive tract, but smokeless tobacco is also an important risk factor. Cessation of these habits has been shown to be beneficial, reducing the risk of malignancy very close to the level of never smokers after approximately 10 years (7). In addition to tobacco, Betel quid chewing, which is common practice in Asia, also increases the risk of oral and oropharyngeal cancers independent of tobacco and alcohol (8).

Human Papilloma Virus (HPV) as a risk factor for head and neck cancer has also gained significant attention over the past several years. While the significance of HPV and oropharyngeal squamous cell carcinoma has been well defined, the role within oral cavity squamous cell carcinomas continues to show little effect. The identification of transcriptionally active HPV infection from transient infection is associated with p16 positive staining, which is a surrogate of the E7 oncogene (9). While many p16 positive tissue samples are identified when evaluating surgical specimens of OSCC, significance is still unknown (10). This is in contrast to p16 positive lesions of the oropharynx, which tend to occur in younger, non-smokers, is more responsive to chemo and radiation therapy, and has a better prognosis than non-HPV OPSCC (11). For Squamous cell carcinoma of the lip, fair complexion and sun exposure, often associated with an outdoor occupation, are major risk factors. While the survival of other SCC of the head and neck are rather low, 5 year survival for lip SCC is around 90% (12).

### **1.1.3 Prognosis**

It is often noted that despite advances in management, the 5-year survival of oral squamous cell carcinoma is still only 50% which has remained relatively unchanged over the last several decades. While therapeutic modalities have improved, the relatively stable measure of outcomes is likely due to the late stage of initial diagnosis (13). Early detection and management of OSCC leads to statistically significant better outcomes as was identified by Gomez et al in their 2009 meta-analysis (14). It has been reported that there is significant improvement in 5-year survival for stage 1 disease relative to stage 4 (15). Interestingly, in a retrospective database analysis conducted by Cheraghlou et al from Yale in 2019, they report that survival has increased significantly over the last

several decades. They note that for early-stage disease, 3-year survival has risen from 78.0% from 1973-1980, to 92.2% from 2011-2014. Additionally, they report that patients with late stage disease have also seen improvements over those same time frames from 51.9% survival to 70.3% (16). This must be interpreted carefully as it is 3-year survival and not 5-year survival.

In addition to survival outcomes, quality of life (QoL) outcomes are also important. In a study by Gurney et al, eighty seven patients with previous treatment of their head and neck cancer were asked to participate in a survey utilizing a quality of life questionnaire asking about domains including eating, speech, emotion and pain. Of the 87 patients, 71 had carcinoma of the oral cavity, though there was no statistical difference in QoL based on site of primary tumour. Interestingly, patients with early-stage carcinoma at the time of diagnosis scored statistically higher QoL scores in the eating domain. Emotion, Speech and pain were no different. Patients that had recurrence, complications, or gastrostomy tubes all scored lower (17).

As of the 1990s, a concerted effort was made to standardize treatment of OSCC, with the advent of nationally available guidelines first printed in 1997. The goal was to enhance and control cancer treatment by developing protocols for management. This would allow for proper allocation of resources for efficient care (18). In addition, patients are funnelled toward high volume centres with dedicated head and neck oncology teams which independently improve outcomes (19).

#### **1.1.4 Clinical identification**

Appropriate diagnosis of OSCC requires a thorough history, physical exam, imaging and tissue biopsy. Early detection and management of OSCC leads to statistically significant

better outcomes as was identified by Gomez et al in their 2009 meta-analysis. They found that the early detection of oral lesions showed a greater difference in prognosis and outcome than oropharyngeal lesions, likely due to early metastasis of the oropharyngeal lesions (14). The reliability of symptoms alone for early detection is low, as many patients present with vague symptoms (20). In this study, no symptom complex was reliable in determining early oral squamous cell carcinoma. Glottic cancer was the only head and neck cancer subsite that was detected early because of symptomatology. It was also reported that the duration of symptoms was not indicative of the time of actual tumor presence. In another study by Grunfeld, 17 consecutive patients diagnosed with oral squamous cell carcinoma were interviewed, regarding their beliefs about symptoms and their decision to seek medical assessment. After self-discovery of the symptoms, delay ranged from 1 to 48 weeks before seeking help. 24% of patients in the study waited longer than 3 months before seeking help. It was found that oral symptoms were often interpreted as minor and a misunderstanding of how oral squamous cell carcinoma presents led to the delay. Socioeconomic barriers were also mentioned by some as reasons for delay. Many reported changing their diet, or self medicating in hopes of improvement (21). Symptoms of OSCC include painless neck mass, loose teeth, nonhealing ulcers, nonhealing extraction sockets, and pain (4). When a tumour is identified it can present in one of several typical presentations; exophytic, which grow outward, endophytic which grow primarily inward, and ulcerated, which has lost epithelium (22).

Once a lesion within the oral cavity is identified, a tissue biopsy is required for histopathologic assessment and diagnosis, including low or high grade differentiation,

and extent of invasion. 5 mm increments have been identified as significant with respect to depth of invasion in that it effects the staging and treatment of the patient (23). High grade tumours are those with poorly differentiated cells found on histological assessment. Further imaging studies such as computed Tomography (CT), Magnetic Resonance imaging (MRI), Ultrasound (US) and Positron Emission Tomography (PET) are required to formulate the Stage of the cancer based on TNM staging protocols established by the American Joint Committee on Cancer. The staging is dependant on the location of the primary, its size and involvement of adjacent structures, nodal involvement and the presence of distant metastases, the most common of which are found in the lungs or bones (22).

### **1.1.5 Management**

Definitive management for OSCC involves surgical resection, with the potential for adjuvant radiation and chemotherapy. The treatment plan is dependent upon the TNM stage of the OSCC which is based on the size of the primary tumor, the extent of spread both locally and into adjacent structures, the depth of invasion, whether or not positive margins were present on the surgical specimen, and whether or not re-resection is possible. Nodal involvement and distant metastases further comprise the stage, and it is this system that best correlates with 5 year survival (24)(23).

Surgery includes resection of the primary tumour. Additionally, depending on the severity of the disease, a neck dissection to remove lymph nodes, and reconstruction, potentially involving free tissue transfer, may be required. Increasing severity of disease requires more aggressive therapy, therefore, early intervention results in less invasive management, better survival and improved quality of life (24). Surgical resection of the

tumour aims to achieve a 1.5 cm margin around the tumour if possible. If bone is involved, partial or complete resection of the bone is required to achieve clear margins (25). Unfortunately up to 45% of patients present with neck node involvement, and as such surgical resection of lymph nodes is required (26). The extent also depends on the location and amount of involvement. Depending on the site and extent of the primary tumor, modifications of the pattern of neck dissection can be carried out. Neck dissections can be selective, removing specific levels of lymph nodes, to radical, which involves all nodes, the submandibular gland, the tail of the parotid and sensory branches of the cervical plexus (27) (28). Definitive management of the neck is important as many studies have pointed out that cervical lymph node metastases is the most important prognostic indicator in these patients (29).

While surgical treatment is the modality of choice for initial care of oral cancer, radiation can be used alone, with surgery or with chemotherapy depending on the initial presentation and course of the management of the oral cancer (30). Standard treatment protocols involve 2 Gy/fraction, for 35 fractions for a total of 70 Gy. Hyper-fractionation has also proven successful and tolerable for patients. 1.2 Gy is delivered twice daily for 35 days, totalling 81.6 Gy. This was compared against standard treatment protocols in a large multi-center trial, which demonstrated improved locoregional control and survival at 5 years post treatment. It was also shown that risks of complications were not significantly different between the study populations (31). Postoperative radiotherapy is used in cases of advanced local disease, or multiple lymph node involvement (25). When used post operatively, radiation therapy lowers recurrence both locally and in the neck, and increases survival (32). In a study by Lavaf et al, 8795 patients who underwent

surgery alone or combined surgery and radiation therapy, were evaluated with a median follow up of 4.3 years. Adjuvant radiation therapy improved 5-year survival with 43.2% survival in the RT group as compared to 33.4% in the surgery alone group (33).

Radiation therapy is not without its complications. Radiation toxicity can include mucositis, esophagitis, xerostomia, pharyngitis, odynophagia and dysphagia. While these are troublesome, they are not life threatening (30). Osteoradionecrosis (ORN) of the jaws a relatively rare complication with variable morbidity. By definition, it is exposed irradiated bone that fails to heal over a period of 3 months without evidence of local recurrence (34). A study by Aarup-Kristensen et al in 2019 reports an incidence ORN of only 4.2%. (35). With improvement in delivery techniques, the incidence of ORN is decreasing (36). While major risk factors for the development of ORN include mandibular surgery and high doses of radiation to large volumes of the mandible, the exact threshold is not well defined. In a study by Lee et al in 2009, 198 patients with oral and oropharyngeal squamous cell carcinoma were evaluated who had undergone radiation therapy over a 10-year span, from 1990, to 2000. This study found that patients who had a mandibular procedure such as an extraction, were at increased risk, as were those who had received on average, greater than 54 Gy (37). The study by Aarup-Kristensen et al reported a mean dose of 39 Gy for their irradiated patient cohort, and reported that those that developed ORN received higher than average doses of radiation though fail to delineate a threshold (35). Nabil and Samman conducted a systematic review in 2010, and they report that the greatest risk belongs to those that have a tooth extracted in the field of radiation, as well as those that receive greater than 60 Gy (38). Despite surgical excision and radiation therapy, systemic therapy can be required to

improve outcomes. Some head and neck cancer patients with perineural invasion, oral cavity cancer, positive surgical margins, multiple positive lymph nodes, and extracapsular spread of lymphatic disease are at greater risk for poor outcomes as compared to others (25). Systemic therapy refers to chemotherapy and immunotherapy which continue to play an increasingly important role in treatment of patients (39). These agents can be administered before, during or after loco regional management which equate to induction, concomitant and adjuvant chemotherapy respectively (40). Additionally, these agents can be used alone or together with radiation therapy, as radiation sensitizers (39). Numerous studies have evaluated the utility of systemic agents. Assessing 70 randomized trials from 1965 to 1993, Pignon et al conducted a meta-analysis evaluating the effect of chemotherapy on head and neck squamous cell carcinoma. Studies evaluated the efficacy of chemotherapy, as well as the timing of chemotherapy. While the data did demonstrate an absolute survival benefit of 4% at 2 and 5 years, there was considerable heterogeneity within the data. Therefore, conclusions could not be drawn based on this data (41). The group repeated the study and published in 2009. They included 24 randomized trials from 1994-2000 (40). In this meta-analysis, concomitant chemotherapy demonstrated benefit over induction chemotherapy with an absolute benefit of 6.5% at 5 years. Chemotherapy in conjunction with radiotherapy shows increased benefit.

Two large trials were then carried out which evaluated the use of cisplatin in addition to standard therapy of surgery and post-operative radiation therapy (PORT). These studies were important for further characterizing which patients would go on to benefit from the chemotherapy as compared to those that would not(42) (43). These too demonstrated

improved locoregional control and distant disease free survival, while the Cooper et al study demonstrated an improvement in overall survival (42). Cetuximab is another chemotherapeutic utilized to improve long term outcomes in patients with locoregionally advanced squamous cell carcinoma of the head and neck. It is a monoclonal antibody against epidermal growth factor receptors (39). In a study published in the New England Journal of Medicine in 2006, it was shown to significantly improve locoregional control when used with radiation therapy as compared to radiation therapy alone (24.4 months vs 14.9 months) (44). It also demonstrated improved overall survival with a median of 49.0 months when combined with radiation therapy as compared to 29.3 months for radiation therapy alone. In addition to these agents, 5-fluorouracil (5-FU), docetaxel, paclitaxel, hydroxyurea, and carboplatin have been studied and used in various combinations for post-operative and induction chemotherapy (39).

### **1.1.6 Follow up**

Long term follow up for these patients is required as they are at increased risk of new OSCC either at the site of the original excision, or at a different site (45). This highlights the need for continued follow up with a medical professional. In a study conducted by Thomson, Goodson and Smith, 99 patients that developed cancer from a pool of 590 patients with OPMLs were closely reviewed. Of the 99 that developed OSCC, 28 of these patients went on to develop malignant lesions at the same or a different site, supporting the argument for long-term follow up (46).

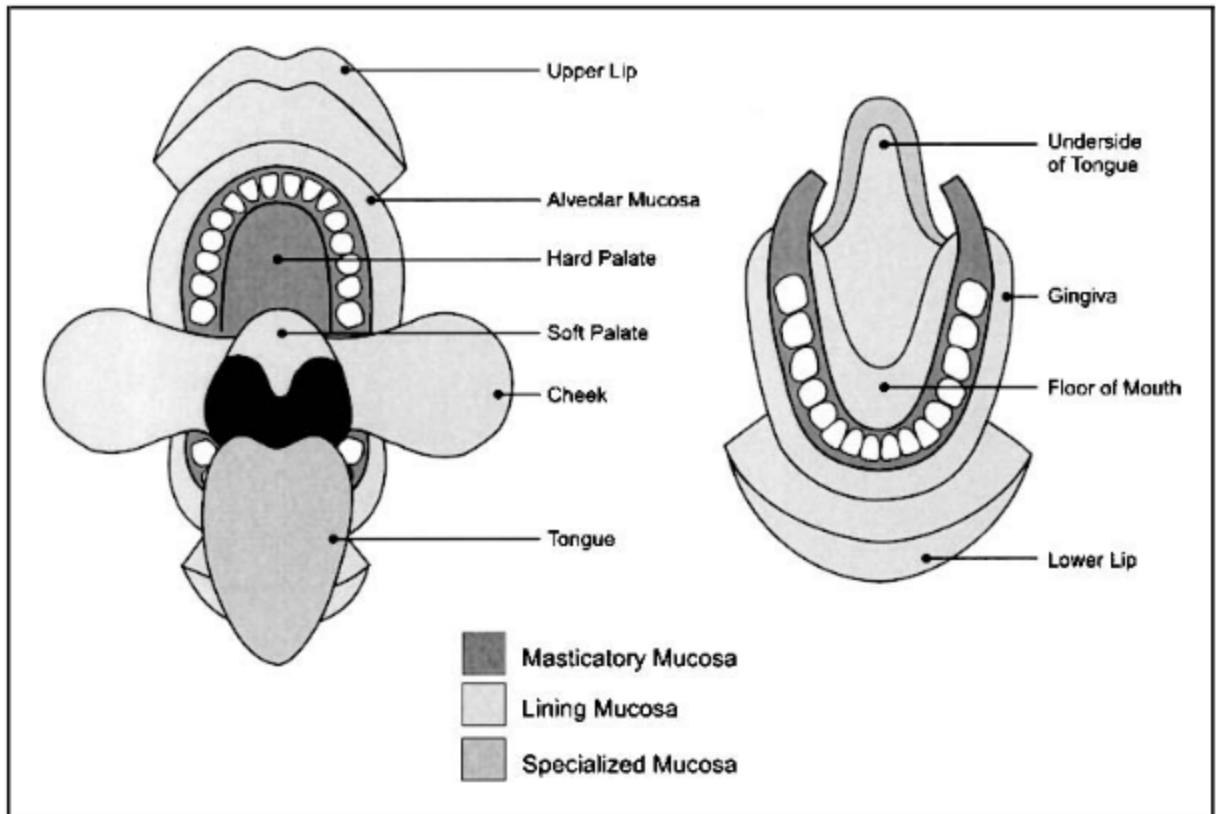
### **1.2 Normal oral mucosa**

The oral mucosa is roughly analogous to the skin, in that there is an epithelium overlying connective tissue. In the oral cavity, the epithelium is comprised of stratified squamous

cells, which are situated on a connective tissue base, referred to as lamina propria. The morphology of the epithelium varies based on location and functional demands within the oral cavity, serving several purposes including immunological barrier, protective mechanical barrier, and host specialized cells such as glands and nerves for lubrication and enhanced perception(47).

The cells of the epithelium are the ones that are considered when discussing oral premalignant lesions. In this case, the layers of the mucosa are dependant on their location; in areas where masticatory forces are present, such as the dorsal tongue, palate or gingiva, the surface is lined by a layer of ortho or parakeratin and as such is called masticatory mucosa. Non-keratinized, lining mucosa, allows for improved flexibility and is found at the floor of mouth, soft palate, cheeks, lips, alveolar mucosa and vestibule (Figure 1.1) (48)(49). Additionally, the tongue is covered by a specialized epithelium which is both keratinized and nonkeratinized and contains papilla, responsible for special features of the tongue surface (48)(50). The relative amount of each type of epithelium that comprises the oral mucosa is approximately 25% masticatory, 60% non-keratinized, and 15% specialized epithelium (51)(48).

**Figure 1.1: Demonstration of types and anatomic location of mucosa within the oral cavity.** This figure was originally published in *Squier CA, Kremer MJ. Biology of oral mucosa and esophagus. J Natl Cancer Inst Monogr. 2001;52242(29):7–15*. This figure is being reproduced for educational purposes only and not for commercial use. The figure is included in the MSc. dissertation with attribution.



The layers of squamous cells within the mucosa represent a progressive maturation from basal membrane to superficial layer, with the most superficial layer becoming cytokeatin filled cells called keratinocytes(47). Interestingly however, the differentiation is not solely dependent on the departure away from the basal lamina, as cells that are prevented from migrating and remain affixed in place, can still differentiate (47). The layers within the masticatory mucosa from deep to superficial include: stratum basale (basal layer), stratum spinosum (prickle cell layer), stratum granulosum (granular cell layer), and stratum corneum (keratinized layer) (Figure 1.2). Only the basal and prickle layers are present in the lining mucosa. Unlike epidermis, there is no stratum lucidum (47). Within the basal layer, are progenitor cells that are present at or near the basal lamina in thin and thick epithelium respectively, and tend to occur in clusters at the depth of the

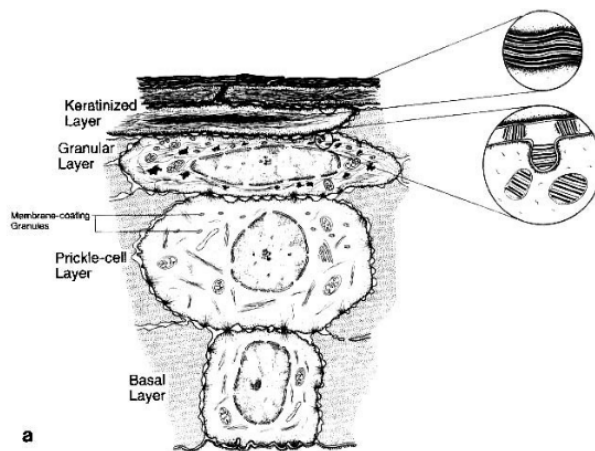
rete ridges (48). These progenitor cells give rise to daughter cells that either stay within the basal layer to maintain progenitor potential of the tissue, while the other daughter cell becomes an amplifying cell, which undergo mitosis, increasing in number and maturing(48)(52). As the cells mature they migrate toward the surface and eventually desquamate(48). These cells are at the least differentiated stage of their maturation with limited organelles for secretion and protein production. There are organelles responsible for production of components of the basal lamina, tonofilaments and keratin (47).

Superficial to the basal layer is the stratum spinosum. This layer is several cells thick demonstrating further maturation and differentiation as the cells migrate. Intracellular processes required for the production of new proteins such as cytokeratins are expressed. The proteins involved in intercellular adhesion, such as desmosomes also increase in number, and as the cells pull away at nonadherent portions of the cells, contributes to the spines which appear on microscopy. The cells of the parabasal layer are characterized by a combination of features of the prickle layer and basal layer, and are still capable of replication (47).

The next layer cells are larger and flatter than the deep layer, and are regarded as the granular layer. Within this layer, most organelles are gone, and the cytoplasm is comprised of tonofilaments and tonofibrils, with an increase in the number of granules called keratohyaline granules. These contain profilagrin, the precursor to fillagrin, which holds the keratin filament network together. Additionally, the granules that are present in the prickle layer now fuse with the lipid membrane and release their contents into the intercellular space. This is a lipid rich material which helps prevent water loss and improve impermeability, while involucrin and loricrin stabilize the cell membranes (47).

The outermost layer is the keratinized layer, in which the cells have matured, and will eventually desquamate. These cells have lost all intracellular organelles, with their intracellular content mostly comprised of keratin.

**Figure 1.2: Layers of keratinized mucosa.** Modified from *Squier CA, Kremer MJ. Biology of oral mucosa and esophagus. J Natl Cancer Inst Monogr. 2001;52242(29):7–15.* This figure is being reproduced for educational purposes only and not for commercial use. The figure is included in the MSc. dissertation with attribution.



Homeostasis within the epithelium is maintained by a balance between cell proliferation, and apoptosis, desquamation of the surface layer of cells and to a lesser extent, necrosis.

This is evident as the epithelium continues to grow throughout life, yet the number of cells within the epithelium stays relatively constant in normal healthy tissue. Regulation of these processes is complex, with a significant number of molecules involved. In general, three types of receptors are involved in proliferative or inhibitory pathways; Kinases, G protein coupled receptors, and steroid binding molecules which have the ability to move into the nucleus once bound, to bind and alter gene expression (53).

Kinases and phosphatases are two classes of enzymes which regulate a number of cellular processes via the transfer of phosphate groups onto organic molecules. These enzymes have opposing function, with the kinases acting to phosphorylate their target molecules,

either Tyrosine residues, or Serine and Threonine residues, while the phosphatases dephosphorylate them (53). Both mechanisms are involved in the regulation of mitosis, and apoptosis.

Keratinocyte cell proliferation and rate of differentiation within the epithelial layer is dependant upon the location of the cells in the oral cavity and whether they are in the keratinized or non-keratinized mucosa. Lining epithelium in the floor of mouth and ventral tongue having the greatest rate of proliferation, and the keratinized tissue of the gingiva and palate having slower rates (5). Using calculations and results from Thomson et al, the turnover time, or time it takes for a cell to mature through the epithelium and shed, ranges from 14-24 days in the oral cavity, which is faster in the non-keratinized than keratinized tissue (48). Sulcular epithelium, immediately adjacent to the tooth, turns over the most rapidly, with a turn over time of approximately five days (47).

### **1.3 Oral potentially malignant lesions**

#### **1.3.1 Overview**

Oral potentially malignant lesions are relatively common morphological alterations to the oral soft tissue with an increased risk of dysplastic and cancerous transformation relative to normal epithelium (54). The definition is based on the following: 1) In longitudinal studies, areas of tissue with certain alterations in clinical appearances identified at the first assessment as 'precancerous' have undergone malignant change during follow-up. 2) Some of these alterations, particularly red and white patches, are seen to co-exist at the margins of overt oral squamous cell carcinomas. 3) A proportion of these may share morphological and cytological changes observed in epithelial malignancies, but without frank invasion. 4) Some of the chromosomal, genomic and molecular alterations found in

clearly invasive oral cancers are detected in these presumptive ‘precancer’ or ‘pre-malignant’ phases (55).

### **1.3.2 Epidemiology**

Lesions which are now considered to be potentially malignant are numerous and identified in table 1.1. In addition to those included on the list, a new set of lesions have been also considered OPML since 2017. These include: chronic hyperplastic candidiasis, oral lichenoid lesions, exophytic verrucous hyperplasia, and oral lesions of graft versus host disease (56). Information is somewhat limited on the prevalence of these disorders, but overall, based on a systematic review in 2018 conducted by Mello et al, the pooled prevalence of oral potentially malignant lesions was 4.47%. There is variability of the prevalence, occurrence geographically, and gender with each of the lesions. Submucous fibrosis was the most common with a prevalence of 4.96%, followed closely by leukoplakia, with a prevalence of 4.11%. Erythroleukoplakia was rare, with a prevalence 0.17% (57). A study conducted in 1987 out of Sweden evaluated the prevalence of all white patches inside the oral cavity to be 24.8% in Swedish adults, however, when re-evaluated with newer definitions considered, prevalence was only 3.6% (56)(58).

**Table 1.1: List of oral potentially malignant lesions.** From El-Naggar AK, Chan J, Grandis J. World Health Organization Classification of Head and Neck Tumours. Vol. 9. 2017.

<b>Oral Potentially Malignant Disorders:</b>
Erythroplakia
Erythroleukoplakia
Leukoplakia
Oral submucous fibrosis
Dyskeratosis congenita
Smokeless tobacco keratosis
Palatal lesions associated with reverse smoking
Chronic candidiasis
Lichen planus
Discoid lupus erythematosus
Syphilitic glossitis
Actinic cheilitis (lip only)

From the review by Mello, oral potentially malignant lesions were seen in greatest number in Asian populations, with an overall incidence of 10.54%, with leukoplakia occurring with a prevalence of 7.77%, and oral submucous fibrosis at 4.96%. The lowest prevalence was in North America, with a prevalence of 0.11%, while in the Caribbean and South America, the prevalence is 3.93% with leukoplakia and erythroplakia occurring with a prevalence of 3.32%, and 0.32% respectively. For Europe, the prevalence was 3.07%, while in the middle east it was 3.72%. Male and female patients represented 59.99% and 39.89% of cases respectively (57).

### **1.3.3 Risk factors**

The occurrence of these lesions appears to be dependent upon gender, tobacco habits and age according to several studies, however, research on these tend to be observational and retrospective. The data is heterogeneous and it is difficult to control for all variables (59). There are a limited number of studies focusing on the characteristics of OPMLs, which

tend to focus on very specific populations. Patients with oral premalignant lesions from developing nations tend to be identified 5-10 years earlier than developed nation, where individuals tend to be identified in their fourth to seventh decade of life (59). Gender also demonstrates variability between males and females and appears to depend on the population evaluated. In a retrospective chart review from India in 2019, 630 patients were evaluated, 375 of which had an OPML or OSCC. Patients attended either a regional dental school, or one of twenty dental clinics. The male to female ratio was 2.28:1, and the average age was 42.64 years with a range from 18-72 years. Submucous fibrosis was the most common OPML occurring in 49.33% of the patients, followed by leukoplakia, which occurred in 29.33% of the 375 patients. The buccal mucosa was the most common site, with 33.01% followed by the tongue and floor of mouth with 22.53% and 14.92% of the lesions respectively. 65% of the patients had at least one risk factor such as tobacco use, alcohol consumption or areca nut (60).

In another retrospective review, all cases with the diagnosis of OPMLs by the Oral Pathology lab at the University of Rio de Janeiro were evaluated. A total of 684 patients were included with OPMLs, with 392 (57%) being female. The age range of patients was seven to 100 years old, with 82% of the patients being between 41 and 82 years old. The mean age for males was 55 years old, while females was 60 years old. Within the oral cavity, the most common site for OPMLs was the lateral boarder of the tongue, with 23% of lesions occurring there. The lower lip and buccal mucosa were second and third most common, occurring in 20% and 19% respectively. 82% of the lesions were leukoplakia. None of the lesions were considered pure erythroplakia. 53% of the patients had a tobacco use history, and 30% reported alcohol consumption. This was more frequent in

males in both cases (61).

Yet another study evaluating a number of oral white lesions in 20333 Swedish adults, 24.8% of patients had a white lesion in their mouth. When cheek and lip biting and smokers palate were excluded, the prevalence dropped to 20.1%. The lesions were found more frequently in males. With respect to location, the commissures and buccal mucosa were the most frequent site for leukoplakia (62).

#### **1.3.4 Leukoplakia**

Leukoplakia is a clinical term describing a white plaque of questionable risk having excluded known diseases or disorders that carry no increased risk of cancer. Examples of non-leukoplakias include frictional hyperkeratosis, leukoedema, and white sponge nevus (55). The term is meant to convey information between the clinician and pathologist, and does not include any information regarding histological features, such as acanthosis, hyperkeratosis, dysplasia, or a combination of any of the three (55). Historically, leukoplakia has been used interchangeably with the dysplasia, however this is incorrect and should be differentiated (63).

Causes of leukoplakia have been debated for many years. While tobacco use, areca nut and alcohol have all been strongly linked to malignancy, their role in the development of leukoplakia is less well known. It has been shown in a number of studies that lesions are more frequent in smokers, and that when smokers stop using tobacco, a number of lesions regress or resolve (64). This is contested in a recent review which stated that newer studies with better statistics indicate that there is not a cause and effect relationship between smoking and leukoplakia (63). Likewise, alcohol consumption and its relationship with leukoplakia is reviewed in this same article. Much the same argument is

made, in that a cause and effect relationship could not be established. In addition, they further note that amount of alcohol consumed may be a factor (63).

There are 2 general classifications of leukoplakia, homogenous and non-homogenous (65). Homogenous is grossly uniform, smooth, white and grossly flat. With respect to non-homogenous, there appears to be roughly 3 variants: speckled, nodular and verrucous. The speckled variety is often referred to as erythroleukoplakia, which is a predominantly white lesions, with red patches interspersed. The nodular lesions are polypoid, while the verrucous lesions are corrugated and appear thicker than homogenous leukoplakia. In a retrospective study of 216 patients with OPML conducted over a 12-year period, it was noted that clinical diagnosis was significantly associated with the risk of malignant transformation, and therefore points to the importance of identifying high risk lesions. They note that non-homogenous lesions had a 4.2 times greater risk of dysplasia as opposed to homogeneous lesions (66).

### **1.3.5 Erythroplakia**

Erythroplakia is a rare epithelial lesion often not included in the category of oral potentially premalignant lesions likely due to the scarcity of its occurrence. A large study by Mehta where a total of 59 915 individuals were evaluated, only 9 cases (0.02%) were found to be erythroplakia (67). This was relatively similar to a survey of 6000 villagers in Burma in which 5 cases were diagnosed with a prevalence of 0.83% (68). When discovered in the oral cavity, erythroplakia tends to have significant features concerning for advancement to oral squamous cell carcinoma (69). One particular study of a series of 58 cases of erythroplakia found that 91% of the lesions were either already invasive, carcinoma in situ, or severe epithelial dysplasia (70). When discovered, these lesions

should be treated as malignancy.

### **1.3.6 Malignant transformation**

The malignant transformation rate of oral leukoplakia has been reported to be within the range of 3.54% to 9.70% (71)(72). 9.70% was established in a meta-analysis of prevalence studies in 2020 that looked at a total of 23 489 lesions. In addition to the transformation rate in general, they noted the high heterogeneity based on geographic region. They therefore ascertained that country of origin was an important risk factor for malignant transformation. This should be viewed cautiously though as there is significant variability of habits by geographic region as well (71). The lower transformation rate of 3.54% was from a 2016 meta-analysis in which 11 423 lesions were identified (72). The 2016 study was restricted to observational studies, as well, they applied a consistent definition of oral leukoplakia to older studies, limiting the total number of lesions that truly represent oral leukoplakia.

Further evaluation of the data within these studies revealed a gender difference in malignant transformation with the 2020 study reporting a transformation rate of 7.6% in males, and 12.6% in females (71). This is corroborated by the 2016 study, which also reports a higher transformation rate among women based on the analysis of twelve studies. The cause of this discrepancy is unknown (72).

Transformation rate and time to follow up was evaluated, which showed that the longer the time to follow up, the greater the chance of malignant transformation. In addition, time to malignant transformation was included as an outcome of interest, which was reported as 11-132 months. The difficulty with this number is that there was a high degree of heterogeneity, making it impractical to complete a meta-analysis of this data

(71).

Age and malignant transformation rate was also considered with 11 of 34 papers reporting the age of the patient at diagnosis (72). Amongst the included studies, there was considerable heterogeneity in age and transformation rate. However, in conjunction with other studies, evidence does support the notion that the greater the age, the greater the risk of malignant transformation (59). A Swedish study found the greatest rate of transformation occurred in patients 70-89 years at 7.5% of patients and only 1% in those under 50 years old (73). In another article, it was found that the peak incidence of leukoplakia occurred in the sixth decade, and the greatest incidence of transformation to carcinoma was in the seventh decade(74). It may be speculated that changes in the immune system with advancing age may contribute to the increase in transformation rate(75)(76).

The duration of the lesion is also a significant factor that appears to correlate with malignant transformation rate (59). It appears that the greatest risk for malignant transformation occurs within the first 5 years of the development of the leukoplakia. Vigilance is required beyond 5 years however, as the risk of malignant transformation still exists, with one study even noting malignant transformation of oral leukoplakia 16 years after diagnosis of the original lesion(77).

Malignant transformation rate and site of the oral leukoplakia has also been evaluated. It seems the most frequent location for the development of oral leukoplakia is the buccal mucosa, however, the most likely site for malignant transformation is the floor of mouth and lateral borders of the tongue, as oral squamous cell carcinomas appear disproportionately at these sites (59). This however is not uniform in all studies. While

some report similar findings with high risk sites for transformation amongst patients from Denmark, Hungary, England and California; other studies show no association between site and malignant transformation in patients from Netherlands (59). Increased malignant transformation at the floor of the mouth and ventrolateral tongue may be due to the pooling of carcinogens in this area where the mucosa has the greatest permeability (78)(64).

Clinical appearance of the leukoplakia seems to be a differentiating factor for those lesions at greater risk of becoming malignant. As previously mentioned, leukoplakia can be described as homogenous or non-homogenous. These have also been referred to as simplex verrucous or erosive (74). The literature supports the notion that the non-homogenous leukoplakia carries an increased risk of malignant transformation relative to the homogenous group(59).

A limited number of studies have also found size of the lesion to be a relevant factor in malignant transformation(69). In the Netherlands, it was found that the greatest transformation rate was thought to be most likely in lesions greater than 200 mm<sup>2</sup> while in Denmark, lesions greater than 5.5cm<sup>2</sup> were thought to be at increased risk(79)(80).

Additionally, an Irish study found that patients with single lesions were at greater risk of transformation than those with multiple or confluent lesions. As such, it appears that larger singular lesions carry a greater risk of transformation as compared to smaller lesions, or those with multiple lesions (81).

Interestingly, the effects of tobacco use and malignant transformation of oral leukoplakia are not firmly established as there are conflicting conclusions about the existing data. While several studies highlight the risk of developing oral leukoplakia in tobacco users as

significant, the malignant transformation of oral leukoplakia to oral squamous cell carcinoma, is not as clearly defined or supported by the data(59)(69)(82)(83). For example, Silverman found that of the patients who developed oral leukoplakia, 74% used tobacco, however, only 47% went on to develop oral squamous cell carcinoma. Of the non-smokers in the group, those that smoked and then quit did demonstrate a reduction in their cancer risk (3). As such, it appears that tobacco use and oral leukoplakia maybe linked, however, the transformation from oral leukoplakia to squamous cell carcinoma is not as strongly linked as one would expect. In fact, oral leukoplakia that develops in patients with no history of tobacco use, are often referred to as idiopathic leukoplakia, appear to be at a greater risk of malignant transformation(59)(69)(3)(73)(84)(64). There may be a difference in leukoplakia that is caused by an irritant, and those that arise spontaneously.

Dysplasia within the biopsy specimen of leukoplakia or erythroleukoplakia has an increased risk of malignant transformation, however this is contested. While the classification of dysplasia is problematic and will be discussed later, in general, several studies have reported oral lesions which demonstrate dysplasia histologically, carry a greater risk of malignant transformation than lesions that do not demonstrate dysplasia. The risk of malignant transformation as noted by Burkhardt and Maerker in 1978 has been noted to be 3%, 4% and 43% for mild, moderate and severe dysplasia (64). With respect to malignant transformation, this is corroborated in the study by Silverman, in which 36% of dysplastic lesions progressed to malignancy. Interestingly however, 16% of leukoplakias that did not demonstrate dysplasia on histological examination, also progressed (3). This is also supported by Schepman, who in their study 166 hospital

based patients, those with moderate and severe dysplasia on their histological evaluation had a statistically significant increased risk of malignant transformation (84).

Additionally, another study reported that lesions with moderate or severe dysplasia had a 2-3 times increased risk of malignant transformation relative to hyperkeratosis or mild dysplasia (85). However, not all studies agree. In 2009, a group from Italy studied 207 patients with long term follow up and failed to find any significant value in any grade of dysplasia, with respect to malignant transformation relative to non-dysplastic lesions (86).

### **1.3.7 Management**

Management of oral leukoplakia is not certain. Some lesions progress while others do not, and some lesions recur after treatment, while others do not and there is no clear method of differentiating which lesions will benefit from invasive management (87).

Options for management include watchful observation, surgical resection, laser ablation, topical and systemic agents and photodynamic therapy (87). For surgical management, the logic is that removal of the lesion decreases the risk of malignant transformation. For NSAIDs, cyclo-oxygenase is inhibited, which may prevent the production of prostaglandins that could contribute to malignant transformation. Chemotherapeutics are intended to destroy cells which have already become neoplastic (88).

Removal of oral leukoplakia by either surgical excision or laser ablation has not convincingly demonstrated a reduction in the malignant transformation rate (86)(79)(84). Therefore, a patient may undergo a surgical excision that has considerable morbidity but gain no true benefit with respect to risk mitigation. This is however contested, and surgical excision with mitigation of other risk factors can have a positive effect on

mitigating the risk of malignant transformation(82). Of 520 patients with leukoplakia who received some form of treatment, those that had removal of etiological factors and surgical excision of the lesion showed the greatest resolution as compared to nonsurgical methods such as topical agents. In contrast, Einhorn and Wersall found an increased transformation rate amongst those who underwent surgical excision (73). When compared to the nonsurgical management group at 2, 5 and 15 years, malignant transformation amongst the excision group was 1.6%, 2.3% and 4.6% versus 0.4%, 1.1% and 2.5% respectively. This paper does mention that there is likely selection bias as lesions at greater risk of malignant transformation are typically the most concerning lesions clinically, and therefore it was these lesions that likely underwent excision. In a cohort study from the UK, 100 patients were followed for 10 years following laser ablation of leukoplakia in the floor of the mouth. Of the 100 patients, 62 patients remained disease free, while 17 went on to develop leukoplakia at the same site, 14 developed leukoplakia at another site, 5 developed OSCC at the same site and 2 developed OSCC at a different site (89).

Photodynamic therapy is a method of management for oral leukoplakia considered to be nonsurgical. There are 3 components 1) a light source, 2) a photosensitizer, 3) tissue oxygen. The photosensitizer is applied then a light source is used. This results in the production of reactive oxygen species (ROS), which causes oxidative damage to the premalignant and malignant cells (90). Two recent systematic reviews, completed in 2015 and 2019 revealed that the photodynamic therapy was effective at either eliminating or reducing the lesion, however, in both cases, recurrence at the original site was 36% and up to 60% respectively. Overall malignant transformation rates were not a part of

either of the reviews (91)(90).

With respect to topical agents and chemotherapeutics, a Cochrane review from 2016 was conducted. In this review, beta carotene, NSAIDs, Vitamin A topical bleomycin and herbal remedies were evaluated. The outcomes for studies included malignant transformation and resolution of the lesions themselves. While Vitamin A and beta carotene may effectively improve the leukoplakia, none were overly effective for prolonged resolution or prevention of malignant transformation (88).

## **1.4 Dysplasia**

### **1.4.1 Introduction**

Histological diagnosis of oral lesions is the gold standard for evaluating and diagnosing dysplastic lesions. Dysplasia is a precancerous lesion of stratified squamous epithelium characterized by a continuum of cellular atypia, with loss of normal maturation and stratification. Carcinoma in situ indicates that the atypia and abnormal maturation of stratification is at or near full thickness (92). Varying degrees of dysplasia exist and these differences are stratified into mild moderate or severe dysplastic changes by the WHO grading system (93). The grade into which the specimen is characterized as is dependant upon the relative degree of change from the basal layer to the epithelium. The characteristic histological changes that are evaluated are present in table 1.2.

**Table 1.2: Criteria for identifying and grading oral epithelial dysplasia.**

*Warnakulasuriya S, Reibel J, Bouquot J, Dabelsteen E. Oral epithelial dysplasia classification systems: Predictive value, utility, weaknesses and scope for improvement. J Oral Pathol Med. 2008;37(3):127–33.*

Architecture	Cytology
Irregular epithelial stratification	Abnormal variation in nuclear size (anisonucleosis)
Loss of polarity of basal cells	Abnormal variation in nuclear shape (pleomorphism)
Basal Cell hyperplasia	Abnormal variation in cell size (anisocytosis)
Drop-shaped rete ridges	Abnormal variation in cell shape (pleomorphism)
Increased number of mitotic figures	Increased nuclear:cytoplasm ratio
Abnormally superficial mitoses	Increased nuclear size
Premature keratinization in single cells	Atypical mitotic figures
Keratin pearls within rete ridges	Increase number and size of nucleoli
	Hyperchromasia

When the changes are full thickness and there is a breach of the basement membrane, squamous cell carcinoma is diagnosed (24). These changes are on a continuum and are simply a continuation of the genetic changes responsible for dysplasia. Many of the OSCCs are well differentiated or moderately differentiated, therefore products such as keratin, in the form of keratin pearls, develop. In these cases, identification of the invasion of epithelial cells is more obvious, where as poorly differentiated carcinomas can have cells which are spindle shaped, or sarcomatoid, which requires special staining techniques to correctly identify the cells as squamous epithelium in origin (24).

**Table 1.3: Grading scheme for oral epithelial dysplasia.** *El-Naggar AK, Chan J, Grandis J. World Health Organization Classification of Head and Neck Tumours. Vol. 9. 2017.*

WHO dysplasia grade (3tier)	Binary grade (2 tier)
Mild dysplasia	Low Grade
Moderate dysplasia	High Grade
Severe Dysplasia	

### 1.4.2 Grading systems

The grading of dysplasia within a specimen is based on the microscopic evaluation of hematoxylin and eosin (H&E) prepared tissue samples, and subjective interpretation of the above features, and their distribution within the epithelium. Mild epithelial dysplasia is considered to demonstrate these architectural features, but the features are confined to the lower third of the specimen, and the cytological changes are relatively minimal. Moderate dysplasia is a continuation along the spectrum of histological changes in the epithelium, with the changes extending into the mild third of the epithelium, or, having sufficiently cytological atypia that the specimen is considered to have moderate dysplasia even if the dysplastic changes do not enter the middle third of the epithelium. Severe dysplasia is found when the architectural changes extend to the most superficial third of the epithelium, or that the cytological changes are significant enough that it is still considered despite the architectural changes not extending into the superficial third. When the tissue is significant for these changes through the whole epithelium, but invasion beyond the basement membrane has not occurred, carcinoma in situ is used (94). In addition to the WHO classification of oral epithelial dysplasia, there is also a binary system based on the same criteria that has been proposed and assessed for utility (95). A

pilot study was conducted in which 28 samples with known outcomes was conducted. 14 tissue samples progressed to cancer, with 14 that did not. The specimens were assessed using the WHO classification system and then evaluated based on the same criteria. It was found that 4 histological and 4 cytological changes was the threshold for classifying a tissue specimen as high risk. This was then tested in a retrospective study, conducted by the same group in which the pathologists were blindly reviewed 68 tissue specimens, with known outcomes. It was found that this binary system had greater interobserver agreement than the WHO classification (Kappa score 0.5, Kappa 0.22 respectively) (95). This new binary system has been embraced with the high risk cut off of 4 architectural and 5 cytological changes (96).

Historically, other grading systems have existed, but have not received widespread acceptance. Smith and Pindborg created a scheme in 1969 where samples were evaluated based on 13 features as either present or not present, slightly present or markedly present, based on a comparison to standard photographs. A score was then assigned (97). The systems flaws however, include the fact that there is no evidence to support the standard photos, and that it is time consuming, therefore it has not caught on universally (94).

### **1.4.3 Predictive value of grading systems**

While pathologists assessing the tissue tend to favour grading tissue as mild, moderate or severe dysplasia, it is well known that this is a flawed system due to the subjectivity of the assignment of these grades. In a Danish study, 4 pathologists were presented with 100 tissue samples and asked to evaluate them as non-dysplastic, mild, moderate, or severe dysplasia, and carcinoma in situ. The inter-observer agreement, which was grossly the same regardless of training, was 49-69%, while the kappa values were in the range of 27-

45% (98). A kappa of this value indicates that inter-observer agreement is generally quite low.

An American study compared six oral pathologists by having them evaluate 120 pre-diagnosed lesions. Several months later, they were given 60 of those same tissue samples to re-evaluate. In the first round of assessment, agreement with the original diagnosis of the tissue sample was 50.5%, with 90.4% of the diagnoses within one histological grade of the originally diagnosis. During the second round of evaluation intra-observer diagnoses was assessed with agreement averaging 50.8%, with 92.4% within one histological grade of their original diagnosis. The ability for the pathologists to recognize dysplasia from non-dysplasia was 81.5%, while agreement with themselves with respect to the same question was 80.3% (99). These numbers indicate that the variability in the interpretation of the tissue sample is significant.

Inter-observer variability was assessed in another study out of the UK, where the exact features of the WHO architectural and cytological variables were documented in order to assess which caused the greatest variation, and those that were most agreed upon within a given sample. In the study of four pathologists, architecturally the most agreed upon features included increased number of mitotic figures (kappa of 0.46), drop shaped rete ridges (kappa of 0.42). With respect to cytoplasmic changes, increased nuclear size and abnormal variation in cell shape (kappas of 0.21 and 0.20 respectively) were the most agreed upon. Irregular epithelial stratification, loss of polarity of basal cells, abnormal variation in nuclear size, atypical mitotic figures, and hyperchromatism were the source of greatest disagreement (100).

The binary system was also assessed for clinical outcomes. The sensitivity and specificity

for predicting malignant transformation was found to be 85% and 80% respectively. Progression free survival for patients considered low grade was 84.8%, while those deemed high grade had progression free survival of only 20%. This was not compared to the original WHO grading system. Based on this study, it appears that the original WHO and binary system are at least comparable, and that there is potential for utility (95).

When the binary and original WHO classification systems were then assessed by Nankivell et al, it was found that the interobserver agreement was superior to the original WHO ( kappa 0.59 versus 0.49 respectively), the prognostic ability was similar (101).

While the classification systems regarding oral epithelial dysplasia is not perfect, they are currently our most used and accepted methods of predicting outcomes. The utility can be viewed from several metrics: risk of progression to OSCC, cancer free survival and survival. Few studies have evaluated this as a primary outcome. In an Irish study by Napier et al published in 2001, 50 patients whose initial biopsy demonstrated dysplasia, only half developed into OSCC, with a positive predictive value of 0.52 (94). In another study involving 257 patients with leukoplakia, 22 were found to have dysplasia, 8 of whom developed OSCC at these sites. The difficulty is that 23 patients without dysplasia in the leukoplakia went on to develop OSCC demonstrating current difficulty in predicting transformation (3).

In keeping with these results, Sperandio et al evaluated 1379 patients for 5-15 years who had been diagnosed with dysplasia. 6/105, 14/76, and 15/38 patients with mild, moderate and severe dysplasia respectively developed OSCC. 14/1182 nondysplastic lesions transformed to OSCC (102). Therefore, while dysplasia is an important predictive tool, the grade of dysplasia does not completely identify those lesions which will transform.

This has a significant effect on management of these lesions.

#### **1.4.4 Management of oral epithelial dysplasia**

Currently, the only method believed to be beneficial in managing dysplastic lesions is surgical excision. In a Cochrane review that evaluated management strategies for OPMLs, methods including herbal extracts, topical bleomycin, Bowman-Birk inhibitor, non-steroidal anti-inflammatory drugs (NSAIDs), Carotenoids, and Vitamin A were assessed (103). According to the analysis, all of the treatments appeared to be well tolerated but there is a lack of strong data as to the efficacy of any of them. Surgical management does appear to decrease the risk of malignant transformation but does not eliminate it. In a study from Australia, 590 patients with OPLs were evaluated, 88% of whom had dysplasia and underwent laser excision. Of those with carcinoma in situ and severe dysplasia, 9% demonstrated persistence and 16% had recurrence (104). Similar results were discovered by Holmstrup in which 296 lesions were biopsied, 94 of which were excised, 71% of which had some grade of dysplasia. Recurrence occurred in 13% and carcinoma developed in 12%(79). These results were in agreement with a retrospective study in Italy in which 207 patients underwent biopsy, 135 of which had mild dysplasia, 50 had moderate, and 22 had severe. Over the 16 years of observation, 128 underwent excision, 5 underwent cryotherapy and 74 elected to observe their lesions. Of the 207 lesions, 39.4% of the lesions disappeared, 19.66% remained stable, 33.7% had a recurrence and 7.24% developed squamous cell carcinoma. It was reported in the study that histological grade of dysplasia was not significant for identifying lesions that became malignant (86). A protocol has been established in Liverpool which attempts to consider factors such as patient age, location of the lesion, as well as grade of dysplasia as to

whether an observation as compared to surgical excision is required. Those lesions deemed higher risk were lesions in non-smokers, were non-homogenous, were on the lateral border of the tongue, and larger than 200mm<sup>2</sup>. The goal of the research team was not to have their protocol established as guidelines, but create further discussion regarding what they felt was an important subject matter, driving further research (105). Due to the risk of recurrence of these lesions, or progression from dysplasia to OSCC, follow up is required. The complicating factor is that due to the variable progression of these lesions, and our inability to reliably detect which lesions will progress as opposed to those that will not, there is no consensus as to the frequency or duration of follow up that is required in patients with dysplasia. It has been suggested that a frequency of every 6 months is satisfactory, but the duration of follow up is unknown, potentially as long as 20 years (106).

### **1.5 Theories of carcinogenesis: Field cancerization**

The theory of field cancerization can help explain malignant transformation regardless of surgical excision. There are two prominent theories regarding field cancerization. One theory is that prolonged exposure to carcinogens results in multiple independent tumors forming due to chronic exposure damaging the cells within the mucosa equally within an anatomical region. The concept originated in 1953 when oropharyngeal, lip and oral cavity squamous cell carcinoma tissue samples from 783 patients were reviewed and several conclusions were made: 1) the seemingly normal mucosa at the margin of a malignancy was in fact abnormal, 2) multiple independent lesions could be found within the resected tumour, 3) the development of second primary tumours within the patient population was high, 4) often, the two separate tumours were from the same anatomical

space, and 5) the recurrence rate of oral squamous cell carcinoma is high. Of the 783 patients in the study, 88 developed second primary lesions 43 within the same anatomical region. The research team felt the cells in the anatomic region were exposed to the same amount and intensity of carcinogen, resulting in greater recurrence than random chance within these sites. This was further evidence supporting the theory for field cancerization (107).

The second theory is that a mutated patch of clonal cells develops from a stem cell which has developed a mutation. Clonal expansion occurs as the mutation confers growth advantage and the colony escapes normal growth control, thus developing a competitive advantage. As the clonal expansion continues, normal cells are displaced. Eventually within the patch, further genetic hits occur creating areas with subclone populations of cells. This occurs multiple times until eventually, a tumour develops. In addition to head and neck cancers, field cancerization has been identified in lung, esophageal, vulva, cervix, colon, breast bladder and skin cancers. This can then be used to explain the development of second primary tumors, and must be considered post resection as portions of the patch of clonal cells likely remains in situ (108). Therefore, regardless of excision of the original lesion, the atypical cells within the area are also at risk of malignant transformation.

This is supported by Bedi et al who evaluated 8 women who had either synchronous or metachronous head and neck squamous cell carcinomas. They evaluated genetic changes, specifically the pattern of X-chromosome inactivation of multiple primary tumours. The logic was, that if the pattern of X-chromosome inactivation were the same in the different tumors, then they were likely from the same origin. X-chromosome

inactivation was used as the marker as this occurs during embryogenesis and is random. This random deactivation is then passed along to all daughter cells prior to malignant transformation. In the study, 8 female patients were assessed who had 2 or more synchronous primary tumours within the oral cavity. Unfortunately only 4 of the cases were able to be used do to loss of heterozygosity at the androgen receptor, though all 4 had identical patterns of inactivation of the X-chromosome which they felt supported their argument (109).

## **1.6 Biomarkers for oral epithelial dysplasia**

### **1.6.1 Introduction**

Assessing the molecular and structural changes for malignant transformation in oral dysplasia is of the utmost importance in secondary prevention. If a lesion can be identified for its true malignant potential early, than patients can be monitored more appropriately based on risk. As previously noted, H&E staining and interpretation by pathologists is subjective, highlighting the importance of other means, as primary or adjunct methods for identifying these lesions. Markers for oral dysplasia with the greatest risk of malignant transformation include genomic markers, such as DNA aneuploidy, chromosome aberrations, and alterations to oncogenes and tumor suppressor genes such as p53. Proliferation markers, differentiation markers and epigenetics may also be of some value. A molecular marker that could identify lesions that are truly at increased risk of malignant transformation as compared to others would be significantly beneficial. The ideal marker would be easily stained and have sufficiently high sensitivity and specificity.

(64).

### **1.6.2 S100A7 in oral epithelial dysplasia and oral squamous cell carcinoma**

The S100 family is comprised of a large number of low molecular weight proteins. The gene family was first identified in bovine brain tissue, during experimentation to identify proteins unique to the nervous system. It was named S100 because it was soluble in 100% saturated ammonium sulfate solution (110). Approximately 15-17 S100 protein genes are present on the epidermal differentiation complex (EDC) on chromosome 1q21(111)(112). These genes are closely related within the complex with other genes that are responsible for terminal differentiation of keratinocytes. In addition to S100 proteins these genes encode trichohyalin, profilaggrin, involucrin, SPRR3, SPRR2A, SPRR1B, and loricrin (113). These genes are part of 3 main gene families that are present in the EDC, namely Small Proline Rich proteins (SPRR), the Late Cornified Envelope (LCE), and S100 (111). The effects of the S100 proteins has been seen both intracellularly and extracellularly (114). The S100 proteins serve as calcium sensor proteins, which once bound work to upregulate, activate, or alter the subcellular distribution of their target proteins (115). Structurally, they contain two EF hand calcium binding domains (loop-helix-loop). These domains have an N-terminus and a carboxy-terminus, with a hinged component in between. It is the carboxy terminus that is variable amongst the S100 protein family, and imparts specificity for different targets (116). The monomers are bound together in an antiparallel fashion, forming dimers within the cells, with or without calcium bound. However, when calcium is present and bound, a cleft is revealed in each of the monomers which exposes the functional domain to the target proteins. When the clefts are bound with their targets, which are at opposite ends due to the antiparallel orientation, the S100 dimer acts as a connection between the two target proteins (117). S100A7 is 11.4kDa protein first identified in psoriatic epidermis by Madsen et al in an

attempt to isolate proteins unique to the skin condition. The upregulation of S100A7 mRNA was determined with immunoblotting and in situ hybridization (118). Expression of S100A7 within normal epidermis is minimally present but is found within the spinous and granular layers with very scarce expression in the basal layer. In this study, in which immunohistochemistry was utilized, both cytoplasmic and nuclear staining were appreciated (119). Interestingly, another study of both normal and psoriatic plaques and the expression of S100A7 it was found that S100A7 was expressed in the basal layer and the spinous layer. In the basal layer, it was found that there was expression in both the nucleus and the cytoplasm, however, the expression of S100A7 in the spinous layer was predominantly found at the plasma membrane (120). In the oral cavity, it appears that typical staining is confined to superficial layers of tissue and is rarely present in the basal layer (121). Additionally, it was found that the staining of S100A7 within the spinous layer appears to be cytoplasmic and concentrates at the plasma membrane (120).

Functionally, the S100A7 role within the cell has not been completely defined. It has been proposed to be involved in keratinocyte differentiation, inflammation and immunology. With respect to differentiation, S100A7 has been found to be induced when differentiation was promoted by factors such as high extracellular calcium and loss of contact with the extracellular matrix (122). It was found that there was essentially no expression in the undifferentiated cells of the basal layer, and more significantly expressed in the differentiated layers, carcinoma in situ, and well differentiated SCC. The expression was proportional to the level of differentiation (122). Unfortunately, the role that S100A7 plays in the process of differentiation is unknown. Further studies have

shown that expression of S100A7 may also coincide with regulation of tight junctions via GSk-3 and MAPK, as well as keratinization proteins such as Beta-Catenin and E-Cadherin and therefore altering the innate immunity of the keratinocytes (123). The expression of S100A7 was also investigated along with other defense/immune proteins. Cell stress such as UV-B light has demonstrated expression of S100A7 in addition to Beta-defensins-2,-3, and ribonuclease 7 (124). This upregulation in response to cell stress maybe regulated through cellular expression of Il-22, a cytokine present within epithelium, produced by NK and Th1 cells (125). While S100A7 appears to have extracellular function as a CD4<sup>+</sup> chemotactic agent, its secretion and mechanism is unclear (126)(114). Furthermore, expression of interleukin-1 alpha as part of the inflammatory response occurs via p38, with knockdown of p38 resulting in an absence of interleukin-1 alpha (127).

Identification of S100A7 as a biomarker initially came from the evaluation of tissue from patients with head and neck squamous cell carcinoma. In an attempt to identify a reliable biomarker, Ralhan et al, preformed quantitative proteomics on tissue homogenates from patients with head and neck squamous cell carcinoma. Via isobaric tag for relative and absolute quantitation (iTRAQ), and verified with western blot, RT-PCR, and immunohistochemistry, differential expression of proteins between a normal control group and the cancer group were evaluated. 811 non-redundant proteins were identified. Of these tests, the 3 best performing proteins were stratifin (14-3-3 sigma), YWHAZ (14-3-3 zeta) and S100A7 which were identified as possible biomarkers that were upregulated in the squamous cell carcinoma group, and not in the control group (128).

With this knowledge, the same group then evaluated tissue homogenates of oral

dysplastic lesions as well as normal oral mucosa to determine proteins present in dysplastic tissue that were nonredundant. In total 459 proteins were identified. Furthermore, they then completed immunoblotting, RT-PCR and immunohistochemistry to further verify these proteins. Interestingly, S100A7 was not originally identified as a non-redundant protein, however, given its performance in the head and neck squamous cell carcinoma trials, S100A7 and prothymosin (PTHA in this study, PTMA in others) were added to the immunoblotting, RT-PCR and immunohistochemistry with the other well performing proteins, stratifin and heterogeneous nuclear ribonucleoprotein K (hnRNPK). The end result was the identification of 5 biomarkers that were significantly upregulated in the dysplastic tissue (129).

Following this study, the 5 biomarkers identified as potentially useful were tested using immunohistochemistry in 110 patients with previously diagnosed dysplasia. This group of patients were unique to this study, and there was no overlap between this and the previous two studies. The patients were followed for a mean of 43 months, with a maximum of 150 months. Of the 110 patients, 39 developed squamous cell carcinoma. Mean time to transformation was 27 months. The 5 biomarkers were evaluated in those that transformed and those that did not. While each of the biomarkers were upregulated in the dysplastic lesions, it was the S100A7 that demonstrated a statistically significant difference between those that transformed and those that did not with a p-value of 0.014. They did not find any correlation between grade of dysplasia and overexpression of S100A7. This led to further evaluation of the S100A7 expression with Kaplan-Meier survival analysis which demonstrated that lesions with overexpression of S100A7 in the cytoplasm had a greater reduction in oral cancer free survival when compared to those

with less cytoplasmic staining (130).

Armed with this information, immunohistochemistry (IHC) with S100A7 staining was carried out to further assess S100A7 and prognostic utility. In this study, S100A7 IHC was carried out in normal, squamous hyperplasia, dysplastic and malignant tissue samples. They found that there was a specificity of 95% for nuclear staining in squamous hyperplasia, dysplasia and squamous cell carcinoma, and 84% for cytoplasmic staining (131). Additionally, they found that nuclear staining led to a greater reduction in cancer free survival as compared to cytoplasmic staining.

### **1.6.3 Straticyte™**

A diagnostic test called Straticyte™, created in Toronto Canada by Proteocyte Diagnostics Inc., utilizes S100A7 expression within dysplastic tissue samples to establish a risk of malignant transformation. A proprietary algorithm is utilized to quantify the expression and create a 5-year cancer risk score. One hundred and fifty (150) oral epithelial dysplasia tissue samples from patients with known outcomes were collected then split into 2 groups randomly: 110 into the learning group, 40 into the test group. The algorithm was recompiled, using the training set. Probability cut offs were established, with less than 21% indicating low risk of progression, and greater than 55% indication high risk of progression. 22-54% is intermediate risk. Compared to standard histopathological assessment, Straticyte™ had improved separation between the 3 groups, with a sensitivity of 95% for low, intermediate and high risk as compared to 75% for mild, moderate and severe dysplasia (132). Interestingly, S100A7 staining was not found to be useful in detecting a progression of grade of dysplasia. A recent study from our lab evaluating S100A7 via manual immunohistochemistry scoring as well as

Straticyte™, found no significant relationship with respect to S100A7 staining and predictability of progression of dysplastic lesions from mild to moderate to severe (121). This seems somewhat counter intuitive as progression of dysplasia would seemingly also likely predict a progression to squamous cell carcinoma. It may also highlight the low reliability and subjectivity of traditional grading methods.

#### **1.6.4 S100A7 in other cancers**

S100A7 has been identified as a potentially significant biomarker in other cancers as well. With respect to the bladder carcinoma, one study evaluated the presence of protein within the urine of patients with bladder carcinomas. While transition cell carcinoma is the most common bladder cancer, a small subset of patients develop squamous cell carcinoma. Urine was analyzed in patients post surgically, and it was found that those with squamous cell carcinoma of the bladder had S100A7 present within the urine samples. As such, the potential benefit for these patients would be to monitor for recurrence, utilizing urine S100A7 as a non-invasive modality for monitoring for recurrence (135).

For ductal carcinoma of the breast, S100A7 mRNA appears to be up-regulated in lesions that are in-situ as compared to the invasive form of the cancer which does not have elevated levels of S100A7. Tissue samples were initially obtained from 3 separate cases, and later confirmed using 32 independent breast tissue specimens (136). Contradicting this slightly was the study by Al-Haddad et al, in which they evaluated not only ductal carcinoma, but lobular, mucinous, medullary and tubular cancers in an attempt to evaluate S100A7 expression. Fifty-seven (57) invasive breast tumors were evaluated. It was found via RT-PCR and western blotting, that S100A7 is over expressed in more

aggressive breast tumors regardless of type, and that it was not exclusive to ductal carcinoma. The thought at the time of the study was that inflammation caused by the cancer cells may be involved in the upregulation of S100A7, however, further studies were required (137).

Additionally, a number of proteins within the S100 family studied to assess their differential expression in esophageal cancer. Sixteen S100 genes were identified, with primers fabricated. A semi-quantitative assessment via RT-PCR was carried out to determine the expression of each of the genes. Of the 16 genes, 11 were significantly down regulated, with only the S100A7 being significantly upregulated, which again strengthens the argument that S100A7 plays a role in epithelial carcinomas (138). In keeping with these epithelial findings, Real time RT-PCR was used to evaluate mRNA levels of IL-8 and S100A7 in precancerous lesions, squamous cell carcinomas and basal cell carcinomas of the skin. While S100A7 mRNA was upregulated in each of the lesions, only SCC had increased levels of both IL-8 and S100A7. This would suggest that S100A7 does play a role in tumourigenesis, and may be independent of inflammation and differentiation in keratinocyte tumours (139). Lastly, RT-PCR, immunoblotting and immunohistochemistry were used to evaluate the presence of S100A7 RNA and protein within different lung tissues, including normal and benign tumour tissue, squamous cell carcinoma, large cell carcinoma, adenocarcinoma and small cell carcinoma. In addition, sera from the above tissue samples were also analyzed with ELISA to determine if S100A7 expression was variable. It was found that S100A7 protein and RNA were upregulated in SCC, adenosquamous carcinoma and large cell carcinoma, but not in small cell or adenocarcinoma. Minimal levels were detected in the benign tumours, and none

was found in normal tissue. The sera of the squamous cell carcinomas demonstrated elevated levels of S100A7, which could have further diagnostic value as a useful biomarker (140).

### **1.7 Mitogen activated protein kinase (MAPK)**

In general, there are 3 conventional enzymatic pathways involved in Mammalian MAPK signalling: Extracellular signal related kinase (ERK), p38, and Jun Kinase (JNK) pathways (141). These pathways share similar organization with 2 serine/threonine kinases, and one double specificity threonine/tyrosine kinase. Starting from upstream, there are at least 3 enzymatic reactions that are activated sequentially, which tend to be generically named MAPK kinase-kinase (MAPKKK), MAPK kinase (MAPKK), and MAPK. Each of the intermediate levels phosphorylates the next level down (142). These enzyme pathways convert extracellular stimuli into a vast number of intracellular responses as the signal is integrated, relayed, and amplified(143). The activation of these pathways alters gene expression, division and replication, metabolism, survival apoptosis and differentiation (141).

The activity of the pathways varies slightly. For the MAPK/ERK pathway, which is also considered the classical pathway, the downstream effect is dependant not only on the timing, duration and intensity of the signal, but that spatial localization of the enzyme as well. As such, this highly regulated cascade can be regulated by extracellular signals such as growth factors and interactions with other cells, as well as internal signalling pathways related to DNA damage and internal metabolic stress stimuli. Activation of these pathways results in cell proliferation, and can be mutated in malignant processes(142). With binding of the plasma membrane growth factor receptors, the signal

cascade is initiated resulting in activation of ERK1/2 once phosphorylated. Once activated, ERKs translocate into the nucleus and alter expression of genes related to replication and growth (143). The cyclin D1-cdk4/6 complex assembly is regulated post-transcriptionally by activated products of the ERK1/2 pathway, and as such ERK1/2 contributes to regulation and passage of the G1/S check point. This is because cyclin-cdk4/6 is involved in the phosphorylation of Rb and therefore activation of E2F transcription factor (143). Additionally, Cdk2 translocation into the nucleus is directly affected by ERK1/2, and cdk2 is required for activation of cyclinA and cyclinE, which are also involved in allowing passage of the cell through the G1/S check point, and progression the S phase (143).

There are multiple isoforms of JNK which are the product of splicing between 3 genes, Jnk1, Jnk2, Jnk3. While Jnk1 and Jnk2 are expressed throughout the body, Jnk3 has been found to be expressed in the brain, heart and testis only (144). JNK is known as a stress activated pathway, and as such, is activated by inflammation, environmental stress, ionizing radiation, oxidative stress DNA damage, and growth factors (143). Once activated, JNK phosphorylates a number of transcription factors, including p53, which in turn bind target genes and either upregulate or downregulate (144). Additionally, they are involved in metabolism, cell transformation and actin reorganization, and is involved with insulin inhibition both in inflammatory states, and as a feedback inhibitor during stimulus states (145).

p38 also plays a role in the inflammatory response and immune response. There are 4 isoforms alpha, beta, delta and gamma. Of these forms, alpha is the most prominent. p38 is present in the cytoplasm and nuclei in quiescent and active cells, phosphorylating

substrates in both compartments. They may come together in the nuclei when stressors are present. Extracellular stressors that have been identified as activators of p38 include UV radiation, hypoxia, ischemia, oxidative stress, inflammatory cytokines, interleukin-1, and tumor necrosis factor alpha. Many of these stressors also activate the JNK pathway and many of the enzymes within the activation pathway are shared. The function of p38 is predominantly involved in the production of pro-inflammatory cytokines by modulating transcription factors or mRNA targets(141). With respect to inflammation within the epithelium, down regulation of p38 alpha appears to decrease inflammation and expression of inflammatory genes (146). This is supported by the fact that Il-1 alpha activation via S100A7 is mitigated through knock down of p38 (147). As such, activity of p38 appears to be involved in cell cycle inhibition by preventing the expression of Cyclin D1 and by regulating the passage of the cell through the G1/S check point as its activity is required for cdc42 arrest (143). It also regulates the cell through mitosis by arresting the cell at the spindle assembly stage of division(148).

### **1.8 Digital slide assessment and QuPath**

Digital slide assessment has been a point of interest since the 1960s, and has continued to draw interest with the improvement of technology (149). While originally difficult, Whole Slide Imaging is now utilized to digitally capture histopathologic specimens in high resolution, for diagnostic and research laboratories (150). Whole Slide Imaging has been validated in a number of studies, including a systematic review which indicated with high quality studies that the use of whole slide imaging was comparable to the use of light microscopy (151).

The benefit of using virtual slides for digital pathology are numerous as these slides can

be added to digital charts, utilized as pooled samples from different sites for research, and allow for cooperation between people in different fields and in different locations to analyze the same slide (152). Additionally, it allows for extraction of quantitative information from the sample by allowing measurement of length or area, cell counts such as mitotic figures, or structure identification and pattern recognition. There is also potential for improved efficiency and productivity with validated algorithms, which could improve workflow (150).

For example, Keenan et al found that digital image analysis could be used to accurately map out nuclear location and crowding within cells in their assessment of cervical biopsies. They found that the automated computer based assessment was efficient and able to accurately distinguish CIN 3 from normal tissue in 98% of cases, demonstrating the possibility of value in computer based assessments (153). This could enhance the reproducibility of biomarker interpretation, as there is considerable intra- and inter-laboratory differences when it comes to assessment, particularly in samples demonstrating moderate amounts of staining(154).

Interpretation of biomarkers becomes more difficult with tumor heterogeneity and this can be made more readily interpretable with the assistance of image analysis with the addition of annotation tools or grids to improve the objective nature of the assessment (150).

Qupath is an open source software application that is a tile-based whole slide image viewer. According to its creator, what distinguishes it from other software applications for whole slide viewing is its object based data model. This means that an object within the image can be created and manipulated by annotation tools which allow drawing, or

segmentation commands for the detection of specific cells. Each annotated area can be grouped and assessed separately or as a whole, allowing for measurement or classification. Ultimately this allows QuPath to represent relationships between a very large number of objects across gigapixel images (155).

## **CHAPTER 2: HYPOTHESIS AND AIMS**

### **2.1 Hypothesis**

S100A7 protein expression is high in oral epithelial lesions which transform to malignancy.

### **2.2 Rationale**

The early detection and diagnosis of oral squamous cell carcinoma improves patient outcomes (14). Oral squamous cell carcinomas are often preceded by lesions with dysplasia present on microscopy. A problem for clinicians is that not all oral epithelial dysplastic lesions progress to malignancy, and therefore it is difficult to identify which lesions require close follow up as opposed to those that do not.

Additionally, the diagnosis of oral dysplasia is via microscopic evaluation. Epithelial dysplasia within the oral cavity is commonly classified as mild, moderate, severe, or carcinoma in situ. Unfortunately, there is significant inter and intra-observer variability in evaluation and diagnosis. Therefore, other methods that could assist in the diagnosis of dysplasia and specifically identify dysplastic lesions at risk of malignant transformation would be of significant value.

Many biomarkers have been evaluated, with S100A7 showing potential promise as a useful predictive aid. If there is a statistically significant, identifiable difference in expression of S100A7 between dysplastic lesions that progress to OSCC, and those that do not, it could lead to significant real world benefit to patients and practitioners.

### **2.3 Aims**

1. Determine the level of S100A7 in oral epithelial dysplasia samples that transform to malignancy and those that do not.
2. Examine the utility of S100A7 immunoreactivity, 2- and 3-tier grading systems, and the S100A7 based Straticyte™ assay in predicting malignant transformation of oral dysplasia.

## **CHAPTER 3: MATERIALS AND METHODS**

### **3.1 Case selection, review and diagnosis**

#### **3.1.1 Case selection**

This study was approved by the Office of Human Resources and Ethics at Western University. REB(#105954).

Formalin fixed paraffin embedded (FFPE) tissue samples and hematoxylin and eosin (H&E) stained slides were retrieved from the archives of the division of Oral Pathology, and London Health Sciences Centre, department of Pathology and Laboratory Medicine, Schulich School of Medicine and Dentistry at Western University. Samples with a diagnosis of hyperkeratosis, dysplasia and squamous cell carcinoma were collected from 2001 to 2019, searched within the Oral Pathology database. Each tissue sample is assigned a code based on diagnosis and recorded in a spreadsheet. Each diagnosis corresponds with a specific numerical code. Cases were retrieved by searching the data for the relevant code.

Inclusion criteria were: 1) Hyperkeratosis: the tissue sample collected from within the oral cavity does not demonstrate any dysplasia. Selection of only hyperkeratosis allows for homogeneity within the control group. 2) Non-progressing dysplasia: two or more biopsies collected consecutively from the same anatomical site, collected at separate encounters which shows either the same, lower, or higher grade of dysplasia but did not progress to oral squamous cell carcinoma (OSCC); or on a single occasion, demonstrating dysplasia, but with no further progression after 4 year follow up. 3) Progressing dysplasia, tissue samples collected from the same anatomical site, with an initial biopsy demonstrating hyperkeratosis, dysplasia, or another epithelial lesion, which

progressed to squamous cell carcinoma at that same site. If there were multiple biopsies, the first one demonstrating dysplasia was used.

Tissue samples from the oropharynx were excluded. Cases were also excluded if the first biopsy collected demonstrated oral squamous cell carcinoma. If there were multiple biopsies, the first one demonstrating dysplasia was used.

### **3.1.2 Tissue grading and diagnosis**

Using light microscopy, the H&E slides were reviewed by a histopathologist and the graduate student author to confirm the diagnosis. The H&E assessment was carried out together initially for calibration, then carried out individually. The diagnosis categories of the 3-tier grading system for oral epithelial dysplasia include mild, moderate, or severe dysplasia.

### **3.1.3 Binary scoring**

In addition to the WHO 3-tier (mild, moderate, severe) grading, each biopsy was assigned either low grade or high grade status using the 2-tier binary grading system. This was carried out by the pathologist as well as the graduate student author. Both were blinded to the 3-tier diagnosis. Initially the samples were reviewed together for calibration, then independently. The 2-tier grading system is based on cellular and architectural features (Table 3.1), with an established cut off for low grade and high grade classification to be 4 histological and 5 cytosolic features (96).

**Table 3.1: Criteria for identifying and grading oral epithelial dysplasia.**

*Warnakulasuriya S, Reibel J, Bouquot J, Dabelsteen E. Oral epithelial dysplasia classification systems: Predictive value, utility, weaknesses and scope for improvement. J Oral Pathol Med. 2008;37(3):127–33. Also presented as Table 1.2 in Chapter 1.*

Architecture	Cytology
Irregular epithelial stratification	Abnormal variation in nuclear size (anisonucleosis)
Loss of polarity of basal cells	Abnormal variation in nuclear shape (pleomorphism)
Basal Cell hyperplasia	Abnormal variation in cell size (anisocytosis)
Drop-shaped rete ridges	Abnormal variation in cell shape (pleomorphism)
Increased number of mitotic figures	Increased nuclear:cytoplasm ratio
Abnormally superficial mitoses	Increased nuclear size
Premature keratinization in single cells	Atypical mitotic figures
Keratin pearls within rete ridges	Increase number and size of nucleoli
	Hyperchromasia

### 3.1.4 Case organization

Cases were grouped based on inclusion criteria described above, into:

1. Hyperkeratosis/Controls (Controls)
2. Non-progressing dysplasia (Non-progressing)
3. Progressing dysplasia in which oral squamous cell carcinoma developed, (Progressing)

A total of 149 cases from all three groups were originally considered for inclusion. After review of the biopsies, some cases were excluded based on biopsies obtained from different locations within the oral cavity, or due to difficulty in obtaining tissue samples.

Consequently, a total of 108 cases were included. 25 hyperkeratosis control samples were used and compared with 35 non-progressing dysplastic samples, and 48 samples that progressed to squamous cell carcinoma from the original dysplastic biopsy. The first

biopsy for each case was identified as the tissue sample of interest for standardization (Table 3.2).

**Table 3.2: Cases retrieved and included in the study**

<b>Diagnosis</b>	<b>Total cases retrieved</b>	<b>Total number of biopsies all cases</b>	<b>Total first biopsies from included cases</b>
<b>Controls</b>	31	31	25
<b>Non-progressing</b>	50	58	35
<b>Progressing</b>	68	106	48
<b>Total</b>	149	195	108

**Demographic data was collected from the biopsy referral form. Data collected included age, gender, location of the biopsy, smoking history, alcohol consumption.**

### **3.2 S100A7**

#### **3.2.1 Tissue preparation and staining**

Formalin fixed paraffin embedded tissue blocks were placed on an ice bath and allowed to cool for 20 minutes. The microtome was set to 5 $\mu$ m, and each block was trimmed to expose a full surface. The fresh surface was then placed back onto the ice bath. The 5  $\mu$ m tissue sections were cut from the block, then floated onto a 45°C warm water bath. A positively charged glass slide was used to collect each section.

Once the tissue was on the slide, it was placed into a slide rack which was then placed into a 37°C incubator for at least 24 hours before removal. Tissue was cut for negative and positive experimental controls, H&E stain, S100A7 stain, and for MAPK signaling pathway proteins p38, ERK1/2 and JNK.

### **3.2.2 Establishment of optimal staining conditions**

A decloaking chamber was used for antigen retrieval. Optimal conditions for antigen retrieval were established by altering the decloaking chamber settings (112.5°C or 125°C). Buffer solutions were also trialed. One solution contained Tris (Sigma Aldrich, St. Louis, MO, USA) + EDTA (Sigma Aldrich, St. Louis, MO, USA) + Tween20 (Sigma Aldrich, St. Louis, MO, USA), was compared to a buffer solution containing just Tris+EDTA. It was determined that the best antigen retrieval occurred with the decloaking chamber set to 112.5°C with a buffer solution of Tris+EDTA+Tween20, pH 9.

### **3.2.3 S100A7 immunohistochemistry**

Using the tissue slides prepared above, S100A7 immunohistochemistry was completed using the same protocol for each round of tissue staining. The rehydration sequence began by placing the slides in 100% xylene three times (5:5:3 minutes), then into 100% ethanol two times (2:1 minutes), 95% ethanol two times (2:1 minutes), 70% ethanol once (2 minutes), and finally distilled water (dH<sub>2</sub>O for 2 minutes). The tissue was then placed into Tris-EDTA buffer, pH 9, with 0.05% Tween 20 in a decloaking chamber. The chamber was set to reach 112.5°C for 90 seconds then cooled to 90°C for 10 seconds.

The slide racks were then cooled with indirect cold tap water. The slides were placed in a humidified chamber and washed with Tris Buffered Saline-0.01% Triton X (TBS-T) on the shaker three times, for three minutes each time. Once washed, the slides were blocked with 125µl of MACH 4 background punisher (Inter Medico, Markham, ON, Canada, Catalogue number: BC-BP974L) per slide, for 15 minutes. This is done to reduce non-specific background staining.

100 µL of anti-S100A7 (Psoriasin) mouse monoclonal antibody (IgG 1Kappa) (Novus Biologicals Canada, Oakville, ON, Canada, Catalogue number: NB 100-56559; clone: 47C1068), diluted to 1:2000 with 1.5% horse serum (VWR International, Toronto, ON, Canada, Catalogue number: 10015-630) in Tris Buffered Saline (TBS), was added to each slide. The negative controls received 100 µL of 1.5% horse serum only. These were then incubated at room temperature for one hour. Once the incubation was complete, the slides were again washed with TBS-T then placed on the shaker three times for 3 minutes. After the wash, 3% H<sub>2</sub>O<sub>2</sub> in TBS was applied to the slides for 10 minutes to block endogenous peroxidase activity, then washed again with TBS-T once for three minutes.

After the wash, 125µl MACH 4 Mouse Probe (Inter Medico, Markham, ON, Canada, Catalogue number: BC-M4U534L) was added to each slide and incubated for 15 minutes. Once complete, the slides were washed three times, for three minutes each time, in TBS-T on the shaker. Next, 125µl MACH 4 HRP (horseradish peroxidase) Polymer (Inter Medico, Markham, ON, Canada, Catalogue number: BC-M4U534L) was added to each slide. These were then allowed to incubate for 15 minutes. After the incubation, the slides were rinsed with TBS-T and placed on the shaker for five minutes, three times.

100 µL of DAB (3,3'-Diaminobenzidine) (MJS BioLynx Inc., Brockville, ON, Canada, Catalogue number: VECTSK4100) was then added to react with the HRP and develop the slides. The DAB was left on the slides for no more than five minutes to avoid excessive background staining. DAB was made fresh and used immediately each time the staining protocol was completed. The DAB was prepared with 5 ml of dH<sub>2</sub>O, 2 drops

(~84µl) buffer, 4 drops (~100µl) DAB and 2 drops (~80 µl) of H<sub>2</sub>O<sub>2</sub>. This was thoroughly mixed prior to use.

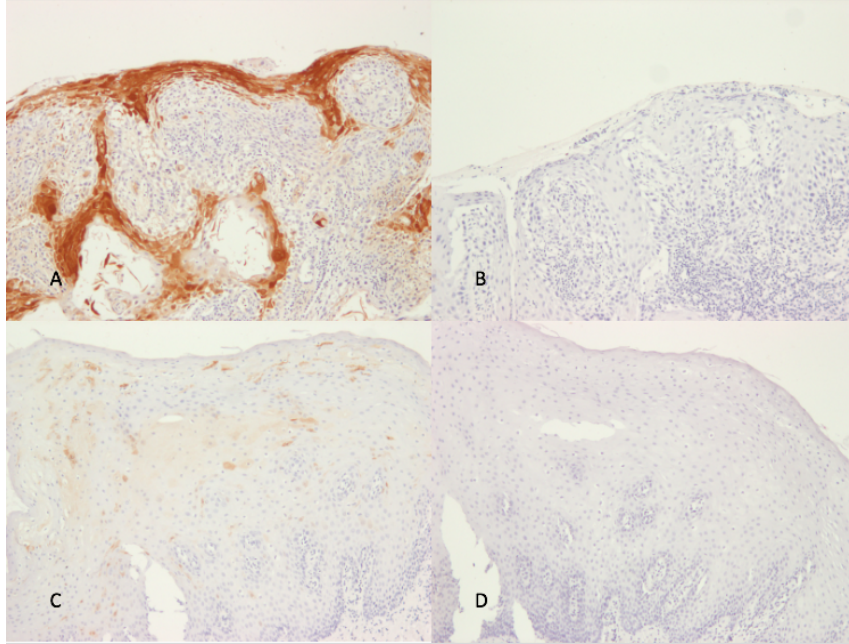
Once the DAB/HRP reaction was complete, slides were rested for up to 5 minutes, then rinsed in dH<sub>2</sub>O and counterstained with Harris haematoxylin (Leica Biosystems Inc., Concord, ON, Canada) for one minute before being rinsed under tap water. The slides were differentiated in 1% acid alcohol (HCl/70% Ethanol) before washing them again with running tap water. The sections were blued in 2% ammonium hydroxide/70% ethanol, and again, the slides were washed in water.

Dehydration of the slides was then carried out in the following manner: the slides were placed in 70% Ethanol for one minute, 95% Ethanol for one minute twice, 100% Ethanol for one minute three times, and finally Xylene for five minutes twice. Cover slips were applied to the slides utilizing Cytoseal™ mounting medium (ThermoScientific, Runcorn Cheshire, WA, USA). The slides were then left to dry, lying flat for at least 24 hours.

### 3.2.4 Staining controls

With each round of S100A7 staining, a known high risk (dysplasia with high level of S100A7 protein staining) and low risk (dysplasia with low level of S100A7 protein staining) tissue samples were included. Positive (S100A7 stained) and negative (primary antibody omitted) were included (Figure 3.1). Information pertaining to Straticyte™ risk stratification can be found in the section labelled, *Straticyte™: Establishing Risk Groups*.

**Figure 3.1 Staining controls: Representative high and low risk S100A7 (magnification x100). A) High risk S100A7 staining with antibody and B) no antibody. C) Low risk S100A7 staining with antibody and D) no antibody.**



### 3.2.5 Microscopic evaluation of S100A7 manual scoring

The immunohistochemistry was analyzed manually via light microscopy. Quantitatively, the scoring was based on both intensity (0-3), and percentage of cells stained (0-5). The sum of this number was then tabulated and a score out of 8 was calculated creating the manual score (Tables 3.3 and 3.4). When evaluating the slides, the epithelium was scanned and then scored based on a representative portion of the tissue. The intensity score was based on the overall impression of the cells stained as compared to our high risk control tissue sample that was included in each run of the staining protocol, while the percent of cells stained was determined by evaluating the epithelial layer in full. This takes into account areas of intense staining as well as other areas of mild or no staining. Qualitatively, the layers within the epithelium were also assessed for the location of the staining. The epithelium was divided into the following layers: corneum, granular, spinous, parabasal and basal layers. Additionally, the distribution of the staining was also noted, as either focal or diffuse, as staining may be minimal, but across the entire

specimen, or it can be full thickness but only within a small portion of the sample. The presence of staining and the relative amount of staining within each layer was also recorded.

**Table 3.3: Intensity scores of S100A7 staining via light microscopic evaluation**

Score	Intensity
0	None
1	Mild
2	Moderate
3	Intense

**Table 3.4: Proportion score for S100A7 staining via light microscopic evaluation**

Score	Percent cells stained (%)
1	1-20
2	21-40
3	41-60
4	61-80
5	81-100

The assessment was conducted by a histopathologist and the graduate student author. Calibration was carried out prior to scoring, using random tissue samples to reach consensus. Once all tissue samples were evaluated and scored, 10 random samples were evaluated by both evaluators to confirm that calibration was maintained. Differences on

the intensity and percentage scores of greater than 1, were discussed and consensus was determined.

### 3.3 Straticyte™ assessment and risk determination

#### 3.3.1 Image and risk analysis

The tissue samples were sent to Toronto for qualitative analysis via Straticyte™. Using the Hamamatsu Nanozoomer-XR slide scanner (Toronto Centre for Phenogenomics, Toronto, Ontario, Canada) the slides were digitally scanned and imported into Visiopharm VIS (Hoersholm, Denmark). Up to five regions of interest (ROIs) were identified within the epithelial layers in areas of high S100A7 staining. These regions had 500 µm diameters. The positive S100A7 and average cell size were calculated and used to generate the Straticyte™ risk category and probability of cancer progression scores. The risk category was determined based on the percent chance of progression to cancer (Table 3.5).

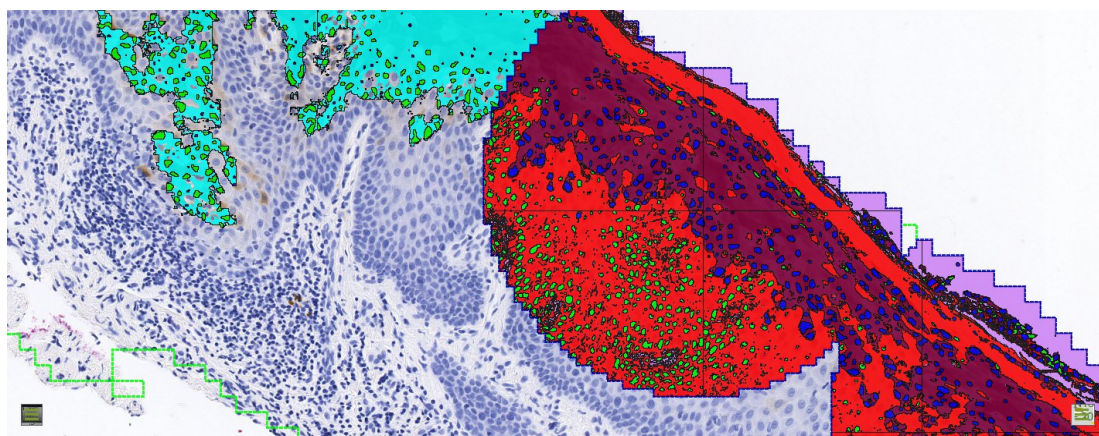
**Table 3.5: Straticyte™ 5-year probability of malignant transformation and risk category**

Risk category	Percent probability of malignant transformation (%)
Low	<19
Medium	20-59
High	>60

Figure 3.2 provides an example of the Straticyte™ assessment. The green outline of the specimen simply identifies the tissue, while the teal area is S100A7 staining. The green dots outside of the ROI represent S100A7 negative nuclei. The blue line outlines the

specific ROIs within the tissue sample. Within the ROI, maroon represents the areas with S100A7 staining, while the red areas are S100A7 negative. The light purple areas are representations of the background glass in areas of tissue porosity. Within the ROI, the green dots indicate S100A7 negative nuclei, while the blue ones are positive. With this tissue sample, the Straticyte™ Risk was medium, with a 5-year malignant transformation risk of 31%.

**Figure 3.2: Straticyte™ image analysis. Control from the gingiva with detail containing ROI in red. Image provided by Dr. Jason Hwang, Proteocyte AI, Toronto, ON, Canada**



### 3.4 QuPath image analysis

As an additional method of evaluating the tissue slides, an open source software, QuPath™ (<https://qupath.github.io>) was used for objective measurements. Ten tissue samples were selected consecutively. Tissues with folds were excluded. These were sent for Whole Image Scanning using an Aperio scanner (Leica Biosystems Inc, Wetzler Hesse, Germany). Utilizing one of the QuPath annotation tools, the total area of the epithelium, as well as the total area of stained cells was calculated. From this, “Percent Cells Stained score” (area of stained cells/ area of total epithelium) was calculated. A raw area was obtained and documented. As with the manual S100A7 scoring, demonstrated in

Tables 3.3 and 3.4, this was converted to a score out of five, and added to the intensity score out of three to create a total QuPath score, as was done for the manual scoring.

### **3.5 Mitogen-Activated Protein Kinase staining**

Consecutive tissue samples from the three populations; Hyperkeratosis/Controls, Non-progressing dysplasia, and Progressing to OSCC, were selected for further immunohistochemistry for three Mitogen-activated protein kinase (MAPK) proteins: p38, Erk1/2, and JNK. A total of 30 tissue samples, ten from each population, were stained. Our positive control for each of these staining protocols was an oral squamous cell carcinoma (OSCC), the same used for the S100A7 staining protocols.

#### **3.5.1 p38: immunohistochemistry protocol**

Slides were initially immersed in xylene solution twice, for five then three minutes. This was done in two different containers. Absolute alcohol was next for two minutes then 95% alcohol for two minutes, 95% alcohol for one minute, then 70% alcohol for one minute. They were then placed in water for two minutes.

To quench the tissue, the slides were placed in fresh 3% hydrogen peroxide in methanol for five minutes (prepared from 30% H<sub>2</sub>O<sub>2</sub>) (20 ml 30% H<sub>2</sub>O<sub>2</sub> and 180 ml Methanol).

Once this step was complete, distilled water was used to rinse the slides for five minutes, and then a five minute Phosphate buffered saline (PBS) rinse was completed on the shaker.

Antigen retrieval was completed in citrate buffer, pH 6.0 in a de-cloaking chamber. Once again the slides were rinsed with running tap water, then PBS for 5 minutes each. For blocking, 2.5% horse serum was utilized, and the slides were incubated for 30 minutes at

room temperature in a humidified chamber. After 30 minutes, the 2.5% horse serum was drained onto a paper towel. The slides were then incubated with p38 (P38 MAPK (Tyr323) Rabbit polyclonal, BS5477R, Cedarlane Laboratories, Burlington, ON) at a 1/200 dilution, which was determined by preliminary titrations. Incubation then took place overnight.

The following day, the slides were rinsed with PBS for five minutes on the shaker then incubated with Rabbit ImmPres kit (horse-radish peroxidase micro-polymer solution)(Vectastain Elite ABC- Peroxidase kit, rabbit, VECTPK6101 MJS Biolynx, Inc.) for 30 minutes at room temperature. They were rinsed twice for five minutes with PBS on the shaker. While the samples were rinsing, DAB was prepared as follows: two drops of buffer, with four drops of DAB and two drops of H<sub>2</sub>O<sub>2</sub> were added to 5ml of dH<sub>2</sub>O, in that order. The solution was placed on the vortex between each addition. Then one to two drops of DAB are added to each slide, and then incubated for 10 minutes. The DAB was then rinsed with water into the waste container.

Harris Hematoxylin counterstaining was then completed, with the slides staining for one minute, before being rinsed with running tap water. Slides were dipped 1-2 times in Acid Alcohol (1% Hydrochloric Acid in 70% Alcohol), then rinsed again with running tap water. Slides were then blued in 2% ammonium alcohol and rinsed in running tap water.

The process continued with the following reagents: 70% alcohol for one minute, 95% alcohol for one minute two times, absolute alcohol for two minutes then one minute, then xylene for five minutes and 3 minutes. Cover slips were then placed with Cytoseal® permount in the fume hood.

### 3.5.2 ERK 1/2: immunohistochemistry protocol

Tissue sections were initially immersed in xylene solution twice, for five then three minutes. Absolute alcohol was next for two minutes then 95% alcohol for two minutes then one minute, then 70% alcohol for one minute. They were then placed in water for two minutes.

To quench the slides, they were placed in fresh 3% hydrogen peroxide in methanol for five minutes (20 ml 30% H<sub>2</sub>O<sub>2</sub> and 180 ml Methanol). Once this step was complete, distilled water was used to rinse the slides for five minutes, and then PBS was further utilized for another five minute wash on the shaker.

For the ERK1/2 protocol, antigen retrieval was not necessary. The tissue was blocked with 2.5% horse serum for 30 minutes at room temperature. The blocking serum was then drained. There was no PBS rinse. The slides were then incubated with ERK 1/2 (ERK1+ERK2 (T185+Y187+T202+Y204) Rabbit polyclonal, BS5469R, Cedarlane Laboratories, Burlington, ON) at a 1/400 dilution. This dilution was determined with preliminary titrations. The slides were incubated at 4°C overnight in a humidified chamber.

The following morning the slides were rinsed with PBS for five minutes on the shaker. Once complete, they were incubated at room temperature for 30 minutes with the Rabbit Impress kit (horse-radish peroxidase micro-polymer solution). Again, the slides were rinsed on the shaker with PBS for five minutes. While the samples were rinsing, DAB was prepared as follows: two drops of buffer, with four drops of DAB and two drops of H<sub>2</sub>O<sub>2</sub> were added to 5ml of dH<sub>2</sub>O, in that order. The solution was placed on the vortex

between each addition. Then one to two drops of DAB are added to each slide, and then incubated for 10 minutes. The DAB was then rinsed with water into the waste container.

Harris Hematoxylin counterstaining was then completed, with the slides staining for one minute, before being rinsed with running tap water. Slides were dipped 1-2 times in Acid Alcohol (1% Hydrochloric Acid in 70% Alcohol), then rinsed again with running tap water. The sections were blues in 2% ammonium alcohol and rinsed with running tap water.

The process continued with the following reagents: 70% alcohol for one minute, 95% alcohol for one minute two times, absolute alcohol for two minutes then one minute, then xylene for five minutes and 3 minutes. Cover slips were then placed with Cytoseal® permount in the fume hood.

### **3.5.3 JNK: immunohistochemistry protocol**

Tissue sections were initially immersed in xylene solution twice, for five then three minutes. Absolute alcohol was next for two minutes then 95% alcohol for two minutes then one minute, then 70% alcohol for one minute. They were then placed in water for two minutes. The slides were placed in a humidified chamber and rinsed with TBS-T for 5 minutes. For blocking, 2.5% horse serum (made in TBS) was utilized, and the slides were incubated for 30 minutes at room temperature. The blocking serum was then drained onto a paper towel, no rinsing, and then incubated with JNK (Phospho-SAPK/JNK (Thr183/Tyr185) (81E11) Rabbit mAb, 46685, New England Biolabs, Whitby, ON) at 4°C overnight in a humidified chamber.

The following morning, the slides were rinsed with TBS-T for five minutes on the shaker, then quenched for five minutes using a solution of 9ml TBS, and 1ml H<sub>2</sub>O<sub>2</sub>. The secondary rabbit biotinylated antibody (Vectastain elite ABC- Peroxidase kit, rabbit IgG as VECTPK6101 MJS Biolynx Inc) was prepared to a dilution of 1/200 in 2.5% horse serum, then slides were incubated for 30 minutes at room temperature. After this, sections were rinsed twice with TBS-T for five minutes each time, on the shaker. The tissue was then incubated with ABC reagent for 30 minutes at room temperature. Again, this was rinsed twice with TBS-T on the shaker for five minutes. While the samples were rinsing, DAB was prepared as follows: two drops of buffer, with four drops of DAB and two drops of H<sub>2</sub>O<sub>2</sub> were added to 5ml of dH<sub>2</sub>O, in that order. The solution was placed on the vortex between each addition. Then one to two drops of DAB are added to each slide, and then incubated for 10 minutes. The DAB was then rinsed with water into the waste container.

Harris Hematoxylin counterstaining was then completed, with the slides staining for one minute, before being rinsed with running tap water. Slides were dipped 1-2 times in Acid Alcohol (1% Hydrochloric Acid in 70% Alcohol), then rinsed again with running tap water. Slides were blued in 2% Ammonium Alcohol.

The process continued with the following reagents: 70% alcohol for one minute, 95% alcohol for one minute two times, absolute alcohol for two minutes then one minute, then xylene for five minutes and 3 minutes. Cover slips were then placed with Cytoseal® permount in the fume hood.

#### **3.5.4 Microscopic evaluation of MAPK stained tissue**

The immunohistochemistry was analyzed manually via microscopy. Quantitatively, the scoring was based on both intensity, 0-3, and percentage of cells stained, 0-5. The sum of this number was then tabulated and a score out of 8 was calculated, just as it was for the S100A7 staining. The scoring scale is represented in Tables 3.3 and 3.4. When evaluating the slides, the epithelium was scanned and then scored based on a representative portion of the tissue. The intensity score was based on stained visualized average of the lightness or darkness of staining using the OSCC positive control as a reference, while the percent of cells stained was determined by estimating the number of cells stained in the entire epithelial layer.

Epithelial layers were also assessed for the location of the staining. The epithelium was divided into Corneal, Granular, Spinous, Parabasal and Basal layers. The presence of staining and the relative amount of staining within each layer was recorded, as was the presence of stain within the nucleus or cytoplasm.

The assessment was conducted by a histopathologist and the graduate student author. Calibration was carried out prior to scoring when random tissue samples were selected and consensus was reached. Once all tissue samples were evaluated and scored, ten random samples were evaluated by both evaluators to confirm that calibration was maintained. Differences on the intensity and percentage scores of greater than 1, were discussed and consensus was determined.

### 3.6 Statistical methods

Statistical analysis was carried out using SPSS® (IBM®, Armonk, NY, USA) with the level of significance being set at  $P \leq 0.05$ . For initial assessment of each of the grading and assessment methods, an ANOVA was used to establish if a statistically significant difference existed between the populations. To further characterize differences between populations, a Tukey Multiple comparison was performed for each of the grading and assessment methods. This allowed for more specific data, identifying between which populations differences existed, and whether these were statistically significant for each of the assessment methods.

For correlational information, Pearson Correlation Coefficients were calculated.

Information gathered allowed for identification of correlational relationships between grading and assessment methods for each of the study populations. Statistical analysis was carried out twice: One set of data was from all populations and assessment methods excluding QuPath. The second statistical assessment included a subset of each of the populations, 10 tissue samples from each of the groups, and included QuPath assessment. This was set as a pilot study to assess the feasibility of QuPath S00A7 assessment and determine if a more accurate S100A7 score can be obtained to improve its utility in differentiating the populations.

## CHAPTER 4: RESULTS

### 4.1 Results

#### 4.1.1 Patient Demographics

One hundred and eight tissue samples were selected for the study: 25 within the Hyperkeratosis/Control (Control) group, 35 within the Non-progressing Dysplasia (Non-progressing) group, and 48 from the Progressing to OSCC (Progressing) group. The age at initial biopsy for each of the groups ranged from: 15-72 years (avg. 50.4 years) for the Control group; 31-74 years (avg. 55.4 years) for the Non-progressing group, and 40-86 years (avg. 62.2 years) for the Progressing group was (Figure 4.1).

In the Control group, there were 13 males and 12 females. The average age was 46.9 for males, and 54.1 for females. Within the Non-progressing group, there were 18 males and 17 females. The average age was 57.4 years for males and 50.6 years for females. In the Progressing group there were 25 males, and 23 females with average ages 61.0 years for males and 63.3 years for females. (Tables 4.1 - 4.3).

**Figure 4.1: Average age of patients at initial biopsy from each of the three study populations: Control, Non-progressing, and Progressing**

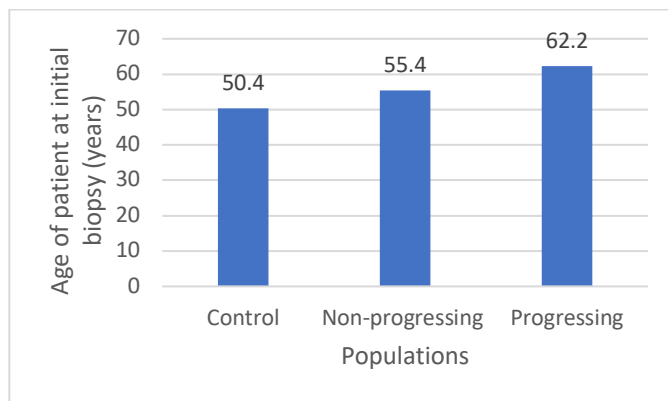


**Table 4.1: Control population gender and average age at first biopsy**

Gender	Count (%)	Average age in years
Male	13 (52)	46.9
Female	12 (48)	54.1

**Table 4.2: Non-progressing dysplasia population gender and average age at first biopsy**

Gender	Count (%)	Average age in years
Male	18 (51)	57.4
Female	17 (49)	50.6

**Table 4.3: Progressing population gender and average age in years at first biopsy**

Gender	Count (%)	Average age in years
Male	25 (52)	61.0
Female	23 (48)	63.3

Other demographic information collected included tobacco and alcohol use. Many of the clinical information forms and biopsy reports made no mention of either of these two risk factors. For the Control group, 10/25 had known tobacco histories, with 7/10 having used tobacco while three had not. Alcohol consumption was not recorded on the clinical information forms for any of the control group. For the Non-progressing group, 23/35 biopsy reports included the patient tobacco history. 21/23 used tobacco, while two did not. 5/35 patients had known alcohol statuses with 4/5 having a history of alcohol consumption, and one reporting no use. In the Progressing group, 15/48 biopsy reports had information regarding tobacco with 12/15 reporting positive histories of tobacco use, while three reported no tobacco use. Only 2/48 alcohol histories were known, with both consuming alcohol. Given the significant deficiency in data with respect to tobacco and

alcohol status, there was insufficient data to complete further statistical analysis, though of known cases, it would appear that tobacco and alcohol use contribute to lesions which result in biopsy.

#### **4.1.2 Lesion Location**

The most common sites involved were the lateral tongue, ventral tongue and floor of mouth (FOM). 16 lateral tongue lesions, and 12 ventral tongue/FOM lesions progressed to OSCC. Lesion located on the buccal mucosa and lip were most prevalent in the Progressing group with six of each while the Non-progressing and Control groups did not have any biopsies from these sites. The dorsal tongue was the least biopsied site from the oral cavity, with one biopsy demonstrating hyperkeratosis. A breakdown of all lesion locations is present in Table 4.4.

**Table 4.4: Location of lesion within the oral cavity for each of the three study populations**

Location	Control		Non- progressing		Progressing	
	n	%	n	%	n	%
Ventral tongue/FOM	5	20	17	49	12	25
Lateral tongue	11	44	11	31	16	33
Soft palate	1	4	5	14	2	4
Hard palate	2	8	0	0	2	4
Gingiva	2	8	1	3	4	8
Retromolar trigone	3	12	1	3	0	0
Dorsal tongue	1	4	0	0	0	0
Buccal Mucosa	0	0	0	0	6	13
Lip	0	0	0	0	6	13
Total	25	100	35	100	48	100

#### 4.1.3 Diagnosis

The diagnosis for each of the initial biopsies is presented in tables 4.5-4.9. The Non-Progressing and Progressing groups included not only dysplasia, but squamous architectural atypia, hyperkeratosis, actinic cheilitis, lichenoid mucositis, verrucous hyperplasia, hyperplastic candidiasis, and traumatic ulcerative granuloma with stromal eosinophilia (TUGSE). For each of the initial biopsies with dysplasia the 3-tier diagnosis as well as the 2-tier diagnosis were recorded.

**Table 4.5: Control group diagnoses**

Diagnosis	Cases (%)
Hyperkeratosis	25 (100%)

**Table 4.6: Non-progressing group diagnoses including the 3-tier dysplasia diagnosis**

Diagnosis	Cases (%)
Hyperkeratosis	4 (11%)
Mild	23 (66%)
Moderate	8 (23%)
Severe	0 (0%)
Total	35 (100%)

The 3-tier diagnoses of the Non-progressing population is present in Table 6. The dominant diagnosis within this group is mild, representing 66% of the initial biopsies.

**Table 4.7: 2-tier diagnoses for the Non-progressing group**

Diagnosis	Cases (%)
Low	27 (77%)
High	8 (23%)
Total	35 (100%)

The 2-tier diagnoses of the Non-progressing group is presented in table 7. Low grade dysplasia was the dominant diagnosis with 77% of all cases.

**Table 4.8: Progressing group diagnoses including the 3-tier dysplasia diagnosis**

Diagnosis	Cases (%)
Atypia/Hyperkeratosis	8 (17%)
Mild	11 (23%)
Moderate	13 (27%)
Severe	5 (10%)
Actinic cheilitis	3 (6%)
Other	8 (17%)
Total	48 (100%)

Table 4.8 contains the 3-tier diagnoses for the sample population Progressing to OSCC. “Other” diagnoses included lichenoid mucositis, verrucous hyperplasia, hyperplastic candidiasis and traumatic ulcerative granuloma with stromal eosinophilia (TUGSE). The most common diagnosis was moderate dysplasia, (27%) followed by mild (23%).

**Table 4.9: Progressing group diagnoses including the 2-tier dysplasia diagnosis**

Diagnosis	Cases (%)
Low grade	10 (21%)
High Grade	33 (69%)
Other	5 (10%)
Total	48 (100%)

When each initial biopsy for the Progressing to OSCC group was graded utilizing the 2-tier system, 33 (69%) of the tissue samples were considered high grade dysplasia. Low grade lesions were diagnosed in 10 (21%) cases (table 4.9). Five of the lesions including those with squamous or architectural atypia and TUGSE were considered dysplastic when applying the 2-tier grading criteria. Lichenoid mucositis, hyperplastic candidiasis, granulation tissue and actinic cheilitis were present in five cases and were classified as such after 2-tier grading (table 4.9: Other).

## **4.2 Immunohistochemistry**

Tissue staining from each of the sample populations is presented in the following figures (4.2- 4.4). For each of the tissue samples presented, the 3-tier, 2-tier, S100A7 manual score, Straticyte™ assessment and QuPath assessment was completed.

### **4.2.1 S100A7 qualitative evaluation of staining**

Immunoreactivity for S100A7 was present in both the cytoplasm and nucleus, though it was more prominent within the cytoplasm. Within the three study populations, staining varied from minimum intensity to heavy. Staining was present in the more superficial layers of the tissue with the basal layer often spared. Stain trapped within the outer keratin layer did occur relatively frequently, interpreted to represent artifact

#### 4.2.2 Control group

**Figure 4.2: Case 6: Hyperkeratosis, from gingiva. A) H&E stain (x100 magnification), B) S100A7 Stain (x100 magnification), C) QuPath total epithelial area, D) QuPath S100A7 total area, E) Straticyte™ ROI analysis, F) Straticyte™.**

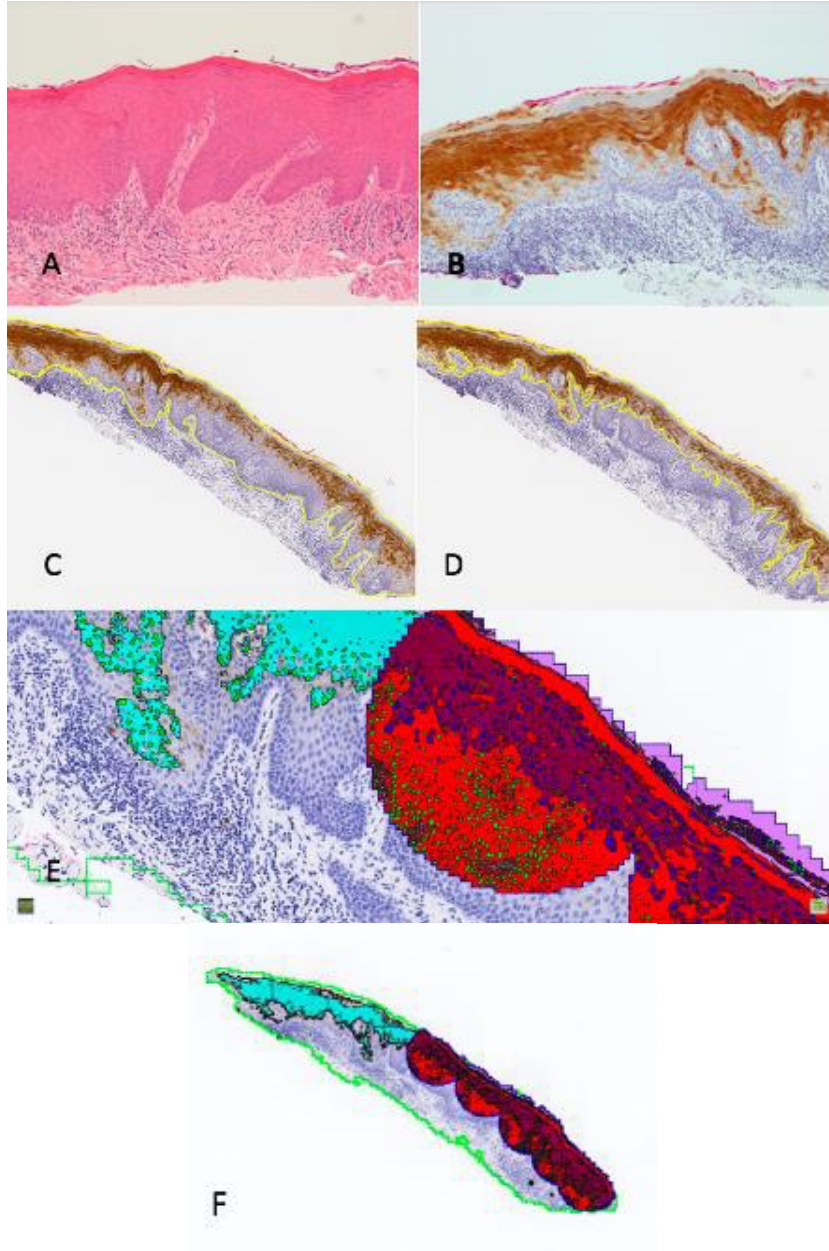
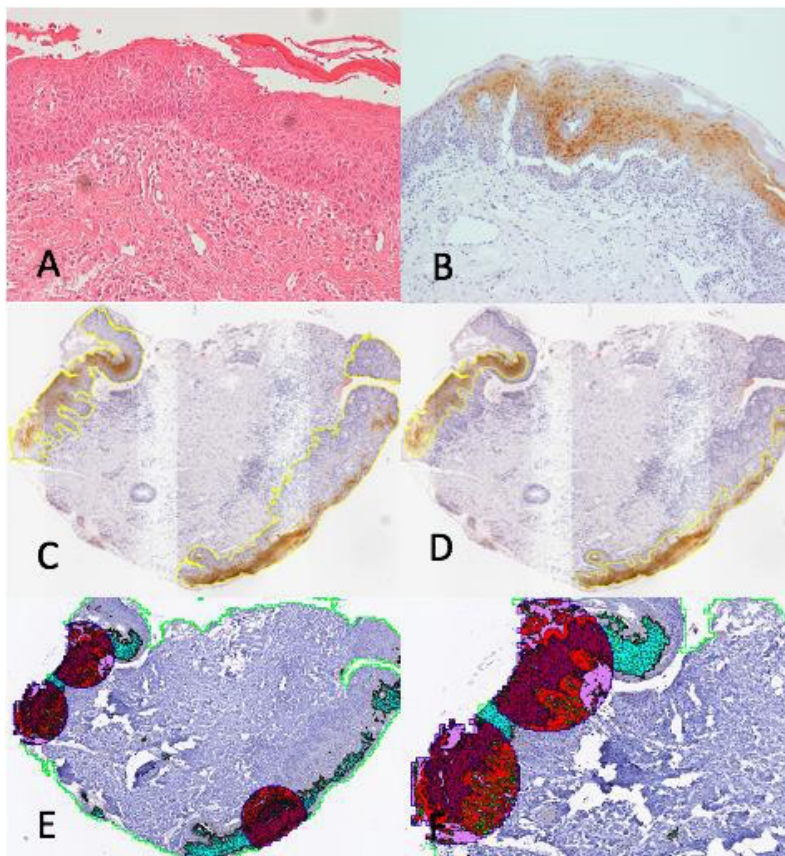


Figure 4.2 shows tissue from the control group, collected from gingiva. The diagnosis was determined based on the H&E slide, with an obvious band of orthokeratin overlying the epithelium (Figure 4.2A). The S100A7 staining is represented in figure 4.2B, and in

this specimen, the manual score was 7 with an intensity score of 3, and a proportion score of 4 which equates to 61-80 percent of cells stained. It can be seen that the S100A7 staining appears to be confined to the upper layers of the mucosa, with only incidental staining within the keratin layer, and no staining in the basal or parabasal layers. Nuclear and cytoplasmic staining can be appreciated. The QuPath staining is depicted in figure 4.2C demonstrating total epithelial area, and figure 4.2D demonstrating total S100A7 area. The Overall QuPath Score was 7 with an intensity score of 3, and a proportion score of 4, matching that of the Manual Score. Figure 4.2F shows the Straticyte™ analysis of the tissue with figure 4.2E providing an enhanced magnification view of a ROI. For this tissue sample, the Straticyte™ Risk was medium, with a 5-year malignant transformation risk of 31%.

### 4.2.3 Non-progressing dysplasia

**Figure 4.3: Case 9: Moderate/High grade dysplasia, from soft palate. A) H&E stain (x100 magnification), B) S100A7 stain (x100 magnification), C) QuPath total epithelial area D) QuPath total S100A7 area E) Straticyte™ analysis, F) Straticyte™ ROI analysis.**

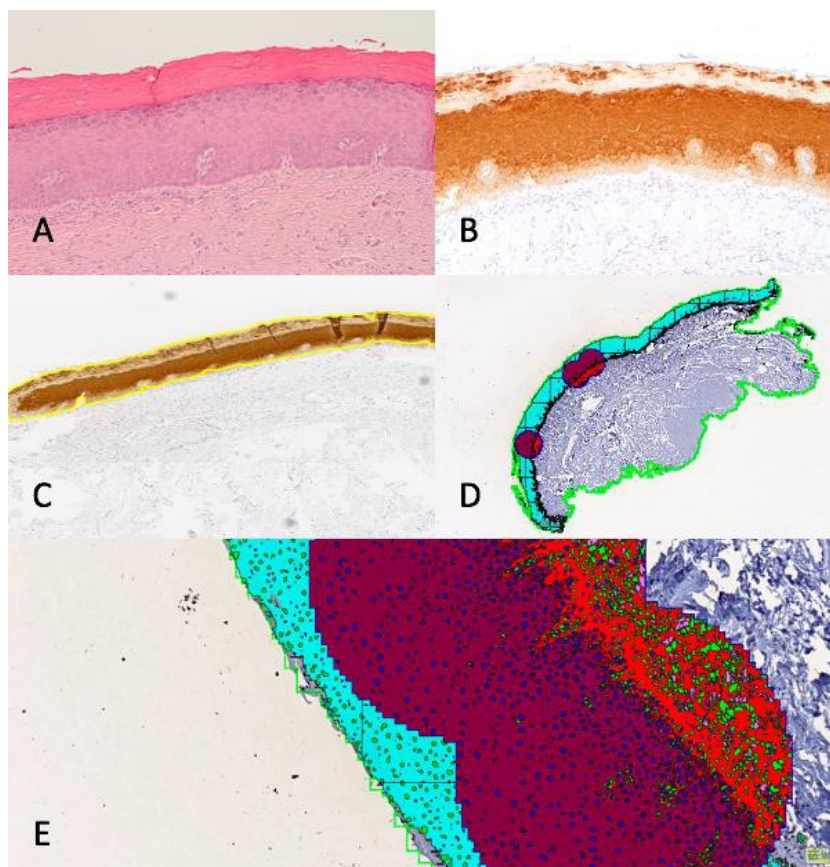


The tissue shown in figure 4.3 is from the soft palate. The initial 3-tier diagnosis was moderate dysplasia with a 2-tier diagnosis of high-grade dysplasia from the H&E stain (Figure 4.3A). S100A7 staining is shown in figure 4.3B. The staining spares the basal and parabasal areas, and both nuclear and cytoplasmic staining are depicted. The manual score for this specimen was 4, with an intensity score of 2 and a proportion score of 2. When QuPath was used to assess the tissue sample the proportion score was based on the total area (Figure 4.3C) and S100A7 area (Figure 4.3D) and was determined to be 1, with

an intensity score of 2 resulting in a QuPath Score of 3. Straticyte™ analysis is shown in figure 4.3E and F with a risk score of medium, and a 5-year malignant transformation risk of 45%.

#### 4.2.4 Progressing to OSCC

**Figure 4.4: Case 4: Mild/Low grade dysplasia, from lateral tongue. A) H&E stain (x100 magnification), B) S100A7 stain (x100 magnification), C) QuPath total epithelial and S100A7 area, D) Straticyte™ analysis, E) Straticyte™ ROI analysis**



The tissue sample in figure 4.4 is mild dysplasia from the lateral tongue. The 2-tier diagnosis was low grade dysplasia (Figure 4.4A). The S100A7 manual score was the maximum score of 8, (based on an intensity score of 3, and a proportion score of 5) (Figure 4.4B). The QuPath™ score was 8 given that the total area of the S100A7 is equal to that of the epithelium (Figure 4.4C). Incidental staining of the orthokeratin layer is

present while there does appear to be faint staining on the basal layer. All other layers of the tissue were evenly stained. Cytoplasmic and nuclear S100A7 staining was present. The Straticyte™ analysis in figure 4.4D and E also demonstrate significant S100A7 staining both inside and outside of the ROI. In this case, the Straticyte™ Risk was high with a 5-year malignant transformation risk calculated to be 69%. Malignant transformation occurred 13 years later.

### **4.3 S100A7 staining**

Results for S100A7 manual scoring are presented in a dot plot (Figure 4.5), and the bar graph represented by figure 4.6 and 4.7. Results for Straticyte™ and the associated risk predictions are presented in tables 4.10-4.12 as well as figures 4.8-4.10. In addition, the QuPath area calculations are provided to demonstrate the capability of QuPath for allowing the user to obtain very specific measurements (Tables 4.13-4.15)(Figures 4.11-4.12). QuPath scores (Figures 4.13-4.15) are present for each of the tissue samples selected. The QuPath score is an intensity and proportion score similar to that of the S100A7 manual score, however, QuPath is utilized to obtain the proportion score. The S100A7 manual scores for the subpopulation of QuPath sampled tissue has also been presented to demonstrate the difference between the two (Figures 4.16 -4.18).

#### **4.3.1 S100A7 manual score assessment**

The dot plot for the S100A7 manual scoring for each of the populations is present in figure 4.5. The range was from 2-8 for each of the groups, though there is a general trend toward greater total scores in the Progressing to OSCC group. The median score for the Progressing, Non-progressing and Control groups were 6, 5 and 4 respectively. Average manual scores were calculated, and the Progressing population had the highest average

S100A7 manual score. The average S100A7 manual score for both the Non-progressing dysplasia and Progressing dysplasia groups was greater than the Control group (Figure 4.6). Median scores were also calculated which were also greatest in the Progressing group (Figure 4.7)

**Figure 4.5: Dot plot for S100A7 manual scores for each of the three populations**

S100A7 Manual Score	Controls	Non-progressing	Progressing
8	•	••••	••••••••
7	••	•••••	••••••••
6	••	•••••	••••••••
5	••	••••••	••••••
4	••••••	••••••	•••••
3	•••••	•••••	•••••
2	•••••	•	••••
1			
0			

**Figure 4.6 Average S100A7 manual score for all three populations calculated from the intensity and proportion scores**

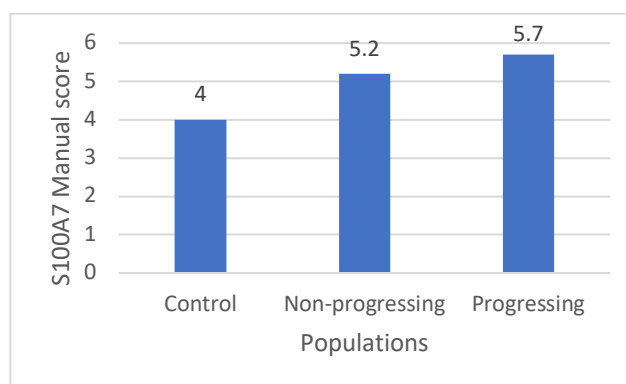
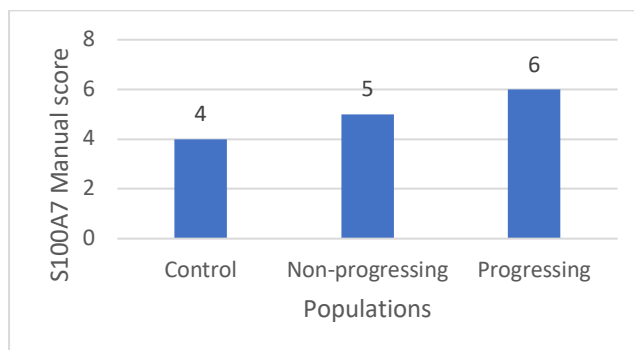


**Figure 4.7: Median S100A7 manual scores for the Control, Non-progressing and Progressing populations calculated from the intensity and proportion score**



#### 4.3.2 Straticyte: S100A7 risk score

The S100A7 staining of the Control group was evaluated utilizing the Straticyte™ test. Eighteen (18) of the 25 samples were considered medium risk, which was the most frequent risk stratification in this population. One of the tissue samples was considered high risk. (Table 4.10)

**Table 4.10: Straticyte™ 5-year risk for malignant transformation: Control group case numbers**

Risk	Count
Low	6
Medium	18
High	1
Total	25

The Straticyte™ score for the initial biopsies for the Non-progressing group were considered medium risk in 27 of 35 cases, were low risk in 7 and high risk in 1 case. (Table 4.11). Of the seven low risk group of tissue samples, one was moderate dysplasia, while six were mild dysplasia. All seven were low grade in the 2-tier grading system. For the 27 tissue samples that were considered medium risk by Straticyte™, seven were moderate dysplasia, 16 were mild dysplasia, and four were hyperkeratosis. With respect

to the 2-tier grading system, eight were high grade, and 19 were low grade. The lone high risk tissue sample was mild dysplasia, and considered low grade in the 2-tier system.

**Table 4.11: Straticyte™ 5-year risk for malignant transformation: Non-progressing group case numbers**

Risk	Count
Low	7
Medium	27
High	1
Total	35

S100A7 staining for the Progressing to OSCC group was evaluated with Straticyte™. Twenty-two (22) cases were medium risk, and 22 were high risk. None of the tissue samples were low risk (Table 4.12). If tissue folds were present in the samples, the Straticyte™ test could not be applied, and was recorded as “unable to assess”, occurring in four cases. In the high risk tissue samples, five cases were mild dysplasia, five were moderate, four were severe, five were hyperkeratosis/architectural atypia, two were verrucous hyperplasia, and one was hyperplastic candidiasis. In the 2-tier system, five were low grade, 16 were high grade, and one was considered not dysplastic with a diagnosis of hyperplastic candidiasis. The Straticyte™ medium risk samples were found to have five mild dysplasia, eight moderate, one severe, one TUGSE, one actinic cheilitis, three hyperkeratosis, two lichenoid mucositis, and one verrucous hyperplasia. When evaluated with the 2-tier system, five were low grade, 15 were high grade, and two were not considered dysplastic and maintained the diagnosis of lichenoid mucocitis.

**Table 4.12: Straticyte™ 5-year risk for malignant transformation: Progressing group case numbers**

Risk	Count
Low	0
Medium	22
High	22
Unable to assess*	4
Total 48	

“Unable to assess” tissue samples that had a tissue fold or “bad sections” which prevented the Straticyte™ assessment.

**Figure 4.8.: Dot plot for calculated Straticyte™ 5 year risk score for each of the three populations**

5 year transformation risk (%)	Control	Non-progressing	Progressing
100			
90			
80			....
70		.	.....
60	.	.	.....
50	...	.....	.....
40	....	.....	..
30	....	.....	.
20	.....	.....	.....
10	....	.....	
0	.		

The dot plot (Figure 4.8) shows the Straticyte™ risk percentage in the study populations. This demonstrates a trend of increasing risk from Controls, to Non-Progressing, to Progressing, with more of the tissue samples falling in the 50-80% range in the Progressing group as compared to the other two populations. The range for the Controls group is from <10 to 60%. The Non-progressing population had a majority of tissue samples within the 10% to 50% range. The range for the tissue samples is from 20% to 80% for the Progressing group, the majority are within 50%-80%. Averages for each

population are present in figure 4.9, and are 31, 37 and 58.7 for the Control, Non-progressing and Progressing groups respectively. The median scores are 30, 39 and 63 respectively (Figure 4.10). These parameters demonstrate a significant difference between the Progressing group and the other two populations.

**Figure 4.9: Average Straticyte™ 5 year risk score for malignant transformation**

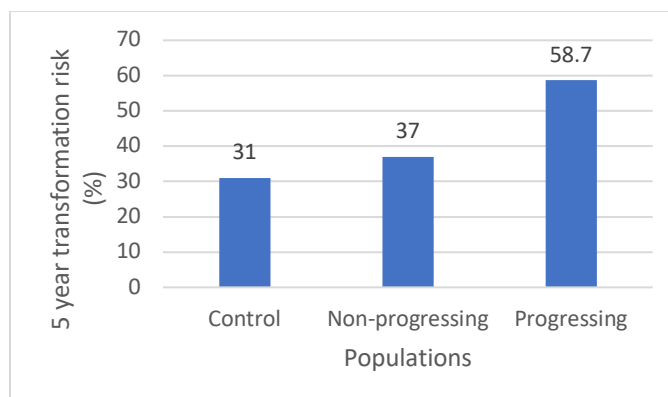
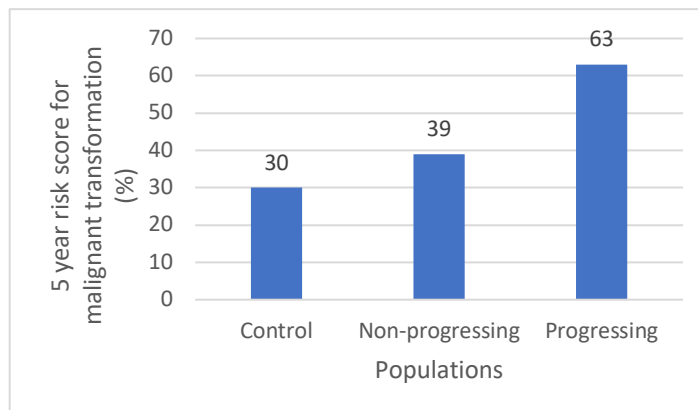


**Figure 4.10: Median Straticyte™ 5 year risk score for malignant transformation**



### 4.3.3 QuPath Assessment of S100A7 staining

Data collected from QuPath include the area of the epithelium, the area of the epithelium stained by S100A7, percent area stained, and finally a conversion of the QuPath staining into an intensity and proportion score to compare to the S100A7 manual score. The area scores for the percentage of area stained calculation are included in tables 4.13 - 4.15.

The data provided in tables 4.13-4.15 is summarized in figures 4.11 and 4.12, with average and median data provided. In these figures we can see that the average area stained is greatest for the progressing group, as is the median percent area stained.

**Table 4.13: Raw score for QuPath assessed epithelial area, S100A7 staining, and percent of epithelium stained in a sub-population of Control tissue samples**

<b>Control</b>			
<b>Case</b>	<b>Total Area (µm<sup>2</sup>)</b>	<b>Stained Area (µm<sup>2</sup>)</b>	<b>Percent stained (%)</b>
<b>1</b>	1632434	1021469	63
<b>2</b>	2937956	897673	31
<b>3</b>	2837717	747630	26
<b>4</b>	6697758	505108	8
<b>5</b>	8239414	8194281	99
<b>6</b>	1573195	962391	61
<b>7</b>	2336883	1246154	53
<b>8</b>	788825	119235	15
<b>9</b>	2623383	293613	11
<b>10</b>	3700602	1073271	29

**Table 4.14: Raw score for QuPath assessed epithelial area, S100A7 staining, and percent of epithelium stained in a sub-population of the Non-progressing tissue samples**

<b>Non-progressing</b>			
<b>Case</b>	<b>Total Area (µm<sup>2</sup>)</b>	<b>Stained Area (µm<sup>2</sup>)</b>	<b>Percent stained (%)</b>
<b>6</b>	4142317	1031980	25
<b>7</b>	2022647	711778	35
<b>9</b>	2280948	971485	43
<b>10</b>	1269091	531520	42
<b>11</b>	3200509	1216982	38
<b>15</b>	7899666	6608	0.1
<b>16</b>	5117732	3947291	77
<b>17</b>	1857471	766041	41
<b>19</b>	2428462	978897	40
<b>23</b>	2634814	795521	30

**Table 4.15: Raw score for QuPath assessed epithelial area, S100A7 staining, and percent of epithelium stained in a sub-population of the Progressing tissue samples**

Progressing			
Case	Total Area ( $\mu\text{m}^2$ )	Stained Area ( $\mu\text{m}^2$ )	Percent stained (%)
2	5587778	4520511	81
4	2444675	2444675	100
5	Tissue folds		
6	11798099	8117504	69
7	1894655	1022796	54
12	1507748	1000659	66
14	549117	339161	62
16	11845915	7284297	61
17	4461147	1987904	45
18	5394605	2295742	43

**Figure 4.11: Average percent of epithelial area stained with S100A7 when assessed with QuPath**

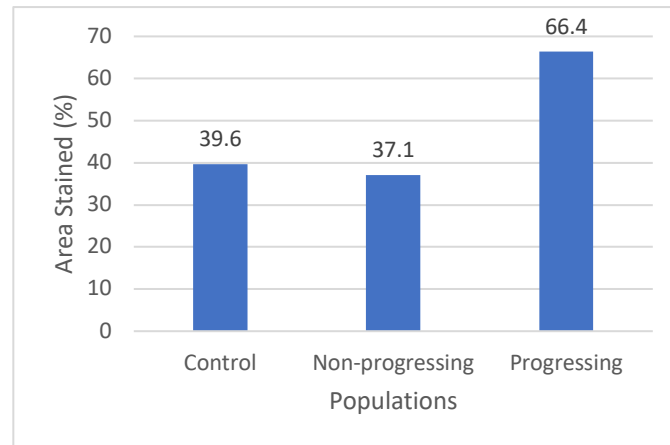


**Figure 4.12: Median percent of epithelial area stained with S100A7 when assessed with QuPath**

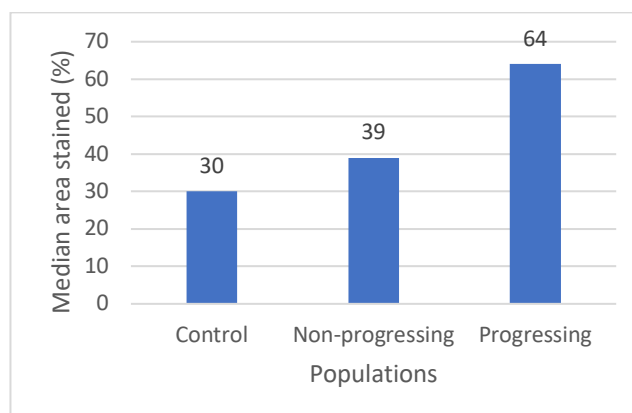


Figure 4.13 shows the scores for QuPath analysis for a subset of 10 cases from each of the populations, when the data is converted to an intensity and proportion score. Figure 4.16 displays the S100A7 manual scores from the same subpopulation of tissue samples. In general, the range of scores is reduced within the Progressing population when QuPath was used for score. The average QuPath scores for the QuPath assessed populations is 4.2, 5.2, 6.6 (Figure 4.14), and the S100A7 manual score average is 4.3, 5.6, 4.9 (Figure 4.17). The median QuPath (Figure 4.15) score for the Control, Non-progressing and Progressing groups were 3.5, 6, and 6.5, respectively, as compared to medians of 3.5, 5 and 5 respectively for the S100A7 manual score (Figure 4.18).

When QuPath was used to assess the tissue, the average and median intensity and proportion scores are highest for the Progressing group (Figures 4.13 - 4.18). As the cases selected were a small sub-sample of each of the populations, the average S100A7 manual score was actually higher for the Non-progressing population compared to the Progressing group (Figure 4.17)

**Figure 4.13: Dot Plot for the subpopulation QuPath S100A7 intensity and proportion scores for each of the three populations**

QuPath intensity and proportion score	Control	Non-progressing	Progressing
8	•		••
7	•	••	•••
6		••••	••••
5	•		•
4	••	•••	
3	••••		
2	•	•	
1			
0			

**Figure 4.14: Average intensity and proportion score for subpopulation of QuPath assessed tissue samples when S100A7 area staining is assessed with QuPath**

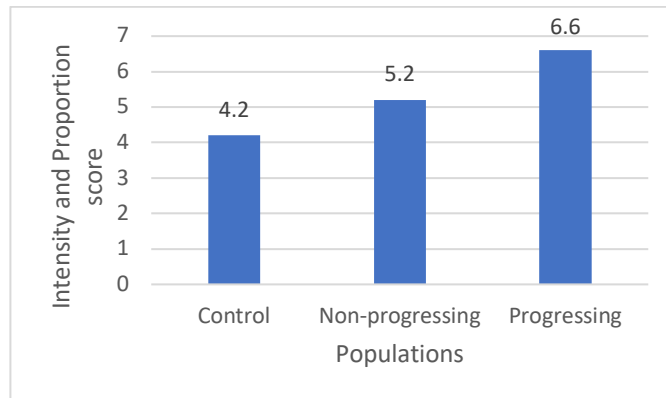


**Figure 4.15: Median intensity and proportion score for the subpopulation of QuPath assessed tissue samples when S100A7 area staining is assessed with QuPath.**

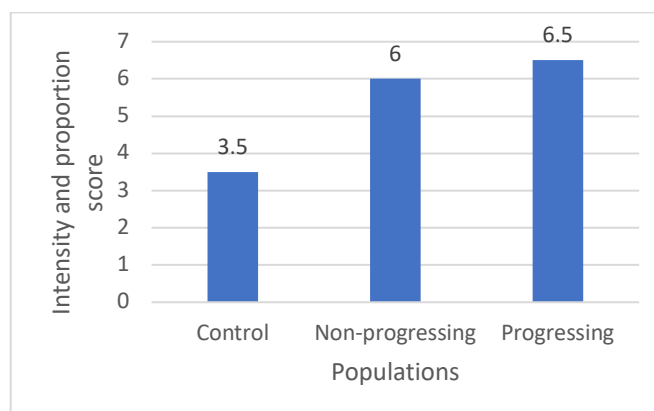


**Figure 4.16: Dot Plot for S100A7 manual scores for the subpopulation of the tissue samples that underwent QuPath assessment**

S100A7 Manual Score	Control	Non-progressing	Progressing
8	•	••	•
7	•	•	•
6	•	•	••
5		•••	••
4	••	••	•
3	••••		••
2	•		•
1			
0			

**Figure 4.17: Average S100A7 manual score for the subpopulation of QuPath assessed tissue samples**

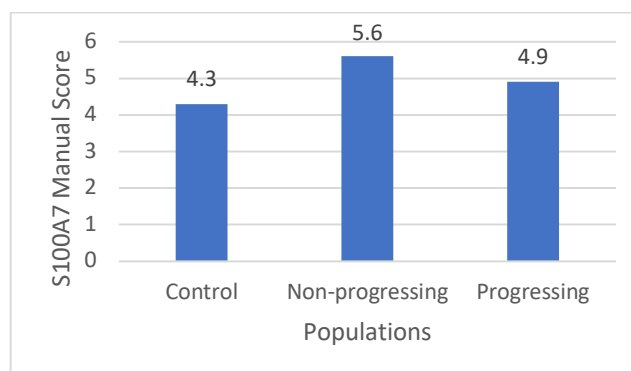
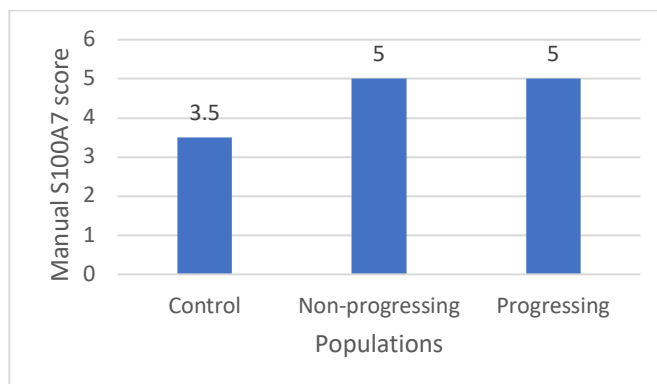


**Figure 4.18: Median S100A7 manual score for the subpopulation of QuPath assessed tissue samples**



#### **4.4 MAPK Activated Phosphorylation Staining**

Figures 4.19 - 4.27 demonstrates immunohistochemical staining of phosphorylated MAPK pathway signaling proteins Erk1/2, p38, and JNK in the tissue samples. These assays are interpreted to have failed, with diffuse, non-specific and extensive background staining occurring in the tissue specimens. Staining for Erk1/2 shows cytoplasmic staining with relative sparing of the nucleus and membrane (Figures 4.19 - 4.21). p38 staining also shows staining of the cytoplasm with nuclear sparing and sparing of the cell membrane (Figures 4.22 - 4.24). Within the cytoplasm, the staining was uniform with very little variation for both proteins. The JNK reagent was interpreted to have failed, as no nuclear staining was apparent in known positive control tissue (Figures 4.25 - 4.27), despite the use of several new antibody batches. As with the Erk1/2 and the p38, the staining appears relatively even within the cytoplasm, sparing the nucleus and the cell membrane.

**Figure 4.19: Erk1/2 Staining, Control group – Case 2 magnification (A) x100, (B) x400**

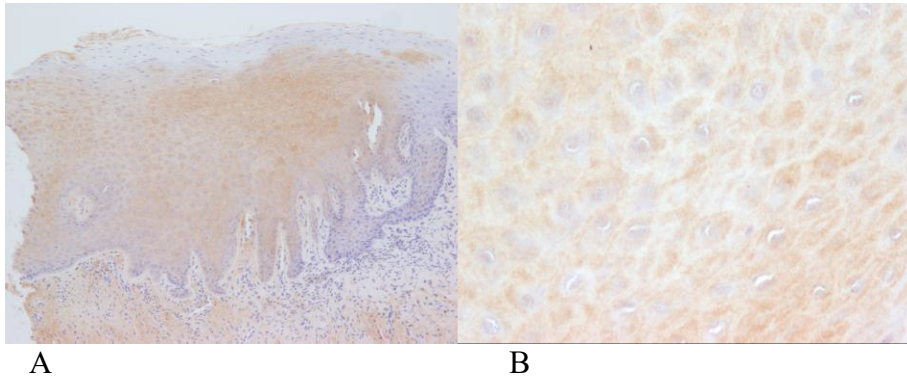


**Figure 4.20: Erk1/2 Staining, Non-progressing group – Case 26 magnification (A) x100, (B) x400**

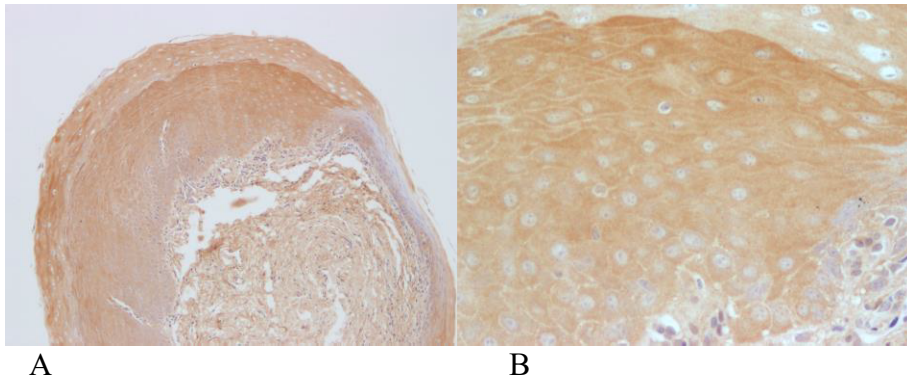


**Figure 4.21: Erk1/2 Staining, Progressing group – Case 4 magnification (A) x100, (B) x400**

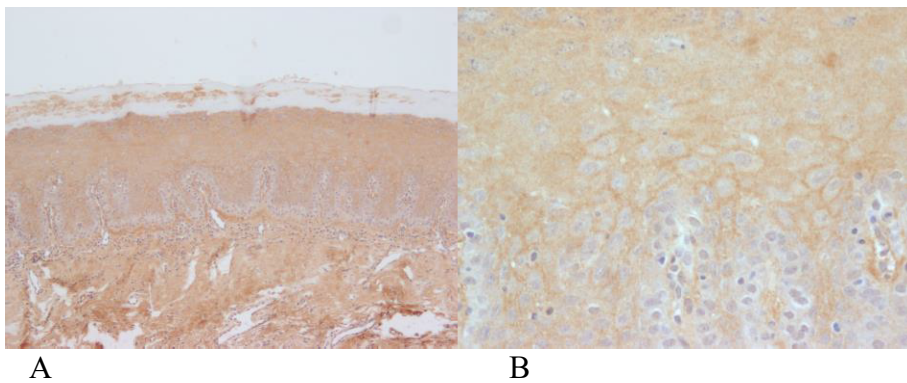


**Figure 4.22: p38 Staining, Control group – Case 2 magnification (A) x100, (B) x400**

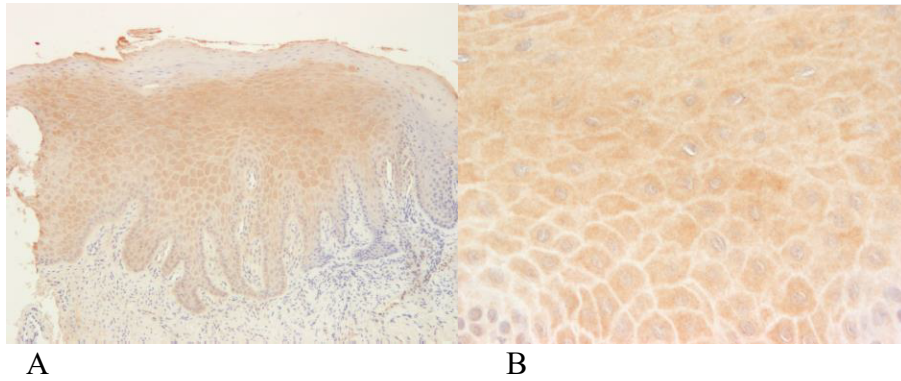


**Figure 4.23: p38 Staining, Non-progressing group – Case 26 magnification (A) x100, (B) x400**

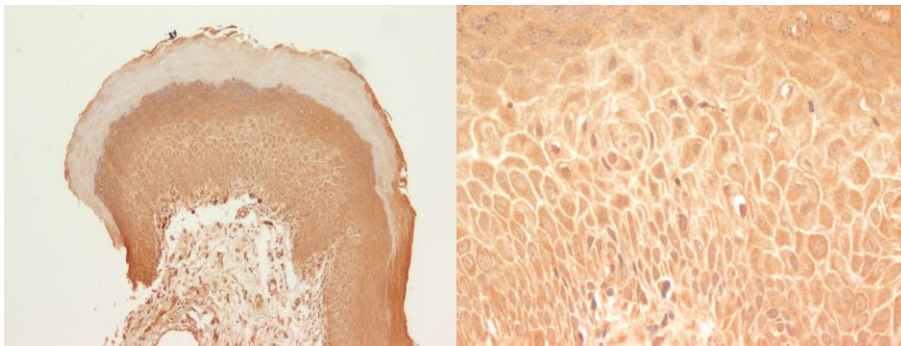


**Figure 4.24: p38 Staining, Progressing group – Case 4 magnification (A) x100, (B) x400**

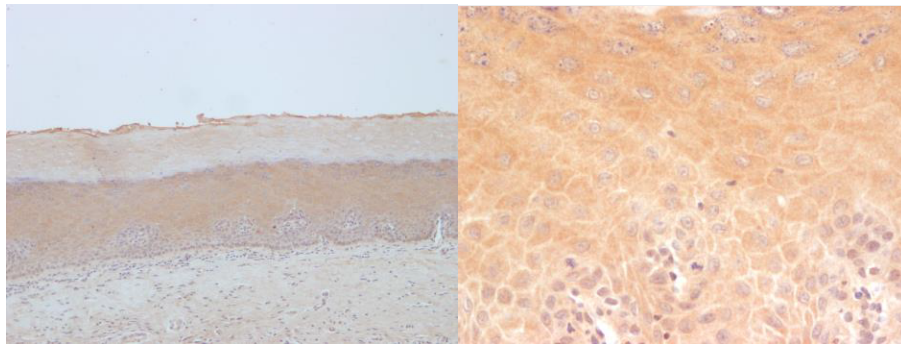


**Figure 4-25: JNK Staining, Control group – Case 2 magnification (A) x100, (B) x400**

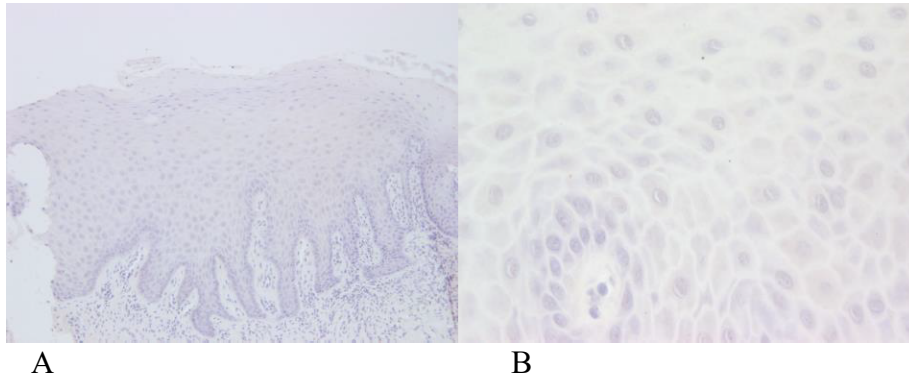


**Figure 4.26: JNK Staining, Non-progressing group – Case 26 magnification (A) x100, (B) x400**

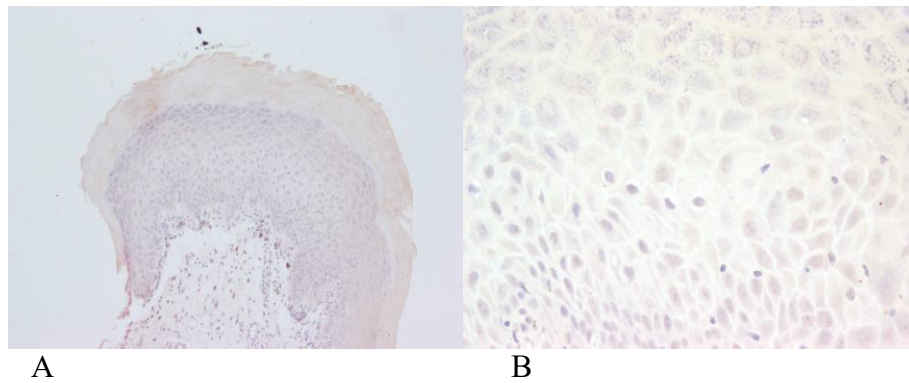
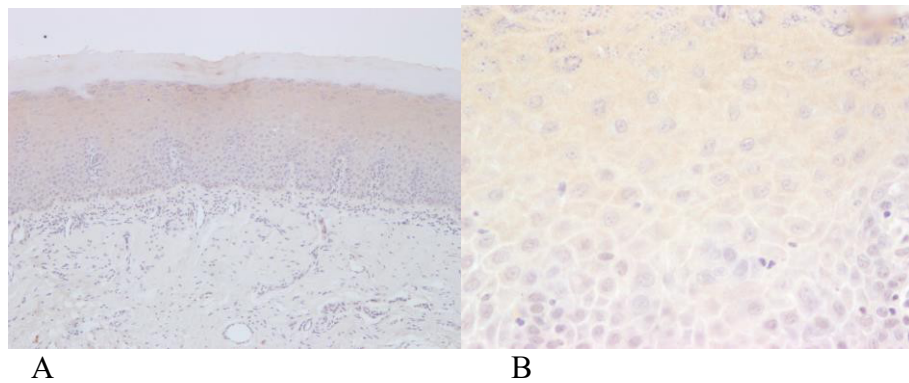


**Figure 4.27: JNK Staining, Progressing group – Case 4 magnification (A) x100, (B) x400**



## 4.5 Statistical analysis

### 4.5.1 Descriptive statistics

**Table 4.16: Descriptive statistics for the 3-tier and 2-tier diagnoses, S100A7 manual scoring, and Straticyte™ risk score**

Descriptive									
		N	Mean	Std. Deviation	Std. Error	95% Confidence Interval for Mean		Minimum	Maximum
						Lower Bound	Upper Bound		
3-Tier	1	39	1.46	1.047	.168	1.12	1.80	0	3
	2	35	1.09	.612	.103	.88	1.30	0	2
	3	25	.00	.000	.000	.00	.00	0	0
	Total	99	.96	.947	.095	.77	1.15	0	3
2-Tier	1	39	2.49	.885	.142	2.20	2.77	1	3
	2	35	1.46	.852	.144	1.16	1.75	1	3
	3	25	.00	.000	.000	.00	.00	0	0
	Total	99	1.49	1.232	.124	1.25	1.74	0	3
Manual	1	39	5.74	1.888	.302	5.13	6.36	2	8
	2	35	5.23	1.682	.284	4.65	5.81	2	8
	3	25	4.00	1.708	.342	3.30	4.70	2	8
	Total	99	5.12	1.886	.190	4.75	5.50	2	8
Straticyte	1	39	59.44	17.641	2.825	53.72	65.15	21	85
	2	35	37.00	16.223	2.742	31.43	42.57	12	71
	3	25	31.00	14.626	2.925	24.96	37.04	3	63
	Total	99	44.32	20.486	2.059	40.24	48.41	3	85

(Manual= S100A7 manual score; Straticyte= Straticyte™ risk score)

The descriptive statistics for each of the predictive parameters for malignant transformation are present in table 4.16. The sample populations were converted to numerical titles for the purposes of statistical analysis. Population 1 is the Progressing group, population 2 is the Non-progressing group and population 3 is the Control group. For statistical analysis, the total number of samples included for the Progressing population is 39, lower than the 48 total samples selected. This is due to the exclusion of

five sets of data from the “Other” diagnoses for not being dysplasia, while an additional four tissue samples due to tissue preparation issues such as tissue folds or poor epithelium. In this case, Straticyte™ was not completed for any tissue sample which contained any tissue folds. Therefore, a total of nine tissue samples was excluded (table 4.17). They remain in the raw data however, because they hold relevance for manual scoring, 3-tier and 2-tier diagnoses

**Table 4.17: Tissue samples excluded from statistical analysis and reason for exclusion**

<b>Case number</b>	<b>Reason for exclusion</b>
5	Tissue folds
16	TUGSE
24	Hyperplastic candidiasis
28	Lichenoid mucositis
40	Tissue lacking enough epithelium
43	Verrucous hyperplasia
50	Verrucous hyperplasia
61	Poor quality tissue section
63	Poor quality tissue section
<b>Total</b>	9

**Table 4.18: ANOVA output for 3 tier diagnosis, 2 tier diagnosis, manual S100A7 scores and Straticyte™ risk scores. The mean difference is significant at  $p < 0.05$**

ANOVA						
		Sum of Squares	df	Mean Square	F	Sig.
3-Tier	Between Groups	33.403	2	16.702	29.454	.000
	Within Groups	54.435	96	.567		
	Total	87.838	98			
2-Tier	Between Groups	94.318	2	47.159	83.177	.000
	Within Groups	54.429	96	.567		
	Total	148.747	98			
Manual	Between Groups	46.938	2	23.469	7.470	.001
	Within Groups	301.607	96	3.142		
	Total	348.545	98			
Straticyte	Between Groups	15222.067	2	7611.033	28.203	.000
	Within Groups	25907.590	96	269.871		
	Total	41129.657	98			

(Manual= S100A7 manual score; Straticyte= Straticyte™ risk score)

The ANOVA output is present in table 4.18. With this data analysis the goal is to determine if there are statistically significant differences between the three populations, Controls, Non-progressing, and Progressing for each of the predictive parameters. The ANOVA indicates that within each of the study populations, there is a statistically significant difference at  $p < 0.05$ , that exists when each of the predictive parameters for malignant transformation: 3-tier, 2-tier, S100A7 manual score, and Straticyte™ risk are applied to the study populations. This means that the predictive parameters are able to identify differences between the groups, however, ANOVA does not indicate between which of the populations the difference exists.

#### **4.5.2 Tukey multiple comparison 3-tier and 2-tier diagnoses**

The 3-tier and 2-tier diagnoses were converted to numerical categories for the sake of statistical analysis. The numerical conversion was as follows: hyperkeratosis/atypia 0,

mild/low grade 1, moderate 2, and severe/high grade 3. While the ANOVA output (Table 4.19) indicates statistically significant differences for each of the two diagnostic parameters, the differences are not clear as to between which populations the difference is significant.

**Table 4.19: Tukey multiple comparison between each of the populations (Control, Non-progressing, Progressing) against one another with the 3-tier and 2-tier diagnoses. Significance is achieved at  $p < 0.05$ . Populations renamed for analysis (1: Progressing, 2: Non-progressing, 3: Controls)**

Multiple Comparisons								
Dependent Variable		(I) Group	(J) Group	Mean Difference (I- J)	Std. Error	Sig.	95% Confidence Interval	
							Lower Bound	Upper Bound
3-Tier	Tukey HSD	1	2	.376	.175	.087	-.04	.79
			3	1.462*	.193	.000	1.00	1.92
		2	1	-.376	.175	.087	-.79	.04
			3	1.086*	.197	.000	.62	1.56
		3	1	-1.462*	.193	.000	-1.92	-1.00
			2	-1.086*	.197	.000	-1.56	-.62
	Bonferroni	1	2	.376	.175	.104	-.05	.80
			3	1.462*	.193	.000	.99	1.93
		2	1	-.376	.175	.104	-.80	.05
			3	1.086*	.197	.000	.61	1.57
		3	1	-1.462*	.193	.000	-1.93	-.99
			2	-1.086*	.197	.000	-1.57	-.61
2-Tier	Tukey HSD	1	2	1.030*	.175	.000	.61	1.45
			3	2.487*	.193	.000	2.03	2.95
		2	1	-1.030*	.175	.000	-1.45	-.61
			3	1.457*	.197	.000	.99	1.93
		3	1	-2.487*	.193	.000	-2.95	-2.03
			2	-1.457*	.197	.000	-1.93	-.99
	Bonferroni	1	2	1.030*	.175	.000	.60	1.46
			3	2.487*	.193	.000	2.02	2.96
		2	1	-1.030*	.175	.000	-1.46	-.60
			3	1.457*	.197	.000	.98	1.94
		3	1	-2.487*	.193	.000	-2.96	-2.02
			2	-1.457*	.197	.000	-1.94	-.98

*. The mean difference is significant at the 0.05 level.
--

Tukey multiple comparison for the 3-tier and 2-tier grading systems was performed. With respect to the 3-tier diagnoses, the mean for the Progressing group was 1.46, the Non-progressing group was 1.09, and the Control group was 0.0 (Table 4.16). According to Tukey multiple comparison (Table 4.19), the difference between the Control group and both dysplasia groups is statistically significant, however, the difference between the Progressing and the Non-progressing group is not. The mean score for each of the populations for the 2 tier diagnoses were 2.49, 1.46, and 0.0 for the Progressing, Non-progressing and Control respectively (Table 4.16). The Tukey multiple comparison (Table 4.19) indicates that the difference between each of the groups is statistically significant at  $p < 0.05$ .

### 4.5.3 Tukey multiple comparison S100A7 manual score

**Table 4.20: Tukey multiple comparison between each of the populations (Control, Non-progressing, Progressing) against one another with the manual S100A7 score. Significance is achieved at  $p < 0.05$ . Populations renamed for analysis (1: Progressing, 2: Non-progressing, 3: Controls)**

Multiple Comparisons								
Dependent Variable		(I) Group	(J) Group	Mean Difference (I- J)	Std. Error	Sig.	95% Confidence Interval	
							Lower Bound	Upper Bound
Manual	Tukey HSD	1	2	.515	.413	.428	-.47	1.50
			3	1.744*	.454	.001	.66	2.82
		2	1	-.515	.413	.428	-1.50	.47
			3	1.229*	.464	.025	.12	2.33
		3	1	-1.744*	.454	.001	-2.82	-.66
			2	-1.229*	.464	.025	-2.33	-.12
	Bonferroni	1	2	.515	.413	.645	-.49	1.52
			3	1.744*	.454	.001	.64	2.85
		2	1	-.515	.413	.645	-1.52	.49
			3	1.229*	.464	.028	.10	2.36
		3	1	-1.744*	.454	.001	-2.85	-.64
			2	-1.229*	.464	.028	-2.36	-.10

\*. The mean difference is significant at the 0.05 level.

(Manual= S100A7 manual score)

The Tukey multiple comparison results from table 4.20 allow us to see if there are significant differences between each of the populations with respect to S100A7 manual scoring. From table 4.16, the mean S100A7 manual score for each of the populations was 5.74, 5.23, and 4.0 for the Progressing, Non-progressing, and Control groups respectively. From the Tukey multiple comparison table, these differences are statistically significant between the Control population and the two dysplastic populations, however, there is no statistical difference between the Non-progressing and Progressing groups. The difference is significant at  $p < 0.05$ .

#### 4.5.4 Tukey multiple comparison, Straticyte™ risk score

**Table 4.21: Tukey multiple comparison between each of the populations (Controls, Non-progressing, Progressing) against one another with the Straticyte™ Risk Score. Significance is achieved at  $p < 0.05$ . Populations renamed for analysis (1: Progressing, 2: Non-progressing, 3: Controls)**

Multiple Comparisons								
Dependent Variable		(I) Group	(J) Group	Mean Difference (I- J)	Std. Error	Sig.	95% Confidence Interval	
							Lower Bound	Upper Bound
Straticyte	Tukey HSD	1	2	22.436*	3.825	.000	13.33	31.54
			3	28.436*	4.209	.000	18.42	38.46
		2	1	-22.436*	3.825	.000	-31.54	-13.33
			3	6.000	4.302	.348	-4.24	16.24
		3	1	-28.436*	4.209	.000	-38.46	-18.42
			2	-6.000	4.302	.348	-16.24	4.24
	Bonferroni	1	2	22.436*	3.825	.000	13.12	31.76
			3	28.436*	4.209	.000	18.18	38.69
		2	1	-22.436*	3.825	.000	-31.76	-13.12
			3	6.000	4.302	.499	-4.48	16.48
		3	1	-28.436*	4.209	.000	-38.69	-18.18
			2	-6.000	4.302	.499	-16.48	4.48

\*. The mean difference is significant at the 0.05 level.

(Straticyte= Straticyte risk score)

The statistical data for the Straticyte™ risk score is also included in table 4.16. The average percent risk for the three populations are 59.44, 37.00 and 31.00, for the Progressing to OSCC, Non-progressing, and Hyperkeratosis/Control groups respectively. When Tukey multiple comparison is applied (Table 4.21), the difference between the Progressing to OSCC group and both the Non-progressing dysplasia and Hyperkeratosis/Control groups is statistically significant at  $p < 0.05$ . The difference between the Non-progressing dysplasia group and the Hyperkeratosis/Control groups is non-significant.

#### 4.5.5 Tukey multiple comparison, QuPath score

A total of 29 tissue samples were assessed with QuPath. Ten tissue samples from each of the populations was originally selected, however case 5 in the Progressing group was not scored by Straticyte because of tissue folds, therefore this group only had 9 cases.

**Table 4.22: Descriptive statistics for the 3-tier and 2-tier diagnoses, S100A7 manual score, Straticyte™ risk score and QuPath score for the subpopulation of QuPath tested tissue samples**

Descriptives									
		N	Mean	Std. Deviation	Std. Error	95% Confidence Interval for Mean		Minimum	Maximum
						Lower Bound	Upper Bound		
3-Tier	1	9	1.11	1.054	.351	.30	1.92	0	3
	2	10	1.50	.707	.224	.99	2.01	0	2
	3	10	.00	.000	.000	.00	.00	0	0
	Total	29	.86	.953	.177	.50	1.22	0	3
2-Tier	1	9	1.78	.972	.324	1.03	2.52	1	3
	2	10	2.20	1.033	.327	1.46	2.94	1	3
	3	10	.00	.000	.000	.00	.00	0	0
	Total	29	1.31	1.257	.233	.83	1.79	0	3
Manual	1	9	4.78	1.986	.662	3.25	6.30	2	8
	2	10	5.60	1.578	.499	4.47	6.73	4	8
	3	10	4.30	2.003	.633	2.87	5.73	2	8
	Total	29	4.90	1.877	.349	4.18	5.61	2	8
Straticyte	1	9	52.11	22.048	7.349	35.16	69.06	22	75
	2	10	38.80	15.591	4.930	27.65	49.95	15	59
	3	10	31.20	12.109	3.829	22.54	39.86	15	55
	Total	29	40.31	18.422	3.421	33.30	47.32	15	75
QuPath	1	9	6.67	1.000	.333	5.90	7.44	5	8
	2	10	5.20	1.619	.512	4.04	6.36	2	7
	3	10	4.20	1.932	.611	2.82	5.58	2	8
	Total	29	5.31	1.834	.341	4.61	6.01	2	8

(Manual= S100A7 manual score; Straticyte= Straticyte™ risk score)

**Table 4.23: Tukey multiple comparison between each of the populations (Control, Non-progressing, Progressing) against one another with the 3-tier, 2-tier, S100A7 manual score, Straticyte™ risk score and QuPath score. Significance is achieved at  $p < 0.05$ . Populations renamed for analysis (1: Progressing, 2: Non-progressing, 3: Control)**

Multiple Comparisons								
Dependent Variable		(I) Group	(J) Group	Mean Difference (I- J)	Std. Error	Sig.	95% Confidence Interval	
							Lower Bound	Upper Bound
3-Tier	Tukey HSD	1	2	-.389	.330	.476	-1.21	.43
			3	1.111*	.330	.006	.29	1.93
		2	1	.389	.330	.476	-.43	1.21
			3	1.500*	.321	.000	.70	2.30
		3	1	-1.111*	.330	.006	-1.93	-.29
			2	-1.500*	.321	.000	-2.30	-.70
	Bonferroni	1	2	-.389	.330	.747	-1.23	.45
			3	1.111*	.330	.007	.27	1.95
		2	1	.389	.330	.747	-.45	1.23
			3	1.500*	.321	.000	.68	2.32
		3	1	-1.111*	.330	.007	-1.95	-.27
			2	-1.500*	.321	.000	-2.32	-.68
2-Tier	Tukey HSD	1	2	-.422	.373	.504	-1.35	.51
			3	1.778*	.373	.000	.85	2.71
		2	1	.422	.373	.504	-.51	1.35
			3	2.200*	.363	.000	1.30	3.10
		3	1	-1.778*	.373	.000	-2.71	-.85
			2	-2.200*	.363	.000	-3.10	-1.30
	Bonferroni	1	2	-.422	.373	.805	-1.38	.53
			3	1.778*	.373	.000	.82	2.73
		2	1	.422	.373	.805	-.53	1.38
			3	2.200*	.363	.000	1.27	3.13
		3	1	-1.778*	.373	.000	-2.73	-.82
			2	-2.200*	.363	.000	-3.13	-1.27

Manual	Tukey HSD	1	2	-.822	.855	.607	-2.95	1.30
			3	.478	.855	.843	-1.65	2.60
		2	1	.822	.855	.607	-1.30	2.95
			3	1.300	.832	.280	-.77	3.37
		3	1	-.478	.855	.843	-2.60	1.65
			2	-1.300	.832	.280	-3.37	.77
	Bonferroni	1	2	-.822	.855	1.000	-3.01	1.37
			3	.478	.855	1.000	-1.71	2.67
		2	1	.822	.855	1.000	-1.37	3.01
			3	1.300	.832	.391	-.83	3.43
		3	1	-.478	.855	1.000	-2.67	1.71
			2	-1.300	.832	.391	-3.43	.83
Straticyte	Tukey HSD	1	2	13.311	7.749	.218	-5.95	32.57
			3	20.911*	7.749	.031	1.65	40.17
		2	1	-13.311	7.749	.218	-32.57	5.95
			3	7.600	7.543	.579	-11.14	26.34
		3	1	-20.911*	7.749	.031	-40.17	-1.65
			2	-7.600	7.543	.579	-26.34	11.14
	Bonferroni	1	2	13.311	7.749	.293	-6.52	33.14
			3	20.911*	7.749	.036	1.08	40.74
		2	1	-13.311	7.749	.293	-33.14	6.52
			3	7.600	7.543	.969	-11.70	26.90
		3	1	-20.911*	7.749	.036	-40.74	-1.08
			2	-7.600	7.543	.969	-26.90	11.70
Qupath	Tukey HSD	1	2	1.467	.728	.128	-.34	3.27
			3	2.467*	.728	.006	.66	4.27
		2	1	-1.467	.728	.128	-3.27	.34
			3	1.000	.708	.350	-.76	2.76
		3	1	-2.467*	.728	.006	-4.27	-.66
			2	-1.000	.708	.350	-2.76	.76
	Bonferroni	1	2	1.467	.728	.163	-.40	3.33
			3	2.467*	.728	.007	.60	4.33
		2	1	-1.467	.728	.163	-3.33	.40
			3	1.000	.708	.509	-.81	2.81
		3	1	-2.467*	.728	.007	-4.33	-.60
			2	-1.000	.708	.509	-2.81	.81

(Manual= S100A7 manual score; Straticyte= Straticyte™ risk score)

\*. The mean difference is significant at the 0.05 level.

Table 4.22 contains the descriptive statistics for the tissue samples that were assessed with QuPath. For these samples, table 4.23 contains the Tukey analysis to determine if differences found between the populations is significant. The Tukey analysis for the smaller sample size for the Manual S100A7 scores demonstrates that there is a statistically significant difference in the scores for the Progressing and Control group, but not the Non-progressing group. There was no statistically significant difference between the Non-progressing and Control groups either. The same can be said for the Straticyte™ assessment, in which the difference between the Progressing and Control groups was statistically significant, yet it was not significant in distinguishing the Progressing from the Non-progressing. The Non-progressing and Controls are also not statistically different.

With the QuPath assessment the same statistical methods were used. The mean score for each of the populations for QuPath was 6.67, 5.20 and 4.20 for the Progressing, Non-progressing and the Control groups respectively (table 4.22). With the Tukey multiple comparison (table 4.23), only the difference between the Progressing and Control was statistically significant. For the Non-Progressing group, just as it was for the Manual S100A7 score and Straticyte scores, there was no statistically significant difference with either of the other two groups.

#### **4.5.6 Pearson correlation coefficients**

Correlational statistics for 3-tier, 2-tier, S100A7 manual score and Straticyte™ risk score

The Pearson Correlation Coefficient allows for comparison of the different predictive parameters of malignant transformation with one another to determine if there is a correlational relationship between them. When analyzed, relationships deemed very

strong have correlational coefficient closer to one (156). The significance of these relationships is indicated by the asterisk with p- values less than 0.01 or 0.05 in the tables below.

**Table 4.24: All populations. Pearson correlation coefficient table for the 3-tier, 2-tier, S100A7 manual score, and Straticyte™ risk score.**

Correlations		3-Tier	2-Tier	Manual	Straticyte
3-Tier	Pearson Correlation	1	.673**	.329**	.422**
	Sig. (2-tailed)		.000	.001	.000
	N	99	99	99	99
2-Tier	Pearson Correlation	.673**	1	.321**	.520**
	Sig. (2-tailed)	.000		.001	.000
	N	99	99	99	99
Manual	Pearson Correlation	.329**	.321**	1	.669**
	Sig. (2-tailed)	.001	.001		.000
	N	99	99	99	99
Straticyte	Pearson Correlation	.422**	.520**	.669**	1
	Sig. (2-tailed)	.000	.000	.000	
	N	99	99	99	99

(Manual= S100A7 manual score; Straticyte= Straticyte™ risk score)

\*\* Correlation is significant at the 0.01 level (2-tailed).

\* Correlation is significant at the 0.05 level (2-tailed).

The 3-tier diagnosis has weak correlation with the S100A7 manual score, at 0.329, and moderate correlation with the Straticyte™ risk score with a correlational coefficient of 0.422. Both of these correlations are statistically significant at  $p < 0.01$ .

The 2-tier system had similar correlation with the S100A7 manual score, with a coefficient of 0.321, however had a slightly improved correlation with the Straticyte™ risk score at 0.520, indicating moderate correlation as well. Again, these relationships are statistically significant at  $p < 0.01$ .

The correlational coefficient between The S100A7 manual score and the Straticyte™ risk score was 0.669, which also indicates a moderate correlation between the two diagnostic

approaches, and assessment of S100A7. The correlational relationship is statistically significant at  $p < 0.01$ .

Further Pearson Correlation was completed for each of the three sample populations to determine if the relationships between any of the diagnostic tests and specific populations were different from the overall population.

**Table 4.25: Progressing population. Pearson correlation coefficient table for the 3-tier, 2-tier, S100A7 manual score, and Straticyte™ risk score**

Correlations					
		3-Tier	2-Tier	Manual	Straticyte
3-Tier	Pearson Correlation	1	.376*	.234	.241
	Sig. (2-tailed)		.018	.151	.140
	N	39	39	39	39
2-Tier	Pearson Correlation	.376*	1	.014	.082
	Sig. (2-tailed)	.018		.934	.619
	N	39	39	39	39
Manual	Pearson Correlation	.234	.014	1	.595**
	Sig. (2-tailed)	.151	.934		.000
	N	39	39	39	39
Straticyte	Pearson Correlation	.241	.082	.595**	1
	Sig. (2-tailed)	.140	.619	.000	
	N	39	39	39	39

(Manual= S100A7 manual score; Straticyte= Straticyte™ risk score)

\*\* Correlation is significant at the 0.01 level (2-tailed).

\* Correlation is significant at the 0.05 level (2-tailed).

For the Progressing population alone, the strongest correlational relationship is between the S100A7 manual score, and the Straticyte™ risk score. The correlation coefficient is 0.595, a moderate strength relationship, with statistical significance at  $p < 0.01$  (Table 4.25).

The correlational relationships for both the 3-tier and 2-tier with the S100A7 manual score and the Straticyte™ risk score both worsened. Negligible correlation existed between the 2-tier and the S100A7 manual score, (correlation coefficient 0.014), and the

2-tier and the Straticyte™ risk score, (correlation coefficient 0.082). Neither of these relationships, however, are statistically significant (Table 4.25). The 3-tier system fared only slightly better with correlation coefficients of 0.234 and 0.241 with the S100A7 manual score and the Straticyte™ risk score respectively. Again, neither of these were considered statistically significant.

**Table 4.26: Non-progressing population. Pearson correlation coefficient table for the 3-tier, 2-tier, S100A7 manual score, and Straticyte™ risk score**

Correlations					
		3-Tier	2-Tier	Manual	Straticyte
3-Tier	Pearson Correlation	1	.486**	.009	.145
	Sig. (2-tailed)		.003	.959	.406
	N	35	35	35	35
2-Tier	Pearson Correlation	.486**	1	.130	.311
	Sig. (2-tailed)	.003		.456	.069
	N	35	35	35	35
Manual	Pearson Correlation	.009	.130	1	.691**
	Sig. (2-tailed)	.959	.456		.000
	N	35	35	35	35
Straticyte	Pearson Correlation	.145	.311	.691**	1
	Sig. (2-tailed)	.406	.069	.000	
	N	35	35	35	35

(Manual= S100A7 manual score; Straticyte= Straticyte™ risk score)

\*\* Correlation is significant at the 0.01 level (2-tailed).

Correlation is significant at the 0.05 level (2-tailed).

The correlation coefficients for the Non-progressing population are presented in table 4.26. The correlation between the 3-tier and 2-tier is moderate at 0.486 and is statistically significant at  $p < 0.01$ . However, the relationship between the 2-tier with the S100A7 manual score and the Straticyte™ risk score, are weak with coefficients of 0.130 and 0.311 respectively, both of which are not statistically significant. The 3-tier had negligible correlation with the S100A7 manual score, (correlation coefficient 0.009), and weak correlation, (correlation coefficient 0.130), with the Straticyte™ risk score. Neither

are statistically significant. The correlation for the S100A7 manual score with the Straticyte™ risk score was (correlation coefficient 0.691), moderately strong, and statistically significant at  $p < 0.01$ .

**Table 4.27: Control population. Pearson correlation coefficient table for the 3-tier, 2-tier, S100A7 manual score, and Straticyte™ risk score.**

Correlations		3-Tier	2-Tier	Manual	Straticyte
3-Tier	Pearson Correlation	.a	.a	.a	.a
	Sig. (2-tailed)		.	.	.
	N	25	25	25	25
2-Tier	Pearson Correlation	.a	.a	.a	.a
	Sig. (2-tailed)	.		.	.
	N	25	25	25	25
Manual	Pearson Correlation	.a	.a	1	.712**
	Sig. (2-tailed)	.	.		.000
	N	25	25	25	25
Straticyte	Pearson Correlation	.a	.a	.712**	1
	Sig. (2-tailed)	.	.	.000	
	N	25	25	25	25

(Manual= Manual S100A7 score; Straticyte= Straticyte™ risk score)

a. Cannot be computed because at least one of the variables is constant.

\*\* Correlation is significant at the 0.01 level (2-tailed).

Correlation is significant at the 0.05 level (2-tailed).

The correlation coefficients for the Control population is present in Table 4.27. Due to the lack of variance in the 3-tier and 2-tier diagnoses, they are interpreted as constants, therefore they cannot be used in correlational coefficient calculations. The correlation coefficient for the S100A7 manual score with the Straticyte™ risk score was 0.692, which is moderately strong, and statistically significant at  $p < 0.01$ .

#### 4.5.7 QuPath correlation

**Table 4.28: All Populations. Pearson correlation coefficient table for the 3-tier, 2-tier, S100A7 manual score, and Straticyte™ risk score and QuPath**

Correlations						
		3-Tier	2-Tier	Manual	Straticyte	Qupath
3-Tier	Pearson Correlation	1	.663**	.391*	.438*	.311
	Sig. (2-tailed)		.000	.036	.018	.100
	N	29	29	29	29	29
2-Tier	Pearson Correlation	.663**	1	.105	.381*	.298
	Sig. (2-tailed)	.000		.588	.041	.117
	N	29	29	29	29	29
Manual	Pearson Correlation	.391*	.105	1	.538**	.632**
	Sig. (2-tailed)	.036	.588		.003	.000
	N	29	29	29	29	29
Straticyte	Pearson Correlation	.438*	.381*	.538**	1	.533**
	Sig. (2-tailed)	.018	.041	.003		.003
	N	29	29	29	29	29
Qupath	Pearson Correlation	.311	.298	.632**	.533**	1
	Sig. (2-tailed)	.100	.117	.000	.003	
	N	29	29	29	29	29

(Manual= S100A7 manual score; Straticyte= Straticyte™ risk score)

\*\* Correlation is significant at the 0.01 level (2-tailed).

Correlation is significant at the 0.05 level (2-tailed).

The All population Pearson correlation for the 29 QuPath tissue samples is present in table 4.28. The primary focus is the QuPath result and whether or not correlational relationships exist for the sample populations with the other predictive parameters. QuPath correlates weakly with both the 3-tier and 2-tier diagnoses with no statistical significance. It correlates moderately with both the S100A7 manual score, and the Straticyte™ risk score with correlational coefficients of 0.632, and 0.533 respectively. Both relationships are statistically significant at  $p < 0.01$

**Table 4.29: Progressing population. Pearson correlation coefficient table for the 3-tier, 2-tier, S100A7 manual score, and Straticyte™ risk score and QuPath**

Correlations						
		3-Tier	2-Tier	Manual	Straticyte	Qupath
3-Tier	Pearson Correlation	1	.027	.610	.371	.158
	Sig. (2-tailed)		.945	.081	.326	.685
	N	9	9	9	9	9
2-Tier	Pearson Correlation	.027	1	-.353	.042	-.214
	Sig. (2-tailed)	.945		.352	.914	.580
	N	9	9	9	9	9
Manual	Pearson Correlation	.610	-.353	1	.514	.713*
	Sig. (2-tailed)	.081	.352		.156	.031
	N	9	9	9	9	9
Straticyte	Pearson Correlation	.371	.042	.514	1	.291
	Sig. (2-tailed)	.326	.914	.156		.447
	N	9	9	9	9	9
Qupath	Pearson Correlation	.158	-.214	.713*	.291	1
	Sig. (2-tailed)	.685	.580	.031	.447	
	N	9	9	9	9	9

(Manual= S100A7 manual score; Straticyte= Straticyte™ risk score)

Correlation is significant at the 0.05 level (2-tailed)

The Progressing population of QuPath assessed tissue samples underwent Pearson correlation, presented in table 4.29. The correlation coefficient for the QuPath score and the S100A7 manual score is 0.713, which is considered a strong correlation relationship. The relationship is significant to  $p < 0.01$ . For the Non-progressing population, the correlation coefficients between QuPath and the S100A7 manual score as well as the Straticyte™ were 0.513 and 0.195 respectively, which are considered moderate and weak correlational relationships. Neither of these relationships are statistically significant (table 4.30). For the Control group, the lack of variance in the 3-tier and 2-tier diagnoses creates constants for each and therefore these cannot be used for correlational assessment. The correlational relationship for QuPath with the S100A7 manual score and Straticyte™ risk

for the Control group are (correlation coefficients 0.959 and 0.767). These are also both significant at  $p < 0.01$  (table 4.31). These relationships are considered very strong and strong respectively.

**Table 4.30: Non-progressing. Pearson correlation coefficient table for the 3-tier, 2-tier, S100A7 manual score, and Straticyte™ risk score and QuPath**

Correlations						
		3-Tier	2-Tier	Manual	Straticyte	Qupath
3-Tier	Pearson Correlation	1	.609	.000	.514	.194
	Sig. (2-tailed)		.062	1.000	.129	.591
	N	10	10	10	10	10
2-Tier	Pearson Correlation	.609	1	-.082	.582	.106
	Sig. (2-tailed)	.062		.822	.077	.770
	N	10	10	10	10	10
Manual	Pearson Correlation	.000	-.082	1	.593	.513
	Sig. (2-tailed)	1.000	.822		.071	.129
	N	10	10	10	10	10
Straticyte	Pearson Correlation	.514	.582	.593	1	.195
	Sig. (2-tailed)	.129	.077	.071		.588
	N	10	10	10	10	10
Qupath	Pearson Correlation	.194	.106	.513	.195	1
	Sig. (2-tailed)	.591	.770	.129	.588	
	N	10	10	10	10	10

(Manual= S100A7 manual score; Straticyte= Straticyte™ risk score)  
Correlation is significant at the 0.05 level (2-tailed).

**Table 4.31: Control population. Pearson correlation coefficient table for the 3-tier, 2-tier, S100A7 manual score, and Straticyte™ risk score and QuPath**

Correlations						
		3-Tier	2-Tier	Manual	Straticyte	Qupath
3-Tier	Pearson Correlation	.a	.a	.a	.a	.a
	Sig. (2-tailed)		.	.	.	.
	N	10	10	10	10	10
2-Tier	Pearson Correlation	.a	.a	.a	.a	.a
	Sig. (2-tailed)	.		.	.	.
	N	10	10	10	10	10
Manual	Pearson Correlation	.a	.a	1	.817**	.959**
	Sig. (2-tailed)	.	.		.004	.000
	N	10	10	10	10	10
Straticyte	Pearson Correlation	.a	.a	.817**	1	.767**
	Sig. (2-tailed)	.	.	.004		.010
	N	10	10	10	10	10
Qupath	Pearson Correlation	.a	.a	.959**	.767**	1
	Sig. (2-tailed)	.	.	.000	.010	
	N	10	10	10	10	10

(Manual= S100A7 manual score; Straticyte= Straticyte™ risk score)

a. Cannot be computed because at least one of the variables is constant.

\*\* Correlation is significant at the 0.01 level (2-tailed).

Correlation is significant at the 0.05 level (2-tailed).

## **CHAPTER 5: DISCUSSION**

### **5.1 Demographics**

#### **5.1.1 Gender**

In general, there was relative gender equality between the Hyperkeratosis/Control (Control), Non-progressing dysplasia (Non-progressing) and Progressing to OSCC (Progressing) populations in this study. The current literature is often mixed with respect to gender differences and OPMLs, and any gender predilection may be linked to habits (59) (156). Interestingly, while lesions maybe reported to occur in males more frequently than in females, malignant transformation has been shown to occur more frequently in the latter (69). It has been shown that women without oral habits such as tobacco use or alcohol consumption are at greater risk of malignant transformation than those that use tobacco and alcohol (84). In this current study, 2 of the 13 cases that had known tobacco consumption were women, though we were unable to draw any strong conclusions regarding malignant transformation and oral habits given the lack of information regarding tobacco and alcohol use.

#### **5.1.2 Age**

The average age at initial biopsy for each of the populations was also noted. The average age and age range of the Control group was 50.4 years with a range of 15-72 years, while the Non-progressing group was 55.4 years, with a range of 31-74 years and the Progressing group was 62.2 years with a range of 40-86 years. The younger age at initial biopsy for the Control group may reflect a significant outlier within the group, as there was a patient whose initial biopsy was at 15 years old which is 16 years younger than the youngest patient in the Non-progressing group. With this outlier removed, the average

age for the Control group was 52 years old, an increase of only 2 years, which is still younger than the other two groups. Median age of the Progressing group was 62, the Non-progressing was 59, and the Control group was 51 years. This is similar to the difference in average age. While Leukoplakia can occur within a large age range, it is most commonly detected in the fourth to seventh decades of life in North America, therefore our findings are in keeping with expectation with published literature (59).

### **5.1.3 Lesion Location**

In this study, the most common lesion sites were the lateral tongue, ventral tongue and floor of mouth (table 4.4). These are all contiguous anatomic sites and are often cited as the most common site for oral dysplastic lesions (69)(3)(66). In all three populations, these were the most common sites to be biopsied with a total of 38 lesions from the lateral tongue and 34 lesions from the ventral tongue and floor of mouth out of a total of 108 lesions. Of the 72 lesions from these sites, 28 (39%) underwent malignant transformation. This transformation rate is higher than other studies which site transformation rates for the tongue with or without floor of mouth as 27%, 14.9%, and 11.8% (82)(84)(66).

Interestingly, amongst the three populations, buccal mucosa lesions were only seen within the Progressing group. A total of six biopsies were obtained from this site.

Evidence regarding the frequency of buccal mucosal lesions is mixed. Buccal mucosal leukoplakia has been found to occur commonly in some studies, with leukoplakia at this site occurring nearly as frequently as the lateroventral tongue and floor of mouth (157)(79) (66)(158). In one particular study, the buccal mucosa was the most common

site for lesions, however these were reported as oral leukoplakia and strongly effected by oral habits such as tobacco and betel quid chewing. With cessation of these habits, many of the lesions resolved. Dysplasia within the buccal mucosa was not common in this study (159). Other studies indicate that the occurrence of buccal mucosal dysplasia and OSCC are not common. A study from Spain found only 7.7% of the major head and neck cancer cases they managed had OSCC of the buccal mucosa (11). In another study by Dost, 260 lesions were compared for site, and histological diagnoses. 79 lesions were found on the buccal mucosa, 41 (52%) were mild dysplasia, and none were OSCC (66). These results are corroborated by a Hungarian study where 170/670 lesions occurred on the buccal mucosa, however, only 5 transformed into OSCC (82). In our current study, the patients with buccal lesions were 77, 71, 48, 81, 82, 43 years of age (average: 67). In a study by Silverman et al, age was evaluated for each of the lesion locations, and they found the average age for patients with buccal leukoplakia which converted to OSCC was 60 years old. This was slightly older than the average age for all patients with lesions which was 57 years. This difference in age was not found to be significant in this study, and the age for each of the lesion locations was roughly the same whether they transformed or not (3). A Brazilian study from 2020, found no significant difference in lesion location and age (61).

Actinic cheilitis of the lower lip was only seen in the group that progressed to OSCC as well. In a 2018 systematic review, the malignant transformation rate was found to be 3.07% for actinic cheilitis (160).

These results may reflect a selection or sample bias based on our initial search criteria. Each of the tissue samples are provided a numerical code based on diagnoses and are logged within a database for the division of Oral Pathology at Western University and London Health Sciences Centre. As part of the search criteria, this numerical code was used to identify tissue samples of a given diagnosis. The lesions that progressed to OSCC from a previous lesion would have been found based on the OSCC code, not that of the original diagnosis. The dysplastic lesions that did not progress to OSCC would have been identified based on a dysplasia code. Actinic cheilitis was coded separately from dysplasia, and would not have been included in the search for hyperkeratosis or dysplastic lesions that do not progress, which would contribute to the discrepancy seen. The same could be said for non-progressing buccal lesions, if they were characterized as a different diagnosis on initial biopsy. This could occur due to the high rate of other types of lesions occurring within the buccal mucosa as previously noted, and potential difficulty differentiating between mild dysplastic and non-dysplastic changes.

#### **5.1.4 Malignant Transformation**

In the current study, 48 tissue samples were selected that eventually progressed to OSCC. Of these tissue samples, the average time to malignant transformation was 4.36 years (range <1-13 years). This is in keeping with a recent systematic review and meta-analysis, in which four studies assessed time to malignant transformation within oral dysplastic tissue samples. In that study, the average time to malignant transformation based on these four studies was 4.3 years (range 0.5-16 years) (161). A more recent study reports a mean transformation rate of 33.56 months (2.8 years) with a range of 6-67 months (0.5-5.58 years) (162).

## **5.2 Utility of predictive parameters of dysplasia**

### **5.2.1 3-Tier and 2-Tier dysplasia grading systems**

Three-tier and 2-tier dysplasia grading systems were evaluated both individually and also compared to one another to determine their utility in predicting malignant transformation. Historically, the 3-tier diagnosis is known to be problematic given the issues regarding inter-observer and intra-observer variability (98)(99)(100). In addition, difficulty arises in differentiating neoplastic mild and moderate dysplasia from non-neoplastic mild dysplastic changes based on histomorphology alone, particularly in inflamed tissue (163). With respect to the Non-progressing dysplasia population, mild dysplasia was the most frequent 3-tier diagnosis and low-grade dysplasia was the most frequent 2-tier diagnosis. None of the tissue samples contained severe dysplasia, though 8 of the tissue samples were interpreted as high grade according to the 2-tier system. Interestingly these do not all coincide with the 8 cases of moderate dysplasia and demonstrates the variability of histopathological interpretation.

The group that progressed to OSCC contained 11 tissue samples with mild dysplasia, 13 tissue samples with moderate dysplasia, and 5 tissue samples with severe dysplasia. In addition, diagnoses also included TUGSE, hyperkeratosis, lichenoid mucositis, and verrucous hyperplasia. While TUGSE and hyperkeratosis are not included in the list of OPMLs, lichenoid mucositis and verrucous hyperplasia are (56). When the lesions were re-evaluated with the 2-tier system, 10 lesions contained low grade dysplasia, while 33 contained high grade dysplasia.

The two dysplastic populations, Non-progressing and Progressing, both contain mild, moderate and severe dysplastic tissue when evaluated with the 3-tier system. When

evaluated with the 2-tier system a combination of low grade and high grade was present in both. While high or severe grade dysplastic lesions carry greater risk of malignant transformation, and the low grade or mild dysplasia carries a lower risk, we found inconsistency in the grading scales ability to truly identify lesions that will progress to OSCC as compared to those that do not, which has often been reported (64)(94). In addition, some lesions without signs of dysplasia or leukoplakia can progress (3). In the current study, 32% of total mild dysplasia progressed to OSCC, and 100% of severe lesions progressed. When utilizing the 2-tier grading system, 80% of the high grade lesions progressed, and 27% of the low grade progressed. In addition, nine lesions with squamous or architectural atypia progressed to OSCC, highlighting the difficulty with the grading systems (164). The progression of the severe dysplasia within our study may also be a result of selection bias as it was discussed earlier that the greatest difficulty lies in identifying mild dysplasias, therefore more emphasis was placed on finding lesions with mild or moderate grade dysplasia as an attempt to underscore potential differences in S100A7 staining.

In this study, a moderate correlation was found between the 3-tier and 2-tier grading systems when all populations were considered together (table 4.21). When correlating grading systems with each population individually, the relationship was moderate for the Non-progressing group, which was stronger than for the Progressing group (tables 4.22, 4.23). The stronger correlation found between the two grading systems in the Non-progressing group may be explained by the number of moderate cases in each of the populations. There were 13 moderate dysplasia cases in the Progressing group, and only 8 in the Non-progressing group. Given the difficulty with distinguishing moderate

dysplasia in the 3-tier system, the greater number of moderate dysplasia cases could be a contributing factor to greater variability in the Progressing 3-tier diagnoses, which would effect the correlation of the two populations. (163).

The use of the 3-tier grading system enabled the pathologist to differentiate the dysplastic populations from the Control population but not the Progressing and the Non-progressing populations, when Tukey analysis was applied (table 4.16). This is consistent with what would be expected in the literature, as lesions with more significant changes are more readily agreed upon and distinguishable from non-dysplastic lesions. As such the hyperkeratosis of the Control group should be readily identifiable as compared to most dysplastic tissue. Distinguishing between the Non-progressing and Progressing groups is difficult as the visual assessment of the tissue samples and identification of dysplasia is the same, therefore the expectation would be that the tissue samples with minimal or no changes would be identifiable when compared to those with significant change (165) (166).

The 2-tier grading system improved upon the 3-tier system. When comparing the three study populations, the 2-tier allowed the examiner to differentiate between not only the dysplastic and non-dysplastic lesions, but between the Progressing and Non-progressing as well (table 4.16). This ability to characterize the tissue samples in our study is in keeping with previous studies regarding the binary grading system (95). This may be due to the removal of moderate dysplastic lesions as seen in the 3-tier system, which has been problematic for pathologist in determining risk of malignant transformation (163).

### 5.2.2 S100A7 manual score

In this study, the potential utility of S100A7 expression as a biomarker for predicting malignant transformation of dysplastic lesions was assessed. Our expectation was that high expression of S100A7 within the epithelium of an oral mucosal dysplastic lesion was indicative of increased risk of malignant transformation.

S100A7 expression was found in all three of the populations evaluated. Staining tended to spare the basal layer, and was most prevalent in the stratum spinosum and the stratum granulosum when present. In tissue sections with very heavy staining, faint staining within the basal layer was appreciated. This is consistent with other studies assessing S100A7 manual scoring of epithelial dysplasia (121).

There was a general trend toward higher total manual score within both the Non-progressing and Progressing groups as compared to the Control group. This finding is in keeping with literature that noted increased expression of S100A7 in tissue with dysplasia relative to histologically normal tissue (129). The Progressing group demonstrated greater expression of S100A7 than the Non-progressing group. When ANOVA was applied to the population data for S100A7, it was noted that there was a statistically significant difference between these populations, and on further statistical analysis, utilizing Tukey multiple comparisons, the S100A7 manual score provided the examiner information to allow them to differentiate the two dysplastic populations from the Control population, however, the S100A7 manual score did not provide utility in allowing the examiner to differentiate the Non-progressing from the Progressing populations. This is clinically important as differentiating dysplastic from non-dysplastic tissue is currently

the basis of the 3-tier and 2-tier systems, and the additional information gained from S100A7 manual scoring may effect the clinical follow up of a patient. Dysplastic tissues are considered to be at increased risk of malignant transformation; yet a significant number of lesions deemed non-OPMLs also progress to OSCC (167). The S100A7 manual score can be applied with little additional effort to tissue samples from the oral cavity, and may contribute to an increased index of suspicion regarding malignant potential of a lesion. The diagnosis of dysplasia increases the frequency with which patients are followed clinically, therefore an assumption can be made that if a lesion is not identified as an OPML, the frequency in which they are followed will remain low. While there is no evidence based clinical follow up regimen, those diagnosed with OPMLs are seen at greater frequency, usually every 3-12 months (105)(87). A set of patients may be identified with the S100A7 manual score that are mild dysplasia or non-OPMLs but carry an increased risk of malignant transformation.

In order to determine a malignant transformation risk based on S100A7 immunohistochemical staining, further work is required to determine a cut off-score that would be specific enough to limit the number of cases deemed high risk, but also sensitive enough to include patients that are truly at risk. A validation study will be required to determine a threshold for risk. This could be completed by the same pathologist, or group of pathologists in order to establish a threshold for which amount of staining is significant. Based on this study, the average score for the Progressing group was 5.74, with a 95% confidence interval of 5.13 to 6.36, therefore any lesion with a manual score over five should be carefully followed. The S100A7 manual score in this study was unable to provide information that allowed the examiner to differentiate the

Non-progressing from the progressing group, and so it could be speculated that there would be a number of patients with dysplasia and a manual score below five that would likely have a lower risk of progression.

### **5.2.3 Straticyte™ assay for S100A7 staining**

Straticyte™ is used to assess S100A7 staining according to a proprietary algorithm, to formulate a five year risk score for malignant transformation (132). Our study demonstrated through Tukey analysis that Straticyte™ has the ability to differentiate a Progressing group from a Non-progressing group of dysplastic tissue (table 4.18). This holds diagnostic importance, as differentiating lesions that progress from those that do not is an area of weakness for the commonly used 3-tier grading system (57)(101)(164). This result supports the work by Hwang et al, in that the quantitative assessment of S100A7 staining of dysplastic oral epithelium utilizing Straticyte™ demonstrates an ability to differentiate lesions that do transform to OSCC from those that do not (132). This allows for closer follow up of oral epithelial lesions with increased risk of malignant transformation, as opposed to all patients with apparent dysplasia, which could potentially be inflammatory and likely to not progress. As such, there is utility in Straticyte™ based on our study, as it will increase efficiency for clinicians by identifying those at greater risk of malignant transformation. Additionally, it can identify patients at greater risk of transformation with lesions that may otherwise be considered low risk on microscopic examination.

#### **5.2.4 S100A7 manual score analysis: 3-tier, 2-tier and Straticyte™**

One of the specific aims of this study was to examine the utility of the different assays used to assess the dysplasia. As part of determining the utility, correlation between S100A7 manual scoring, and the 3-tier or 2-tier grading system was assessed. A Pearson correlation coefficient was calculated to identify a statistically significant relationship involving all populations and another was calculated for each of the individual test populations (tables 4.21, 4.22, 4.23). The expectation prior to carrying out the staining was that severe or high-grade dysplasia would have greater staining. When considering all populations, our study found weak correlation between S100A7 manual scoring and both the 3-tier and 2-tier grading systems. When the populations were evaluated with Pearson correlation individually, the relationship was negligible with only the Progressing group having a weak relationship with the 3-tier system. None of these relationships were statistically significant which makes it difficult to draw conclusions.

One source of discrepancy could lie in the analysis of the whole epithelium as compared to specific ROIs. The grade of dysplasia will be determined by the worst area, which can be very focal on microscopic examination. As such, the diagnosis can potentially be made based on a very small percentage of the overall epithelium present. When the S100A7 manual score was calculated, the whole epithelium was assessed, therefore a very focal area of strong staining would not result in a maximum score, despite a potential focal severe or high grade dysplasia.

Interestingly, when the Pearson correlation was applied to Straticyte™, and the relationships with the 3-tier and 2-tier grading systems were assessed, the correlational

relationships were very similar to the S100A7 manual scores with the 3-tier and 2-tier grading systems, with negligible to weak correlation existing, which was not statistically significant (tables 4.21, 4.22, 4.23). Again, drawing meaningful conclusions is difficult. This is not what was originally expected, given that both Straticyte™ and the 3-tier and 2-tier grading systems rely on specific ROIs to determine the diagnosis. The diagnosis of hyperkeratosis in the Control group is interpreted as a constant in the Pearson correlation, therefore it cannot be assessed individually. The stronger relationships between all populations and the individual populations is likely due to the inclusion of the Control group in the total population calculation (table 4.21 and 4.24).

The Pearson correlation coefficient indicates statistically significant moderate and strong relationships between S100A7 manual scoring and Straticyte™ for all populations (tables 4.21, 4.22, 4.23, 4.24). This is interesting given the discussion above regarding ROIs as compared to whole epithelial assessment, however it is feasible given the theory of field cancerization. Despite the tissue in the surrounding regions appearing histomorphologically normal, intracellular and molecular changes in keeping with the process of malignant transformation could be present well beyond the more obviously dysplastic tissue (168). This is a potential benefit with these tests as the staining occurs at a molecular level, and therefore may identify tissue that appears relatively normal histomorphologically. Based on the validation study of Straticyte™, which demonstrates the ability of Straticyte™ to identify lesions at increased risk of malignant transformation, a strong relationship between S100A7 manual scoring and Straticyte™, could be beneficial in identifying lesions that are at greater risk of malignant transformation, therefore effecting clinical follow up for the specific patient.

### 5.2.5 QuPath assessment of S100A7 staining

Our study also utilized QuPath for assessment of the S100A7 manual scoring in an attempt to improve objective measurement for tissue scoring (tables 4.19, 4.20, 4.25, 4.26, 4.27, 4.28). By utilizing the software's annotation tools, the area of staining was more precisely determined as compared to the more subjective area assessment of the S100A7 manual score. This has the potential to improve reproducibility which addresses significant issues with inter-observer and intra-observer variability when assessing and grading dysplasia. In combination with S100A7 staining, this could be an effective way for pathologists to further characterize tissue. In addition, the software can be utilized for more precise cell counts. This was not relevant in our study due to the diffuse nature of the staining, although the identification of nuclei could improve cell counts and potentially aid in the differentiation of cytoplasmic and nuclear staining. Nuclear staining of S100A7 of epithelial cells has been reported in the literature to be associated with cancer free survival (131). In the study by Tripathi et al, it was demonstrated that the over-expression of nuclear S100A7 staining was a poor prognostic indicator for not only cancer free survival but also overall outcomes. If automated identification of nuclear staining could be achieved and calculated against total nuclei (total cells) within the area of interest, the utility of QuPath could improve.

In this study, ANOVA, Tukey comparison and Pearson correlation were applied to QuPath results, the 3-tier and 2-tier grading systems, S100A7 manual scoring and Straticyte™ for the specific tissue samples used in the QuPath analysis. This showed that the three populations could not be differentiated using the S100A7 manual score, likely due to the small sample size, but when QuPath was utilized to assess the tissue staining, a

statistically significant difference between the Progressing group and the Control group was identified. When Pearson correlation was applied, the QuPath score had the strongest correlation with the S100A7 manual score, for all three populations.

## **5.6 MAPK**

MAPK signaling pathway protein immunohistochemical staining of tissue samples in this study was interpreted to be unsuccessful. While staining was attempted to identify dysregulation in phosphorylated protein activity, the tissue stained relatively uniformly, with what appeared to be significant non-specific staining. While staining of activated phosphorylated proteins is known to be difficult, irregular and unexpected staining may have resulted due to delayed staining of the prepared slides. In this study, some of the tissue was cut and prepared months prior to staining, which may have resulted in loss of specificity for some of the proteins in the pathway due to tissue deterioration.

## **5.7 Future considerations**

Obtaining a biomarker that can sufficiently identify lesions at increased risk of malignant transformation is of vital importance. The potential impact on clinical management could be significant. Possible impacts include increased surveillance of patients with an increased risk of malignant transformation, and decreased clinic visits for those at low risk. For the patient, the benefit is in personalized care. The current model has patients return to clinic for evaluation every 3-6 months, although less than half of dysplastic lesions go on to develop OSCC. In addition, a number of patients with initial diagnoses of non-dysplastic lesions progress and undergo malignant transformation (3)(102). This implies that some of the molecular changes that result in malignant transformation are not

perceptible on initial light microscopy. While the current results indicate S100A7 manual scoring was unable to distinguish between dysplastic lesions that progress to malignancy from those that do not, there was a statistically significant difference between those that progressed and the hyperkeratosis group. Therefore, there is potential utility for S100A7 staining and assessment to determine if these patients are at risk.

This study shows that S100A7 has predictive utility for malignant transformation in potentially malignant lesions. S100A7 manual scoring is relatively inexpensive and quick and can be completed within the same laboratory as the initial tissue sample. The interpretation can be carried out at the same time as other stains during the diagnostic assessment by the pathologist. In order to further increase specificity, ROIs could be assessed as opposed to the total epithelium. By limiting the interpretation of the slides to specific regions of interest, the total area of epithelium assessed would change, which would alter the percentage score component of the S100A7 manual score. This may improve the utility of the S100A7 manual score.

Additionally, the location of S100A7 staining within either the nucleus or cytoplasm could provide value in potentially identifying lesions at risk of malignant transformation. Nuclear staining is used as part of the Straticyte™ protocol, which demonstrated the ability to differentiate the Progressing from the Non-progressing groups. With the integration of staining location with the S100A7 manual score, differentiation of the populations may improve.

## 5.8 Limitations

Further information regarding patient habits both past and present would have improved this study. Unfortunately, the information regarding tobacco or alcohol status was incomplete for most as health care professionals submitting the tissue samples for assessment often failed to provide this information. If complete, this information could be included in the statistical analysis of the S100A7 manual score, which may improve our understanding of the S100A7 expression, and further improve its utility. One way of enhancing the amount of demographic information collected would be to include specific headings on the referral form. As many clinicians are filling out the information regarding the specimen during their busy clinics, and may inadvertently only include minimal information. If prompted, this information is more likely to be provided. The information will have already been collected during the initial consult.

The lack of a statistical difference in S100A7 scores between the two dysplastic populations is likely due to the heterogeneity of each of the groups. Heterogeneity in this case means that despite the identification of seemingly two distinct populations, progressors and non-progressors, within each group, there may be differences that we are unable to identify, that ultimately result in different subgroups within the population. With each subgroup, perhaps different outcomes would be expected if we could identify them. In particular, the progression to OSCC happens over a period of time which is variable, unpredictable at this time, and can occur after many years. This is supported by many studies which indicate that the average time to malignant transformation is three to five years, with some progressing more rapidly, and others taking several decades to transform. In addition, the proportion of dysplastic lesions that progress to OSCC is

greatest within the first two years (106)(169)(3)(85). While we attempted to select cases from four years previous to account for malignant transformation, some transformation can be expected to occur beyond four years. Therefore, despite multiple biopsies without malignant transformation, the Non-progressing population may contain patients who have yet to undergo malignant transformation but are likely to. As such, the heterogeneity is in the fact that there really may be two subgroups within the Non-progressing population, that we are unable to differentiate using our current method of identification; one of which may still undergo malignant transformation and hence truly belong in the Progressing group. It is also conceivable that some patients for whom only one biopsy was found, may have relocated to other parts of the province or country and are no longer receiving care within the catchment of the UWO pathology service. A second biopsy, recurrence or transformation may have occurred without our knowledge. In addition, patients may have died of other causes. In both cases, this would represent sampling bias. 10 patients from the Non-progressing group in our study only had one biopsy, and potentially may have been affected by sampling bias.

With respect to QuPath, a major disadvantage was that the use of the software was time consuming. The main reason for this is that staining of the epithelium and the underlying connective tissue was difficult for the automated annotation tool to differentiate. An over-estimate of the epithelium, with inclusion of the underlying connective tissue was commonly encountered, therefore, the user was still required to manipulate the annotation tool to outline the epithelium accurately. Given the moderate and strong correlation between the QuPath score and the S100A7 manual score, the practical value of the QuPath evaluation may be limited because of the time commitment for each of the tissue

samples, as Pathologists may be more inclined to assess the S100A7 staining directly using the light microscope rather than by using image analysis software. Further assessment of the S100A7 staining with QuPath utilizing ROIs would be beneficial in determining the if the software provides greater value than S100A7 manual scoring alone.

## CHAPTER 6: CONCLUSION

### 6.1 Conclusion

The primary goal of our study was to demonstrate that elevated S100A7 expression in tissue samples correlates with increased risk of malignant transformation. In addition, we looked to evaluate the utility of the 2- and 3-tier grading systems, S100A7 manual scoring and the S100A7 assay Straticyte™ in identifying dysplastic lesions at increased risk of malignant transformation. A subset of patient tissue samples were also evaluated with QuPath, an open source software for evaluation of histopathological specimens. This was done to assess potential utility of the software for improved assessment and scoring of tissue samples.

Each of the modalities was utilized to assess three populations: a Control population comprised of patients with hyperkeratosis, without dysplasia or malignant transformation, a Non-progressing population, with dysplasia which has not become malignant, and a Progressing population. This population demonstrates malignant transformation at a site of a previous lesion or dysplasia.

We attempted to differentiate the three study populations by assessing the proportion and intensity scoring of S100A7 expression within the oral mucosa. Our study showed that with S100A7 immunohistochemical staining, we were able to differentiate dysplastic tissue specimens from the non-dysplastic specimens of the Control group, giving value-added information for the pathologist to consider when grading dysplastic epithelia. This may be beneficial in cases of uncertainty between inflamed tissue or dysplasia. Given this utility, there is still promise, for differentiation of progressing from non-progressing

dysplasia. Perhaps more specific criteria are required to further hone the specificity of the S100A7 assay by including location of staining and evaluating specific regions of interest as opposed to the whole epithelium itself, as demonstrated by the Straticyte™ risk score, which was able to differentiate Progressing dysplasia from Non-progressing dysplasia groups. Utilizing QuPath as a means of evaluating the S100A7 offers potential for improving reproducibility for the S100A7 manual score and provides interesting prospective for further testing of its utility in these cases, as this study demonstrated promising preliminary results.

The current study demonstrates that the strongest correlation exists between S100A7 manual scoring and the Straticyte™ risk score. This correlation existed when applied to the Progressing and Non-progressing populations, and provides valuable information regarding both methods S100A7 staining evaluation.

## BIBLIOGRAPHY

1. World Health Organization. Cancer fact sheets - lip, oral cavity [Internet]. Cancer Fact Sheets. 2020. Available from: <http://gco.iarc.fr/today/data/factsheets/cancers/1-Lip-oral-cavity-fact-sheet.pdf>
2. Torre LA, Bray F, Siegel RL, Ferlay J, Lortet-Tieulent J, Jemal A. Global cancer statistics, 2012. *CA Cancer J Clin*. 2015;65(2):87–108.
3. silverman jr S, Gorsky M, Lozada F. Oral Leukoplakia and Malignant Transformation. *Cancer*. 1984;(53):563–8.
4. Marur S, Forastiere AA. Head and neck cancer: Changing epidemiology, diagnosis, and treatment. *Mayo Clin Proc*. 2008;83(4):489–501.
5. Thomson PJ, Potten CS, Appleton DR. Mapping dynamic epithelial cell proliferative activity within the oral cavity of man: A new insight into carcinogenesis? *Br J Oral Maxillofac Surg*. 1999;37(5):377–83.
6. Hashibe M, Brennan P, Chuang S, Boccia S, Castellsague X, Chen C, et al. Interaction between tobacco and alcohol use and the risk of head and neck cancer: pooled analysis in the INHANCE consortium. *Cancer Epidemiol Biomarkers Prev*. 2009;18(2):541–50.
7. Warnakulasuriya S, Dietrich T, Bornstein MM, Peidro EC, Preshaw PM, Walter C, et al. Oral health risks of tobacco use and effects of cessation. *Int Dent J*. 2010;60:7–30.
8. Guha N, Warnakulasuriya S, Vlaanderen J, Straif K. Betel quid chewing and the risk of oral and oropharyngeal cancers: A meta-analysis with implications for cancer control. *Int J Cancer*. 2014;135(6):1433–43.
9. Pannone G, Rodolico V, Santoro A, Lo Muzio L, Franco R, Botti G, et al. Evaluation of a combined triple method to detect causative HPV in oral and oropharyngeal squamous cell carcinomas: p16 Immunohistochemistry, Consensus PCR HPV-DNA, and In Situ Hybridization. *Infect Agent Cancer* [Internet]. 2012;7(1):4. Available from: <http://www.infectagentscancer.com/content/7/1/4>
10. Hübbers CU, Akgül B. HPV and cancer of the oral cavity. *Virulence*. 2015;6(3):244–8.
11. Capote-Moreno A, Brabyn P, Muñoz-Guerra MF, Sastre-Pérez J, Escorial-Hernandez V, Rodríguez-Campo FJ, et al. Oral squamous cell carcinoma: epidemiological study and risk factor assessment based on a 39-year series. *Int J Oral Maxillofac Surg*. 2020;49(12):1525–34.
12. Warnakulasuriya S. Global epidemiology of oral and oropharyngeal cancer. *Oral Oncol* [Internet]. 2009;45(4–5):309–16. Available from: <http://dx.doi.org/10.1016/j.oraloncology.2008.06.002>
13. Baykul T, Yilmaz HH, Aydin Ü, Aydin MA, Aksoy MÇ, Yildirim D. Early diagnosis of oral cancer. *J Int Med Res*. 2010;38(3):737–49.
14. Gómez I, Seoane J, Varela-Centelles P, Diz P, Takkouche B. Is diagnostic delay related to advanced-stage oral cancer? A meta-analysis. *Eur J Oral Sci*. 2009;117(5):541–6.
15. Evans SJW, Langdon JD, Rapidis AD, Johnson NW. Prognostic significance of STNMP and velocity of tumor growth in oral cancer. *Cancer*. 1982;49(4):773–6.
16. Cheraghlou S, Schettino A, Zogg CK, Judson BL. Changing prognosis of oral

- cancer: An analysis of survival and treatment between 1973 and 2014. *Laryngoscope*. 2018;128(12):2762–9.
17. Gurney TA, Eisele DW, Orloff LA, Wang SJ. Predictors of quality of life after treatment for oral cavity and oropharyngeal carcinoma. *Otolaryngol - Head Neck Surg*. 2008;139(2):262–7.
  18. Carlson RW. *Journal of the National Comprehensive Cancer Network Staying True to a Mission : NCCN Then and Now*. 2014;12(1):146–7.
  19. Eskander A, Merdad M, Irish J, Hall S, Groome P, Freeman J, et al. Volume–outcome associations in head and neck cancer treatment: A systematic review and meta-analysis. *Head Neck*. 2014;36(10):1820–34.
  20. Dolan R. Symptoms in early head and neck cancer: an inadequate indicator. *Otolaryngol Neck Surg*. 1998;119(5):463–7.
  21. Scott SE, Grunfeld EA, Main J, McGurk M. Patient delay in oral cancer: A qualitative study of patients' experiences. *Psychooncology*. 2006;15(6):474–85.
  22. Edge S, Byrd D, Compton C, Fritz A, Greene F, Trotti A. *AJCC CANCER STAGING MANUAL Seventh Ed. AJCC Cancer Staging Manual*. 2017. 21–35 p.
  23. Ettinger KS, Ganry L, Fernandes RP. Oral Cavity Cancer. *Oral Maxillofac Surg Clin North Am* [Internet]. 2019;31(1):13–29. Available from: <https://doi.org/10.1016/j.coms.2018.08.002>
  24. Sciubba J. Oral Cancer: The importance of early diagnosis and treatment. *Am J Clin Dermatol*. 2001;2(4):239–51.
  25. Ow TJ, Myers JN. Current management of advanced resectable oral cavity squamous cell carcinoma. *Clin Exp Otorhinolaryngol*. 2011;4(1):1–10.
  26. Lodder WL, Sewnaik A, Den Bakker MA, Meeuwis CA, Kerrebijn JDF. Selective neck dissection for N0 and N1 oral cavity and oropharyngeal cancer: Are skip metastases a real danger? *Clin Otolaryngol*. 2008;33(5):450–7.
  27. Silver CE, Rinaldo A, Ferlito A. Crile's neck dissection. *Laryngoscope*. 2007;117(11):1974–7.
  28. Li XM, Wei WI, Guo XF, Yuen PW, Lam LK. Cervical lymph node metastatic patterns of squamous carcinomas in the upper aerodigestive tract. *J Laryngol Otol*. 1996;110(10):937–41.
  29. Sivanandan R, Kaplan MJ, Lee KJ, Lebl D, Pinto H, Le Q-T, et al. Long-term Results of 100 Consecutive Comprehensive Neck Dissections. *Otolaryngol - Head Neck Surg*. 2004;130(12):1369–73.
  30. Lin A. Radiation Therapy for Oral Cavity and Oropharyngeal Cancers. *Dent Clin North Am* [Internet]. 2018;62(1):99–109. Available from: <https://doi.org/10.1016/j.cden.2017.08.007>
  31. Beitler JJ, Zhang Q, Fu KK, Trotti A, Spencer SA, Jones CU, et al. Final results of local-regional control and late toxicity of rtog 9003: A randomized trial of altered fractionation radiation for locally advanced head and neck cancer. *Int J Radiat Oncol Biol Phys* [Internet]. 2014;89(1):13–20. Available from: <http://dx.doi.org/10.1016/j.ijrobp.2013.12.027>
  32. Lundahl RE, Foote RL, Bonner JA, Suman VJ, Lewis JE, Kasperbauer JL, et al. Combined neck dissection and postoperative radiation therapy in the management of the high-risk neck: A matched-pair analysis. *Int J Radiat Oncol Biol Phys*. 1998;40(3):529–34.

33. Lavaf A, Genden EM, Cesaretti JA, Packer S, Kao J. Adjuvant radiotherapy improves overall survival for patients with lymph node-positive head and neck squamous cell carcinoma. *Cancer*. 2008;112(3):535–43.
34. Chronopoulos A, Zarra T, Ehrenfeld M, Otto S. Osteoradionecrosis of the jaws : definition , epidemiology, staging and clinical and radiological findings. A concise review. 2018;2014(January 1922):22–30.
35. Aarup-Kristensen S, Hansen CR, Forner L, Brink C, Eriksen JG, Johansen J. Osteoradionecrosis of the mandible after radiotherapy for head and neck cancer: risk factors and dose-volume correlations. *Acta Oncol (Madr) [Internet]*. 2019;58(10):1373–7. Available from: <https://doi.org/10.1080/0284186X.2019.1643037>
36. Berger A, Bensadoun RJ. Dose de tolérance des tissus sains: la mandibule. *Cancer/Radiotherapie*. 2010;14(4–5):295–300.
37. Lee IJ, Koom WS, Lee CG, Kim YB, Yoo SW, Keum KC, et al. Risk Factors and Dose-Effect Relationship for Mandibular Osteoradionecrosis in Oral and Oropharyngeal Cancer Patients. *Int J Radiat Oncol Biol Phys*. 2009;75(4):1084–91.
38. Nabil S, Samman N. Incidence and prevention of osteoradionecrosis after dental extraction in irradiated patients: A systematic review. *Int J Oral Maxillofac Surg [Internet]*. 2011;40(3):229–43. Available from: <http://dx.doi.org/10.1016/j.ijom.2010.10.005>
39. Hartner L. Chemotherapy for Oral Cancer. *Dent Clin North Am [Internet]*. 2018;62(1):87–97. Available from: <https://doi.org/10.1016/j.cden.2017.08.006>
40. Pignon JP, Maître A le, Maillard E, Bourhis J. Meta-analysis of chemotherapy in head and neck cancer (MACH-NC): An update on 93 randomised trials and 17,346 patients. *Radiother Oncol [Internet]*. 2009;92(1):4–14. Available from: <http://dx.doi.org/10.1016/j.radonc.2009.04.014>
41. Pignon JP, Bourhis J, Domenge C, Designé L. Chemotherapy added to locoregional treatment for head and neck squamous-cell carcinoma: Three meta-analyses of updated individual data. *Lancet*. 2000;355(9208):949–55.
42. Cooper J, Pajak T, Forastiere A, Jacobs J, Campbell BH, Saxman SB, et al. Postoperative Concurrent Radiotherapy and Chemotherapy for High-Risk Squamous-Cell Carcinoma of the Head and Neck. *N Engl J Med*. 2004;350(19):1937–44.
43. Bernier J, Domenge C, Ozsahin M, Matuszewska K, Lefebvre JL, Greiner RH, et al. Postoperative irradiation with or without concomitant chemotherapy for locally advanced head and neck cancer. *N Engl J Med*. 2004;350:1945–52.
44. Bonner J, Harari P, Giralt J, Azarnia N, Shin D, Cohen R, et al. Radiotherapy plus Cetuximab for squamous cell carcinoma of the head and neck. *N Engl J Med*. 2006;354(6):567–78.
45. Wan Y, Liang F, Nakasone T, Sunakawa H. Development of new leukoplakias and leukoplakia-associated second/multiple primary oral cancers: A case report and literature review. *J Oral Maxillofac Surgery, Med Pathol [Internet]*. 2014;26(2):166–9. Available from: <http://dx.doi.org/10.1016/j.ajoms.2012.12.001>
46. Palareti G, Legnani C, Cosmi B, Antonucci E, Erba N, Poli D, et al. Profiling Cancer Risk in Oral Potentially Malignant Disorders – a Patient Cohort Study. *J*

- Oral Pathol Med. 2017;46(10):888–95.
47. Berkovitz B, Holland G, Moxham B. Oral Histology and Embryology [Internet]. 4th ed. Mosby; 2010. 222–252 p. Available from: [vbk://978-0-7234-3411-5](http://vbk://978-0-7234-3411-5)
  48. Squier CA, Kremer MJ. Biology of oral mucosa and esophagus. *J Natl Cancer Inst Monogr*. 2001;52242(29):7–15.
  49. Groeger S, Meyle J. Oral mucosal epithelial cells. *Front Immunol*. 2019;10(FEB):1–22.
  50. Qin R, Steel A, Fazel N. Oral mucosa biology and salivary biomarkers. *Clin Dermatol* [Internet]. 2017;35(5):477–83. Available from: <http://dx.doi.org/10.1016/j.clindermatol.2017.06.005>
  51. Collins LMC, Dawes C. The Surface Area of the Adult Human Mouth and Thickness of the Salivary Film Covering the Teeth and Oral Mucosa. *J Dent Res*. 1987;66(8):1300–2.
  52. Hume WJ, Potten CS. Advances in epithelial kinetics—An oral view. *J Oral Pathol Med*. 1979;8(1):3–22.
  53. Kamer AR, Krebs L, Hoghooghi SA, Liebow C. Proliferative and apoptotic responses in cancers with special reference to oral cancers. *Crit Rev Oral Biol Med*. 1999;10(1):58–78.
  54. van der Waal I. Historical perspective and nomenclature of potentially malignant or potentially premalignant oral epithelial lesions with emphasis on leukoplakia—some suggestions for modifications. *Oral Surg Oral Med Oral Pathol Oral Radiol* [Internet]. 2018;125(6):577–81. Available from: <https://doi.org/10.1016/j.oooo.2017.11.023>
  55. Warnakulasuriya S, Johnson NW, Van Der Waal I. Nomenclature and classification of potentially malignant disorders of the oral mucosa. *J Oral Pathol Med* [Internet]. 2007 Jul 26 [cited 2018 Aug 14];36(10):575–80. Available from: <http://doi.wiley.com/10.1111/j.1600-0714.2007.00582.x>
  56. Warnakulasuriya S. Oral potentially malignant disorders: A comprehensive review on clinical aspects and management. *Oral Oncol* [Internet]. 2020;102(May 2019):1045–50. Available from: <https://doi.org/10.1016/j.oraloncology.2019.104550>
  57. Mello FW, Fernanda A, Miguel P, Neves E, Guerra S, Riet E, et al. Prevalence of oral potentially malignant disorders : A systematic review and meta-analysis. 2018;(April):633–40.
  58. Axell T. Occurrence of leukoplakia and some other oral white lesions among 20 333 adult Swedish people. *Community Dent Oral Epidemiol*. 1987;15(1):46–51.
  59. Napier SS, Speight PM. Natural history of potentially malignant oral lesions and conditions: An overview of the literature. *J Oral Pathol Med*. 2008;37(1):1–10.
  60. Kumar K, Abidullah M, Elbadawi L, Dakhil S, Mawardi H. Epidemiological profile and clinical characteristics of oral potentially malignant disorders and oral squamous cell carcinoma: A pilot study in Bidar and Gulbarga Districts, Karnataka, India. *J oral Maxillofac Pathol*. 2019;23(1):90–6.
  61. Pires FR, Barreto MEZ, Nunes JGR, Car-Neiro NS, de Azevedo AB, Dos Santos TCRB. Oral potentially malignant disorders: Clinical-pathological study of 684 cases diagnosed in a brazilian population. *Med Oral Patol Oral y Cir Bucal*. 2020;25(1):e84–8.

62. Axeil T. Occurrence of leukoplakia and some other white lesions among 20333 adult Swedish people. *Community Dent Oral Epidemiol.* 1987;Feb(1):46–51.
63. Arduino PG, Bagan J, El-naggar AK, Carrozzo M. Urban legends series : oral leukoplakia. *Oral Dis.* 2013;19:642–59.
64. Reibel J. Prognosis of oral premalignant lesions: Significance of clinical, histological, and molecular biological characteristics. 2003;14(1):47–62.
65. Warnakulasuriya S. Clinical features and presentation of oral potentially malignant disorders. *Oral Surg Oral Med Oral Pathol Oral Radiol* [Internet]. 2018;125(6):582–90. Available from: <https://doi.org/10.1016/j.oooo.2018.03.011>
66. Dost F, Cao KL, Ford PJ, Hons B. A retrospective analysis of clinical features of oral malignant and potentially malignant disorders with and without oral epithelial dysplasia. *Oral Surgery, Oral Med Oral Pathol Oral Radiol* [Internet]. 2013;116(6):725–33. Available from: <http://dx.doi.org/10.1016/j.oooo.2013.08.005>
67. Mehta F, Pindborg J, Hamner J. Report on oral cancer and precancerous conditions in Indian rural populations, 1966–1969. Basic Dental Research Unit. Tata Institute of Fundamental Research, Bombay. Munksgaard, Copenhagen. 1971.
68. K L, M S, A M, SK K, JJ P. Epidemiologic study of 6000 villagers of oral precancerous lesions in Bilugyun: preliminary report. *Commun Dent Oral Epidemiol.* 1982;(10):152–5.
69. Speight PM, Khurram SA, Kujan O. Oral potentially malignant disorders: risk of progression to malignancy. *Oral Surg Oral Med Oral Pathol Oral Radiol* [Internet]. 2018;125(6):612–27. Available from: <https://doi.org/10.1016/j.oooo.2017.12.011>
70. Shafer WG, Waldron CA. Erythroplakia of the oral cavity. *Cancer.* 1975;36(3):1021–8.
71. Pinto AC. Malignant transformation rate of oral leukoplakia — systematic review. 2020;00(00).
72. Warnakulasuriya S, Ariyawardana A. Malignant transformation of oral leukoplakia : a systematic review of observational studies. 2016;155–66.
73. Einhorn J, Wersall J. Incidence of oral carcinoma in patients with leukoplakia of the oral mucosa. *Cancer* [Internet]. 1967;20(12):2189–93. Available from: [10.1002/1097-0142\(196712\)20:12%3C2189::aid-cnrcr2820201218%3E3.0.co;2-m](https://doi.org/10.1002/1097-0142(196712)20:12%3C2189::aid-cnrcr2820201218%3E3.0.co;2-m)
74. Bánóczy J, Sugár L. Longitudinal studies in oral leukoplakias. *J Oral Pathol Med.* 1972;1(6):265–72.
75. Camous X, Pera A, Solana R, Larbi A. NK cells in healthy aging and age-associated diseases. *J Biomed Biotechnol.* 2012;2012.
76. Castelo-Branco C, Soveral I. The immune system and aging: A review. *Gynecol Endocrinol.* 2014;30(1):16–22.
77. LIND PO. Malignant transformation in oral leukoplakia. *Eur J Oral Sci.* 1987;95(6):449–55.
78. Lesch CA, Squier CA, Cruchley A, Williams DM, Speight P. The Permeability of Human Oral Mucosa and Skin to Water. *J Dent Res.* 1989;68(9):1345–9.
79. Holmstrup P, Vedtofte P, Reibel J, Stoltze K. Long-term treatment outcome of oral premalignant lesions. *Oral Oncol.* 2006;42(5):461–74.
80. Roed-Petersen B. Cancer development in oral leukoplakia follow-up of 331 patients. *J Dent Res.* 1971;50(3):711.

81. Napier SS, Cowan CG, Gregg TA, Stevenson M, Lamey P, Toner PG. Potentially malignant oral lesions in Northern Ireland : size ( extent ) matters. 2003;(July 2002):129–37.
82. Bánóczy J. Follow-up studies in oral leukoplakia. *J Maxillofac Surg*. 1977;5(C):69–75.
83. Bánóczy J, Gintner Z, Dombi C. Tobacco use and oral leukoplakia. *J Dent Educ* [Internet]. 2001;65(4):322–7. Available from: <http://www.ncbi.nlm.nih.gov/pubmed/11336117>
84. Schepman KP, Meij EH Van Der, Smeele LE, Waal I Van Der. Malignant transformation of oral leukoplakia : a follow-up study of a hospital-based population of 166 patients with oral leukoplakia from The Netherlands. *Oral Oncol*. 1998;34:270–5.
85. Lee JJ, Hong WK, Hittelman WN, Mao L, Lotan R, Shin DM, et al. Predicting cancer development in oral leukoplakia: Ten years of translational research. *Clin Cancer Res*. 2000;6(5):1702–10.
86. Arduino PG, Surace A, Carbone M, Elia A, Massolini G, Gandolfo S, et al. Outcome of oral dysplasia: A retrospective hospital-based study of 207 patients with a long follow-up. *J Oral Pathol Med*. 2009;38(6):540–4.
87. Villa A, Woo S Bin. Leukoplakia—A Diagnostic and Management Algorithm. *J Oral Maxillofac Surg* [Internet]. 2017;75(4):723–34. Available from: <http://dx.doi.org/10.1016/j.joms.2016.10.012>
88. Lodi G, Franchini R, Warnakulasuriya S, Varoni EM, Sardella A, Kerr AR, et al. Interventions for treating oral leukoplakia to prevent oral cancer. *Cochrane Database Syst Rev*. 2016;2016(7).
89. Diajil A, Robinson CM, Sloan P, Thomson PJ, Infirmiry RV, Ne T. Clinical Outcome Following Oral Potentially Malignant Disorder Treatment: A 100 Patient Cohort Study. *Int J Dent*. 2013;2013:1–8.
90. Li Y, Wang B, Zheng S, He Y. Photodynamic therapy in the treatment of oral leukoplakia: A systematic review. *Photodiagnosis Photodyn Ther* [Internet]. 2019;25(November 2019):17–22. Available from: <https://doi.org/10.1016/j.pdpdt.2018.10.023>
91. Vohra F, Al-Kheraif AA, Qadri T, Hassan MIA, Ahmed A, Warnakulasuriya S, et al. Efficacy of photodynamic therapy in the management of oral premalignant lesions. A systematic review. *Photodiagnosis Photodyn Ther* [Internet]. 2015;12(1):150–9. Available from: <http://dx.doi.org/10.1016/j.pdpdt.2014.10.001>
92. Pindborg, J.J., Sobin, L.H., Reichart P.A., Smith C.J. van der WI. Histological typing of cancer and precancer of the oral mucosa. Berlin: Springer; 1997.
93. Macdonald G. Classification and histopathological diagnosis of epithelial dysplasia and minimally invasive cancer. In: *Satellite Symposium on epithelial dysplasia and borderline cancer of the head and neck: controversies and future directions*. Joint BSOMP, BSOM, BAHNO. Oxford; 2003.
94. Warnakulasuriya S, Reibel J, Bouquot J, Dabelsteen E. Oral epithelial dysplasia classification systems: Predictive value, utility, weaknesses and scope for improvement. *J Oral Pathol Med*. 2008;37(3):127–33.
95. Kujan O, Oliver RJ, Khattab A, Roberts SA, Thakker N, Sloan P. Evaluation of a new binary system of grading oral epithelial dysplasia for prediction of malignant

- transformation. *Oral Oncol.* 2006;42(10):987–93.
96. El-Naggar AK, Chan J, Grandis J. World Health Organization Classification of Head and Neck Tumours. Vol. 9. 2017.
  97. Smith C, Pindborg J. Histological grading of oral epithelial atypia by the use of photographic standards. Copenhagen; 1969.
  98. Karabulut A, Reibel J, Therkildsen MH, Praetorius F, Nielsen HW, Dabelsteen E. Observer variability in the histologic assessment of oral premalignant lesions. *J Oral Pathol Med.* 1995;24(5):198–200.
  99. Abbey LM, Kaugars GE, Gunsolley JC, Burns JC, Page DG, Svirsky JA, et al. Intraexaminer and interexaminer reliability in the diagnosis of oral epithelial dysplasia. *Oral Surgery, Oral Med Oral Pathol Oral Radiol.* 1995;80(2):188–91.
  100. Kujan O, Khattab A, Oliver RJ, Roberts SA, Thakker N, Sloan P. Why oral histopathology suffers inter-observer variability on grading oral epithelial dysplasia: An attempt to understand the sources of variation. *Oral Oncol.* 2007;43(3):224–31.
  101. Nankivell P, Williams H, Matthews P, Suortamo S, Snead D, McConkey C, et al. The binary oral dysplasia grading system: Validity testing and suggested improvement. *Oral Surg Oral Med Oral Pathol Oral Radiol* [Internet]. 2013;115(1):87–94. Available from: <http://dx.doi.org/10.1016/j.oooo.2012.10.015>
  102. Sperandio M, Brown AL, Lock C, Morgan PR, Coupland VH, Madden PB, et al. Predictive value of dysplasia grading and DNA ploidy in malignant transformation of oral potentially malignant disorders. *Cancer Prev Res.* 2013;6(8):822–31.
  103. Lodi G, Franchini R, Warnakulasuriya S, Varoni EM, Sardella A, Kerr AR, et al. Interventions for treating oral leukoplakia to prevent oral cancer. *Cochrane Database Syst Rev.* 2016;2016(7).
  104. Thomson PJ, Goodson ML, Cocks K, Turner JE. Interventional laser surgery for oral potentially malignant disorders: a longitudinal patient cohort study. *Int J Oral Maxillofac Surg* [Internet]. 2017;46(3):337–42. Available from: <http://dx.doi.org/10.1016/j.ijom.2016.11.001>
  105. Field EA, McCarthy CE, Ho MW, Rajlawat BP, Holt D, Rogers SN, et al. The management of oral epithelial dysplasia: The Liverpool algorithm. *Oral Oncol.* 2015;51(10):883–7.
  106. Mehanna H, Rattay T, Smith J, McConkey C. TREATMENT AND FOLLOW-UP OF ORAL DYSPLASIA — A SYSTEMATIC REVIEW AND META-ANALYSIS. *Head Neck.* 2009;31(12):1600–9.
  107. Slaughter DP, Southwick HW, Smejkal W. “Field cancerization” in oral stratified squamous epithelium. Clinical implications of multicentric origin. *Cancer.* 1953;6(5):963–8.
  108. Braakhuis BJM, Tabor MP, Kummer JA, Leemans CR, Brakenhoff RH. A genetic explanation of slaughter’s concept of field cancerization: Evidence and clinical implications. *Cancer Res.* 2003;63(8):1727–30.
  109. Bedi GC, Westra WH, Gabrielson E, Koch W, Sidransky D. Multiple head and neck tumors: Evidence for a common clonal origin. *Cancer Res.* 1996;56(11):2484–7.
  110. Moore BW. A soluble protein characteristic of the nervous system. *Biochem Biophys Res Commun.* 1965;19(6):739–44.

111. Kypriotou M, Huber M, Hohl D. The human epidermal differentiation complex: Cornified envelope precursors, S100 proteins and the “fused genes” family. *Exp Dermatol*. 2012;21(9):643–9.
112. Volz A, Korge BP, Compton JG, Ziegler A, Steinert PM, Mischke D. Physical mapping of a functional cluster of epidermal differentiation genes on chromosome 1q21. Vol. 18, *Genomics*. 1993. p. 92–9.
113. Mischke D, Korge BP, Marenholz I, Volz A, Ziegler A. Genes Encoding Structural Proteins of Epidermal Cornification and S100 Calcium-Binding Proteins Form a Gene Complex (“Epidermal Differentiation Complex”) on Human Chromosome 1q21. *J Invest Dermatol* [Internet]. 1996;106(5):989–92. Available from: <http://dx.doi.org/10.1111/1523-1747.ep12338501>
114. Donato R. Intracellular and Extracellular Roles of S100 Proteins. *Microsc Res Tech*. 2003;551(January 2002):540–51.
115. Donato R. Functional roles of S100 proteins, calcium-binding proteins of the EF-hand type. *Biochim Biophys Acta - Mol Cell Res*. 1999;1450(3):191–231.
116. Kube E, Becker T, Weber K, Gerke V. Protein-protein interaction studied by site-directed mutagenesis. Characterization of the annexin II-binding site on p11, a member of the S100 protein family. *J Biol Chem* [Internet]. 1992;267(20):14175–82. Available from: [http://dx.doi.org/10.1016/S0021-9258\(19\)49694-4](http://dx.doi.org/10.1016/S0021-9258(19)49694-4)
117. Eckert RL, Broome AM, Ruse M, Robinson N, Ryan D, Lee K. S100 proteins in the epidermis. *J Invest Dermatol* [Internet]. 2004;123(1):23–33. Available from: <http://dx.doi.org/10.1111/j.0022-202X.2004.22719.x>
118. Madsen P, Rasmussen H, Leffers H, Honoré B, Dejgaard K, Olsen E, et al. Molecular cloning, occurrence, and expression of a novel partially secreted protein “psoriasin” that is highly up-regulated in psoriatic skin. *J Invest Dermatol*. 1991;97(4):701–12.
119. Zhu L, Okano S, Takahara M, Chiba T, Tu Y, Oda Y, et al. Expression of S100 protein family members in normal skin and sweat gland tumors. *J Dermatol Sci* [Internet]. 2013;70(3):211–9. Available from: <http://dx.doi.org/10.1016/j.jdermsci.2013.03.002>
120. Broome AM, Ryan D, Eckert RL. S100 protein subcellular localization during epidermal differentiation and psoriasis. *J Histochem Cytochem*. 2003;51(5):675–85.
121. Mclean L, Boeters-Jackson L, Armstrong J, Darling M. Evaluating the Utility of Protein Biomarker, S100A7, and Diagnostic Test, Straticyte, in Predicting the Progression of Oral Dysplasia [Internet]. Western University; 2019. Available from: <https://ir.lib.uwo.ca/etd/6711/>
122. Martinsson H, Yhr M, Enerbäck C. Expression patterns of S100A7 (psoriasin) and S100A9 (calgranulin-B) in keratinocyte differentiation. *Exp Dermatol*. 2005;14(3):161–8.
123. Hattori F, Kiatsurayanon C, Okumura K, Ogawa H, Ikeda S, Okamoto K, et al. The antimicrobial protein S100A7 / psoriasin enhances the expression of keratinocyte differentiation markers and strengthens the skin ’ s tight junction barrier. 2014;742–53.
124. Schro JM. UV-B radiation induces the expression of antimicrobial peptides in human keratinocytes in vitro and in vivo. :1117–23.

125. Wolk K, Witte E, Wallace E, Döcke W, Kunz S, Asadullah K, et al. IL-22 regulates the expression of genes responsible for antimicrobial defense, cellular differentiation, and mobility in keratinocytes: a potential role in psoriasis. *J Invest Dermatol*. 2006;1309–23.
126. Jinquan T, Vorum H, Larsen CG, Madsen P, Rasmussen HH, Gesser B, et al. Psoriasin: A Novel Chemotactic Protein. *J Invest Dermatol*. 1996;5–10.
127. Lei H, Li X, Jing B, Xu H, Wu Y. Human S100A7 induces mature interleukin1 $\alpha$  expression by RAGE-p38 MAPK-calpain1 pathway in psoriasis. *PLoS One*. 2017;12(1):1–13.
128. Ralhan R, DeSouza L V., Matta A, Chandra Tripathi S, Ghanny S, Datta Gupta S, et al. Discovery and Verification of Head-and-neck Cancer Biomarkers by Differential Protein Expression Analysis Using iTRAQ Labeling, Multidimensional Liquid Chromatography, and Tandem Mass Spectrometry. *Mol Cell Proteomics* [Internet]. 2008;7(6):1162–73. Available from: <http://www.mcponline.org/lookup/doi/10.1074/mcp.M700500-MCP200>
129. Ralhan R, Desouza L V., Matta A, Tripathi SC, Ghanny S, Dattagupta S, et al. ITRAQ-multidimensional liquid chromatography and tandem mass spectrometry-based identification of potential biomarkers of oral epithelial dysplasia and novel networks between inflammation and premalignancy. *J Proteome Res*. 2009;8(1):300–9.
130. Kaur J, Matta A, Kak I, Srivastava G, Assi J, Leong I, et al. S100A7 overexpression is a predictive marker for high risk of malignant transformation in oral dysplasia. *Int J Cancer*. 2014;134(6):1379–88.
131. Tripathi SC, Matta A, Kaur J, Grigull J, Chauhan SS, Thakar A, et al. Nuclear S100A7 is associated with poor prognosis in head and neck cancer. *PLoS One*. 2010;5(8):1–10.
132. Hwang JTK, Gu YR, Shen M, Ralhan R, Walfish PG, Pritzker KPH, et al. Individualized five-year risk assessment for oral premalignant lesion progression to cancer. *Oral Surg Oral Med Oral Pathol Oral Radiol*. 2017;123(3):374–81.
133. Hwang JTK, Gu YR, Dickson BJ, Shen M, Ralhan R, Walfish PG, et al. Straticyte demonstrates prognostic value over oral epithelial dysplasia grade for oral potentially malignant lesion assessment. *Oral Oncol* [Internet]. 2017;72:1–6. Available from: <https://doi.org/10.1016/j.oraloncology.2017.06.024>
134. Hwang JTK, Gu YR, Dickson BJ, Shen M, Ralhan R, Walfish PG, et al. Erratum: Straticyte demonstrates prognostic value over oral epithelial dysplasia grade for oral potentially malignant lesion assessment. *Oral Oncol*. 2018;77:138.
135. Celis JE, Rasmussen HH, Vorum H, Madsen P, Honore B, Wolf H, et al. Bladder Squamous Cell Carcinomas Express Psoriasin and Externalize it to the Urine. *J Urol*. 1996;2105–12.
136. Leygue E, Snell L, Hiller T, Dotzlaw H, Hole K, Murphy LC, et al. Differential expression of psoriasin messenger RNA between in situ and invasive human breast carcinoma. *Cancer Res*. 1996;56(20):4606–9.
137. Al-Haddad S, Zhang Z, Leygue E, Snell L, Huang A, Niu Y, et al. Psoriasin (S100A7) expression and invasive breast cancer. *Am J Pathol*. 1999;155(6):2057–66.
138. Ji J, Zhao L, Wang X, Zhou C, Ding F, Su L, et al. Differential expression of S100

- gene family in human esophageal squamous cell carcinoma. *J Cancer Res Clin Oncol*. 2004;130(8):480–6.
139. Moubayed N, Weichenthal M, Harder J, Wandel E, Sticherling M, Gläser R. Psoriasis (S100A7) is significantly up-regulated in human epithelial skin tumours. *J Cancer Res Clin Oncol*. 2007;133(4):253–61.
  140. Zhang H, Zhao Q, Chen Y, Wang Y, Gao S, Mao Y, et al. Selective expression of S100A7 in lung squamous cell carcinomas and large cell carcinomas but not in adenocarcinomas and small cell carcinomas. *Thorax*. 2008;63(4):352–9.
  141. Cargnello M, Roux PP. Activation and Function of the MAPKs and Their Substrates, the MAPK-Activated Protein Kinases. *Microbiol Mol Biol Rev* [Internet]. 2011;75(1):50–83. Available from: <http://mmbbr.asm.org/cgi/doi/10.1128/MMBR.00031-10>
  142. Burotto M, Chiou VL, Lee J-M, Kohn EC. The MAPK pathway across different malignancies: a new perspective. *Cancer* [Internet]. 2014 Nov 15 [cited 2018 Oct 12];120(22):3446–56. Available from: <http://www.ncbi.nlm.nih.gov/pubmed/24948110>
  143. Wei Z, Liu HT. MAPK signal pathways in the regulation of cell proliferation in mammalian cells. *Cell Res*. 2002;12(1):9–18.
  144. Dhillon AS, Hagan S, Rath O, Kolch W. MAP kinase signalling pathways in cancer. *Oncogene* [Internet]. 2007 May 14 [cited 2018 Oct 12];26(22):3279–90. Available from: <http://www.ncbi.nlm.nih.gov/pubmed/17496922>
  145. Raman M, Chen W, Cobb MH. Differential regulation and properties of MAPKs. 2007;3100–12.
  146. Kim C, Sano Y, Todorova K, Carlson BA, Arpa L, Lawrence T, et al. p38 $\alpha$  MAP kinase serves cell type-specific inflammatory functions in skin injury and coordinates pro- and anti-inflammatory gene expression. 2009;9(9):1019–27.
  147. Dey KK, Bharti R, Dey G, Pal I, Rajesh Y, Chavan S, et al. S100A7 has an oncogenic role in oral squamous cell carcinoma by activating p38/MAPK and RAB2A signaling pathway. *Cancer Gene Ther* [Internet]. 2016;23(11):382–91. Available from: <http://dx.doi.org/10.1038/cgt.2016.43>
  148. Takenaka K, Moriguchi T, Nishida E. Activation of the protein kinase p38 in the spindle assembly checkpoint and mitotic arrest. *Science* (80- ). 1998;280(5363):599–661.
  149. Spriggs AI. Automatic scanning frame. *J Clin Pathol*. 1969;2(1):1–6.
  150. Hamilton PW, Bankhead P, Wang Y, Hutchinson R, Kieran D, McArt DG, et al. Digital pathology and image analysis in tissue biomarker research. *Methods* [Internet]. 2014;70(1):59–73. Available from: <http://dx.doi.org/10.1016/j.jymeth.2014.06.015>
  151. Araújo ALD, Arboleda LPA, Palmier NR, Fonsêca JM, de Pauli Paglioni M, Gomes-Silva W, et al. The performance of digital microscopy for primary diagnosis in human pathology: a systematic review. *Virchows Arch*. 2019;474(3):269–87.
  152. Deroulers C, Ameisen D, Badoual M, Gerin C, Granier A, Lartaud M. Analyzing huge pathology images with open source software. *Diagn Pathol*. 2013;8(1):1–8.
  153. Keenan SJ, Diamond J, Glenn McCluggage W, Bharucha H, Thompson D, Bartels PH, et al. An automated machine vision system for the histological grading of

- cervical intraepithelial neoplasia (CIN). *J Pathol.* 2000;192(3):351–62.
154. McShane LM, Aamodt R, Cordon-Cardo C, Cote R, Faraggi D, Fradet Y, et al. Reproducibility of p53 immunohistochemistry in bladder tumors. *Clin Cancer Res.* 2000;6(5):1854–64.
  155. Bankhead P, Loughrey MB, Fernández JA, Dombrowski Y, McArt DG, Dunne PD, et al. QuPath: Open source software for digital pathology image analysis. *Sci Rep.* 2017;7(1):1–7.
  156. Liu W, Shi L, Wu L, Feng J, Yang X, Li J, et al. Oral Cancer Development in Patients with Leukoplakia – Clinicopathological Factors Affecting Outcome. 2012;7(4):1–7.
  157. Jaber MA, Porter SR, Speight P, Eveson JW, Scully C. Oral epithelial dysplasia: Clinical characteristics of western European residents. *Oral Oncol.* 2003;39(6):589–96.
  158. Dost F, Lê Cao K, Ford PJ, Ades C, Farah CS. Malignant transformation of oral epithelial dysplasia: A real-world evaluation of histopathologic grading. *Oral Surg Oral Med Oral Pathol Oral Radiol* [Internet]. 2014;117(3):343–52. Available from: <http://dx.doi.org/10.1016/j.oooo.2013.09.017>
  159. Silverman S, Bhargava K, Mani NJ, Smith LW, Malaowalla AM. Malignant transformation and natural history of oral leukoplakia in 57,518 industrial workers of gujarat, india. *Cancer.* 1976;38(4):1790–5.
  160. Dancyger A, Heard V, Huang B, Suley C, Tang D, Ariyawardana A. Malignant transformation of actinic cheilitis: A systematic review of observational studies. *J Investig Clin Dent.* 2018;9(4):e12343.
  161. Mehanna H, Rattay T, Smith J, McConkey C. TREATMENT AND FOLLOW-UP OF ORAL DYSPLASIA — A SYSTEMATIC REVIEW AND META-ANALYSIS. *Head Neck.* 2009;1600–9.
  162. Wang YY, Tail YH, Wang WC, Chen CY, Kao YH, Chen YK, et al. Malignant transformation in 5071 southern Taiwanese patients with potentially malignant oral mucosal disorders. *BMC Oral Health.* 2014;14(1):1–9.
  163. Câmara PR, Dutra SN, Takahama Júnior A, Fontes KBFC, Azevedo RS. A comparative study using WHO and binary oral epithelial dysplasia grading systems in actinic cheilitis. *Oral Dis.* 2016;22(6):523–9.
  164. Pritzker KPH, Darling MR, Hwang JTK, Mock D. Oral Potentially Malignant Disorders (OPMD): What is the clinical utility of dysplasia grade? *Expert Rev Mol Diagn* [Internet]. 2021;21(3):289–98. Available from: <https://doi.org/10.1080/14737159.2021.1898949>
  165. Montgomery E. Is there a way for pathologists to decrease interobserver variability in the diagnosis of dysplasia? *Arch Pathol Lab Med.* 2005;129(2):174–6.
  166. Speight PM, Abram TJ, Floriano PN, James R, Vick J, Thornhill MH, et al. Interobserver agreement in dysplasia grading: Toward an enhanced gold standard for clinical pathology trials. *Oral Surg Oral Med Oral Pathol Oral Radiol* [Internet]. 2015;120(4):474-482.e2. Available from: <http://dx.doi.org/10.1016/j.oooo.2015.05.023>
  167. Reibel J. Prognosis of oral pre-malignant lesions: Significance of clinical, histopathological, and molecular biological characteristics. *Crit Rev Oral Biol Med.* 2003;14(1):47–62.

168. Willenbrink TJ, Ruiz ES, Cornejo CM, Schmults CD, Arron ST, Jambusaria-Pahlajani A. Field cancerization: Definition, epidemiology, risk factors, and outcomes. *J Am Acad Dermatol* [Internet]. 2020;83(3):709–17. Available from: <https://doi.org/10.1016/j.jaad.2020.03.126>
169. Tilakaratne WM, Jayasooriya PR, Jayasuriya NS, De Silva RK. Oral epithelial dysplasia: Causes, quantification, prognosis, and management challenges. *Periodontol 2000*. 2019;80(1):126–47.